



January 2015

# Dopamine Transporter Phosphorylation, Palmitoylation And Membrane Localization And Mobility In Health And Disease

Madhur Shetty

Follow this and additional works at: <https://commons.und.edu/theses>

---

## Recommended Citation

Shetty, Madhur, "Dopamine Transporter Phosphorylation, Palmitoylation And Membrane Localization And Mobility In Health And Disease" (2015). *Theses and Dissertations*. 1962.  
<https://commons.und.edu/theses/1962>

This Thesis is brought to you for free and open access by the Theses, Dissertations, and Senior Projects at UND Scholarly Commons. It has been accepted for inclusion in Theses and Dissertations by an authorized administrator of UND Scholarly Commons. For more information, please contact [zeinebyousif@library.und.edu](mailto:zeinebyousif@library.und.edu).

DOPAMINE TRANSPORTER PHOSPHORYLATION, PALMITOYLATION AND  
MEMBRANE LOCALIZATION AND MOBILITY IN HEALTH AND DISEASE

By

Madhur Shetty

Bachelor of Science, Mumbai University, India 2008

Master of Science, Bangalore University, India 2010

A Thesis

submitted to the Graduate Faculty

of the

University of North Dakota

in partial fulfillment of the requirements

for the degree of

Master of Science

Grand Forks, North Dakota

December

2015

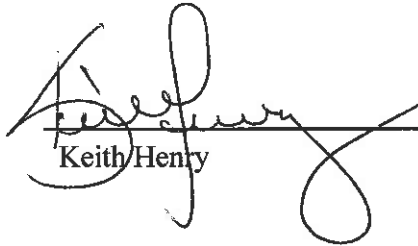
This thesis, submitted by Madhur Shetty in partial fulfillment of the requirements for the Degree of Master of Science from the University of North Dakota, has been read by the Faculty Advisory Committee under whom the work has been done and is hereby approved



James D. Foster (Chairperson)

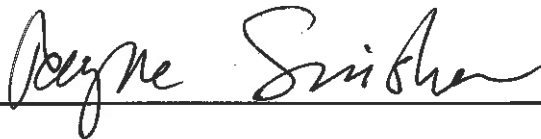


Roxanne A. Vaughan



Keith/Henry

This thesis is being submitted by the appointed advisory committee as having met all the requirements of the School of Graduate Studies at the University of North Dakota and is hereby approved.



Wayne Swisher  
Dean of the School of Graduate Studies



Date

## PERMISSION

Title	Dopamine transporter phosphorylation, palmitoylation and membrane localization and mobility in health and disease
Department	Biochemistry and Molecular Biology
Degree	Master of Science

In presenting this thesis in partial fulfillment of the requirements for a graduate degree from the University of North Dakota, I agree that the library of this University shall make it freely available for inspection. I further agree that permission for extensive copying for scholarly purposes may be granted by the professor who supervised my thesis work or, in his absence, by the Chairperson of the department or the Dean of the School of Graduate Studies. It is understood that any copying or publication or other use of this dissertation or part thereof for financial gain shall not be allowed without my written permission. It is also understood that due recognition shall be given to me and to the University of North Dakota in any scholarly use which may be made of any material in my thesis.

Madhur Shetty

8<sup>th</sup> December 2015

## TABLE OF CONTENT

LIST OF FIGURES .....	vii
LIST OF TABLES .....	ix
ABBREVIATIONS .....	x
ACKNOWLEDGEMENTS .....	xiv
ABSTRACT .....	xvii
CHAPTER	
I. INTRODUCTION .....	1
Neurotransmission and neurotransmitters .....	1
Monoamine neurotransmitters .....	4
Dopaminergic system .....	5
DAT .....	8
DAT structure .....	8
DAT regulation and binding partners .....	19
Reciprocal roles of phosphorylation and palmitoylation .....	23
Psychostimulant drugs .....	24
DAT and diseases .....	29
PD .....	29
Angelman syndrome .....	29
ADHD .....	30
DAT, cholesterol, lipid rafts and lateral membrane mobility .....	32
DHHC palmitoyl transferases enzymes .....	33

II.	ADHD ASSOCIATED DOPAMINE TRANSPORTER MUTANT A559V HAS ALTERED, RECIPROCAL PHOSPHORYLATION AND PALMITOYLATION STATUS ABSTRACT .....	36
1.	ABSTRACT .....	36
2.	INTRODUCTION .....	38
3.	EXPERIMENTAL METHODS .....	41
	Cell culture and site directed mutagenesis .....	41
	Acyl-biotinyl exchange (ABE).....	41
	Cell membrane preparation .....	43
	DAT T53 phosphorylation assay.....	43
	Metabolic [32]PO <sub>4</sub> - labeling.....	44
	Crosslinking immunoglobulin (IgG) to protein-A sepharose beads.....	45
	Immunoprecipitation .....	47
	Immunoblotting .....	47
	Equipment.....	48
	Materials .....	49
4.	RESULTS.....	51
	ADHD associated SNP, A559V and its rat homologue, A558V rDAT, display increased phosphorylation .....	51
	A558V rDAT displays increased phosphorylation at T53 .....	53
	Determining C581A hDAT to be palmitoylation deficient mutant.....	54
	ADHD associated SNP, A559V and its rat homologue, A558V rDAT, display decreased palmitoylation .....	57
	Phosphorylation deficient hDAT and rDAT mutants show enhanced palmitoylation status.....	57
5.	DISCUSSION.....	61

III. ALTERED MEMBRANE LOCALIZATION AND MOBILITY IN ADHD ASSOCIATED DOPAMINE TRANSPORTER MUTANT A559V LINKED TO ALTERED PHOSPHORYLATION/PALMITOYLATION STATUS.....	64
1. ABSTRACT .....	64
2. INTRODUCTION .....	66
3. EXPERIMENTAL METHODS .....	69
Cell culture and site directed mutagenesis .....	69
Confocal microscopy and fluorescence recovery after photobleaching (FRAP).....	70
Sucrose density gradient centrifugation .....	71
Immunoblotting .....	72
Equipment.....	73
Materials .....	74
4. RESULTS.....	76
ADHD associated SNP, A559V hDAT and its rat homologue, A558V rDAT, display increased membrane raft microdomain association .....	76
ADHD associated SNP, A559V hDAT and its rat homologue, A558V rDAT, display increased lateral membrane mobility.....	82
Palmitoylation is a factor affecting lateral membrane mobility .....	87
Phosphorylation deficient mutants displays decreased lateral membrane mobility.....	89
5. DISCUSSION.....	91
REFERENCES .....	94

## LIST OF FIGURES

FIGURE	PAGE
1. Neurotransmission pathway .....	3
2. Monoamine neurotransmitters and the functions they share .....	6
3. Dopaminergic pathways .....	7
4. Amino acid sequence alignment of <i>A. aeolicus</i> LeuT with hDAT homologues for glycine, GABA, DA and 5-HT using Psi-BLAST .....	10
5. LeuT structure .....	11
6. <i>Drosophila</i> DAT structure .....	12
7. Depiction of rDAT in its currently known phosphorylation and palmitoylation sites.....	14
8. Alternating access mechanism for transportation of substrate .....	17
9. DAT and its binding partners .....	22
10. Action of COC and AMPH on DAT .....	25
11. AMPH induced DAT efflux regulated by second messengers.....	27
12. Schematic representation of transporter mediated monoamine efflux .....	28
13. Membrane topology of DHHC proteins and its aligned sequences .....	35
14. A559V hDAT, C581A hDAT and their rat homologues display increased basal phosphorylation levels.....	52
15. A558V rDAT shows increased basal T53 phosphorylation levels.....	55
16. C581A hDAT is a palmitoylation deficient mutant .....	56
17. A559V hDAT and A558V rDAT display decreased palmitoylation levels .....	58
18. Phosphorylation deficient hDAT and rDAT mutants show enhanced palmitoylation levels .....	59



19. A559V hDAT and A558V rDAT display increased membrane raft microdomain localization .....	78
20. AMPH induces an increase in WT membrane raft microdomain localization.	80
21. A559V hDAT, C581A and their rDAT homologues display increased lateral membrane mobility.....	83
22. A559V hDAT and A558V rDAT display increased lateral membrane mobility equivalent to that induced by AMPH treatment .....	85
23. Inhibition of DAT palmitoylation results in increased lateral membrane mobility.....	88
24. Phosphorylation deficient mutants display decreased lateral membrane mobility.....	90

## LIST OF TABLES

TABLE	PAGE
1. The volume of specific antibodies required for crosslinking with the protein-A beads based on the specificity of the antibodies .....	46

## ABBREVIATIONS

2BP	2-bromopalmitate
5-HT	serotonin
ABE	acyl-biotinyl exchange
AD	Alzheimer's disease
ADE	anomalous DA efflux
ADHD	attention-deficit hyperactivity disorder
AMEM	$\alpha$ -minimum essential medium
AMPA	$\alpha$ -amino-3-hydroxy-5-methyl-4-isoxazolepropionic acid
AMPH	amphetamine
ASD	autism spectrum disorder
BPD	bipolar disorder
BSA	bovine serum albumin
CaMKII	calcium/calmodulin-dependent protein kinase II
CaMKII $\alpha$	calcium/calmodulin-dependent protein kinase II alpha subunit
CNS	central nervous system
CO	carbon monoxide
COC	cocaine
COMT	catechol-O-methyl transferase
CRD	Cys rich domain
DA	dopamine
DAT	dopamine transporter

dDAT	drosophila melanogaster DAT
DHHC	Asp-His-His-Cys
DMEM	Dulbecco's modified eagle's medium
DMP	dimethyl pimelimidate
DMSO	dimethyl sulfoxide
DTT	dithiothreitol
EDTA	ethylenediaminetetraacetic acid
EL2	extracellular loop 2
EL4	extracellular loop 4
ER	endoplasmic reticulum
ERK	extracellular signal regulated kinase
FBS	fetal bovine serum
FCS	fluorescence correlation spectroscopy
Flot1	flotillin
FRAP	fluorescence recovery after photobleaching
G418 sulfate	geneticin
GABA	$\gamma$ -aminobutyric
H <sub>2</sub> S	hydrogen sulphide
hDAT	human DAT
HPDP-biotin	<i>N</i> -(6-(biotinamido) hexyl)-3'-(2'-pyridyldithio)-propionamide
IB	immunoblotting
IgG	immunoglobulin
IL3	intracellular loop 3
IPB	ImmunoPrecipitation Buffer
JNK	c-Jun N-terminal kinase

KRH	Krebs's-Ringer HEPES
LeuT	leucine transporter protein
LLC-PK <sub>1</sub>	Lewis lung carcinoma-porcine kidney
MAO	monoamine oxidase
MAPK	mitogen-activated protein kinase
METH	methamphetamine
MMTS	methyl methanethiosulfonate
N <sub>2</sub> A	Neuronal
NE	norepinephrine
NET	norepinephrine transporter
NH <sub>2</sub> OH	hydroxylamine
NO	nitric oxide
NSS	neurotransmitter sodium symporter
NTTs	neurotransmitter transporters
OCD	obsessive compulsive disorder
PAGE	polyacrylamide gel electrophoresis
PAT	protein acyltransferase
PBS	phosphate buffer saline
PD	Parkinson's disease
PI3K	phosphatidylinositol 3-kinase
PKA	protein kinase A
PKC	protein kinase C
PMA	phorbol 12-myristate, 13-acetate
PPTs	palmitoyl-protein thioesterases
PVDF	polyvinylidene difluoride

RACK1	receptor for activated C kinase
rDAT	rat DAT
RIPA	RadioImmunoPrecipitation Assay
Rit2	GTPase Rin
ROI	region of interest
RT	room temperature
SDS	sodium dodecyl sulphate
SERT	serotonin transporter
SLC6	solute carrier 6
SNARE	soluble N-ethylmaleimide-sensitive factor attachment protein receptor
SNc	substantia nigra
SNP	single nucleotide polymorphism
Syn 1A	syntaxin 1A
TMD	transmembrane spanning domain
VMAT	vesicular monoamine transporter
VTA	ventral tegmental area
WT	wildtype
YFP	yellow fluorescent protein

## ACKNOWLEDGEMENTS

I owe my deepest gratitude to my advisor, Dr. James D. Foster for his constant support throughout my graduate studies at UND. His continuous guidance has been a constant source of motivation for me. Questions put forth by Dr. Foster have challenged me to critically think and plan experiments. He has been a perfect role model and an exceptionally good trainer, having put in hours of effort in teaching me the techniques I have mastered since I joined the lab. His encouragement to attend national and international conferences has not only helped me present my research to a larger audience but also helped me get valuable critics from competing lab. I am grateful for his training, encouragement, motivation and support in the lab.

A special thanks to Dr. Sukalski in allowing me to be funded by the department during all my years as a graduate student. I am grateful to the former department of Biochemistry and Molecular Biology and the current department of Basic Sciences for all the funding support.

I would like to thank my committee members Dr. Roxanne A. Vaughan and Dr. Keith Henry for their valuable inputs, comments and suggestions during committee meetings and otherwise. I would also like to acknowledge Dr. Bryon Grove and Sarah Abrahamson for all the training with confocal microscopy.

My journey here would not have been possible without such a wonderful lab environment. I am incredibly grateful to all the lab members of the Foster Lab and Vaughan Lab (Daniel Stanislawski, Danielle Rastedt, Micheal Tomlinson and

Margaret Smith) for their support with extended thanks to Dr. Rejwi Acharya Dahal, Dr. Sathyavathi Challasivakanaka and rest of the transporter group.

I would like to extend my gratitude to the rest of the faculty, staff of the former department of Biochemistry and Molecular Biology and all the present and past graduate students. I am glad to have crossed path with you.

Last but not the least, I would like to thank my loving and ever wonderful parents for their unconditional love and support. Special thanks to my brother, Mihir Shetty and my wife, Jaspreet Kaur Osan for their love, care and ever-lasting support. Thanks for always being there with me.



Dedicated to my parents, brother and wife

## ABSTRACT

The dopaminergic system is a regulatory system of the brain controlling various motor, cognitive and behavioral activities. Neurotransmitter dopamine (DA) plays an important role in modulating brain circuits controlling functions of this system with dopamine transporter (DAT) maintaining its homeostasis. Abnormalities in this homeostasis and/or nucleotide polymorphisms in the DAT structure leads to its association with a wide range of neurological and neuropsychiatric disorders, with attention-deficit hyperactivity disorder (ADHD) being one of them.

Disrupting the normal function of DAT, many psychostimulants such as amphetamine (AMPH) upon being transported via DAT into the pre-synaptic neuron alters DAT properties triggering N-terminal DAT phosphorylation associated DA efflux.

Recently identified, ADHD associated human DAT (hDAT) single nucleotide polymorphism (SNP), A559V, displayed anomalous DA efflux (ADE). Our results showed A559V hDAT and its rat homologue, A558V rat DAT (rDAT), displaying AMPH independent increased phosphorylation, including T53 site (human equivalent being S53), a proline directed phosphorylation site specific for rDAT, further unaffected by AMPH, which may support ADE observed for this polymorphism. These SNPs also showed reciprocal decreased palmitoylation status. With these modifications impacting DAT properties, we found phosphorylation driven increased membrane raft localization for A559V hDAT and other palmitoylation deficient mutants. These membrane rafts serve as a site for localization of phosphorylated DAT

and a platform for DA efflux. These mutants also showed increased lateral membrane mobility, which was reciprocally decreased for phosphorylation deficient mutants (T53A rDAT, S7A hDAT and S53A hDAT) which have increased palmitoylation.

Further, studies confirmed C581 to be a palmitoylation site in humans, with C581A hDAT being a palmitoylation deficient mutant having elevated phosphorylation with membrane microdomain and mobility properties similar to A559V hDAT.

For A559V hDAT, the close proximity of Val substitution to the palmitoylation site could cause a structural alteration in DAT transmembrane spanning domain (TMD) 12 helical structure. The bulkier substitution may mechanistically hinder C581 palmitoylation causing its movement away from DAT core region, lose of flexibility, altered DAT membrane localization, mobility and function. We believe other phosphorylation or palmitoylation deficient mutants might show similar unknown mechanisms, reciprocally regulating post-translational modifications.

With palmitoylation helping in membrane raft partitioning, stabilization of membrane anchoring and integral membrane protein interaction, we demonstrate palmitoylation to be a factor for DAT membrane mobility. We believe the palmitate group affects DAT's interaction with binding partners and cholesterol and that its deficiency leads to increased lateral membrane mobility. This palmitoylation status could be the driving force for phosphorylation driven increased localization of phosphorylated DAT in membrane raft microdomains, leading to increased interaction with binding partners, serving as a platform for phosphorylation-dependent DA efflux either by AMPH-stimulation or by polymorphism.

## CHAPTER I

### INTRODUCTION

#### Neurotransmission and neurotransmitters

The nervous system is a complex system that plays a key role in controlling and coordinating neurological signal transmission as well as various voluntary and involuntary actions. This system is well maintained by a coordinated network of neurons, which communicate with each other by a process called neurotransmission.

Neurotransmission is brought about by endogenous chemicals called neurotransmitters which are stored in small sac like organelles called synaptic vesicles and are released from pre-synaptic neurons upon being excited through an incoming signal. These neurotransmitters then move through neuronal junctions called synapses and are received and recognized by receptors present on the plasma membranes of post-synaptic neurons, causing relaying of signals downstream and bringing about synaptic transmission. Following the transmission of the signals, the neurotransmitters are cleared from the synapses either by diffusing through the plasma membrane into the pre-synaptic neurons or are taken-up by the pre-synaptic neurons with the help of neurotransmitter specific transporter proteins or are taken-up by neighboring glial cells. Within the pre-synaptic neurons, these neurotransmitter substrates are repackaged into synaptic vesicles or are targeted towards metabolic or enzymatic degradation. Clearance of neurotransmitter substrates from synapses is an important step in maintaining synaptic homeostasis and inability to do so leads to over-

stimulation of the post-synaptic receptors. Long term over-stimulation of these post-synaptic receptors could lead to various neurological conditions and diseases.

The neurotransmission cycle occurs within milliseconds and is triggered by an action potential generated by voltage gated ion channels which originates in the cell bodies of the neurons. This action potential moves across the axon terminal, causing depolarization of the pre-synaptic neuronal membranes leading to synaptic transmission. Upon reaching the end of the axon terminal, the action potential triggers the opening of calcium channels causing  $\text{Ca}^{++}$  ions to move from the synapse into the pre-synaptic neurons, in exchange for  $\text{Na}^+$  ions which are pumped to the extracellular side. This buildup of  $\text{Ca}^{++}$  ions triggers the fusion of synaptic vesicles with the plasma membrane causing the release of neurotransmitters into the synapse. New synaptic vesicles are formed by pinching off the plasma membrane within the pre-synaptic neurons where it is filled with neurotransmitters for cycle to continue (Fig. 1) [1].

Within neurons there are many different types of neurotransmitters present and one of the ways of classifying them is into amino acids, peptides and monoamines. Some of the neurotransmitters that fall into these groups are:

- Amino acid neurotransmitters: glutamate, aspartate, D-serine,  $\gamma$ -aminobutyric (GABA) and glycine.
- Monoamines and other biogenic amines neurotransmitters: dopamine (DA), serotonin (5-HT), norepinephrine (NE), epinephrine and histamine.
- Gasotransmitters: nitric oxide (NO), carbon monoxide (CO), hydrogen sulphide ( $\text{H}_2\text{S}$ ).

The uptake of neurotransmitter substrates from the synapses into the pre-synaptic

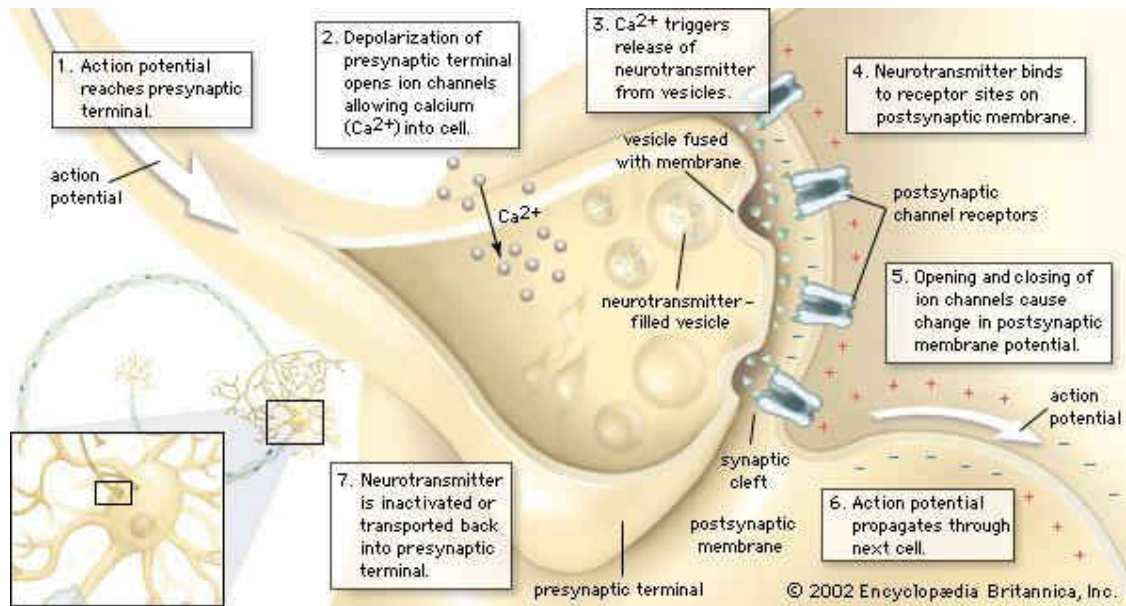


Image courtesy, 2002 Encyclopædia Britannica Inc, with permission.

Figure 1: Neurotransmission pathway.

Neurotransmission is triggered by an incoming action potential which upon reaching the pre-synaptic neuronal terminal opens the ion channels allowing  $\text{Ca}^{++}$  ions to move into the cell. These  $\text{Ca}^{++}$  ions trigger the fusion of synaptic vesicles with the plasma membrane of the pre-synaptic neurons causing the release of neurotransmitters into the synapse. These neurotransmitters then act on the receptors present on the post-synaptic neurons, relaying the signal downstream. These neurotransmitters are then transported back to the pre-synaptic neurons by transporters and are either repackaged into the synaptic vesicles or are targeted towards metabolic or enzymatic degradation.

neurons is brought about by substrate specific neurotransmitter transporter (NTTs) proteins, which are present on the plasma membrane of the pre-synaptic neurons. These NTTs belong to the solute carrier 6 (SLC6) gene family which are widely expressed in the brain. These NTTs are also called neurotransmitter-sodium-symporter (NSS) or  $\text{Na}^+/\text{Cl}^-$  dependent transporters and are named according to the neurotransmitter substrate they transport. The transport of neurotransmitter substrates across the transporter is brought about by an electrochemical gradient, where  $\text{Na}^+$  ions are the source of energy, generated by the  $\text{Na}^+/\text{K}^+$  transporting ATPase. The uptake of substrate through NTTs occurs along with the co-transportation of extracellular  $\text{Na}^+$  and  $\text{Cl}^-$  ions and in some cases intracellular  $\text{K}^+$  ions, with the function of NTTs being regulated by various protein kinases and protein-protein interactions [2-6]. Abnormalities in the function of these NTTs is associated with various neurological disorders such as attention-deficit hyperactivity disorder (ADHD), Alzheimer's disease (AD), obsessive compulsive disorder (OCD), bipolar disorder (BPD), Parkinson's disease (PD), X-linked mental retardation, autism and mood disorders such as depression and anxiety [7-9].

#### Monoamine neurotransmitters

Neurotransmitters that structurally contain an amino group connected to an aromatic ring by a two carbon chain are known as monoamines. These monoamine neurotransmitters, DA, NE and 5-HT, are transported from the synapse to the pre-synaptic neurons with the help of dopamine transporter (DAT), norepinephrine transporter (NET) and serotonin transporter (SERT) respectively. DA and NE are derived from a common upstream amino acid Tyr with DA being the immediate precursor of NE, while 5-HT is synthesized from Trp. These neurotransmitters

together coordinate a wide range of functions including mood, attention, sleep, learning, memory function, obsession, sex and anxiety (Fig. 2) [10].

### Dopaminergic system

The dopaminergic system in the brain is responsible for controlling motor, cognitive, and motivational behavior and plays a role in regulating sleep patterns, moods, attention, memory and locomotion [6, 9, 11-15]. Failure of this system leads to disruption of DA function that has an effect on neurological and psychological illnesses such as PD, AD, ADHD, BPD, drug abuse and addiction [6, 9, 16-21]. The dopaminergic system is categorized into four pathways called the mesocortical, mesolimbic, nigrostriatal and tuberoinfundibular tracks within the brain. Dopaminergic neurons arising from different regions of the brain have different functions. The neurons located within the mesencephalon branch into three neuronal groups: the retrobulbar, the substantia nigra (SNc) and the ventral tegmental area (VTA). While most of the neurons arising from the zona compacta of the SNc are a part of the nigrostriatal pathway projecting into the dorsal striatum and are associated with movement, the neurons arising from the VTA are part of the mesolimbic pathway projecting into the limbic and its connected regions such as the nucleus accumbens, amygdala and hippocampus and are associated with mood, motivation, thought process and reward. Some of the neurons arising from the VTA are also a part of the mesocortical dopaminergic pathway projecting into the prefrontal, cingulate and perirhinal cortex. Other neurons arising from the retrobulbar area project into the hypothalamus and regulate the hormonal secretions from the pituitary (Fig. 3) [22-26]. All of these dopaminergic neurons although present within the central nervous system (CNS) are considered unrelated as they perform different sets of cellular functions, are



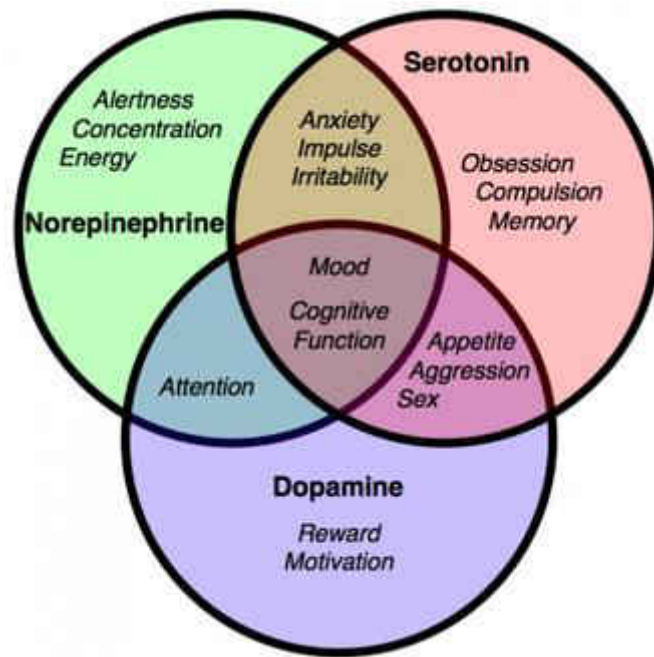


Image courtesy, <http://elitenootropics.com/identify-overcome-low-dopamine/>, with permission.

Figure 2: Monoamine neurotransmitters and the functions they share.

Monoamine neurotransmitters DA, NE and 5-HT coordinate and regulate various different functions individually but also are involved in coordinating a wide range of functions together such as mood, attention, sleep, appetite, anxiety, attention, sex and cognitive functions.

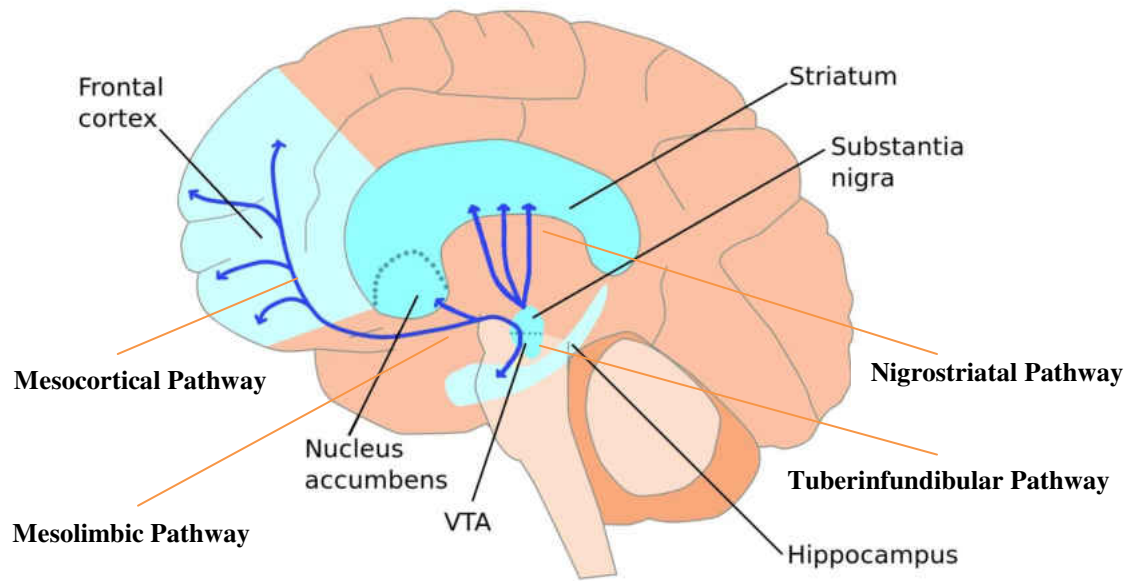


Image courtesy, <https://www.oist.jp/news-center/photos/dopamine-pathways>, with permission.

Figure 3: Dopaminergic pathways.

Dopaminergic neurons are categorized into four pathways: mesocortical, mesolimbic, nigrostriatal and tuberoinfundibular.

located in different positions and project differently. The only common aspect linking them is that they all synthesize DA.

### DAT

DAT plays an important role in maintaining DA homeostasis. Following the release of DA into the synapse, DAT functions to clear the synaptic DA by uptake in presence of an electro-chemical gradient. Upon uptake of DA by DAT into the pre-synaptic neurons, it is either repackaged into synaptic vesicles for reused or is directed towards degradation by oxidation in the presence of monoamine oxidase (MAO) or catechol-O-methyl transferase (COMT). This process of uptake is highly specific to the type of neurotransmitters [3]. DAT belongs to the SLC6 gene family and called SLC6A3 as it is the third member of the group. It is known to be distributed majorly in the CNS while some is also present in the gut [2].

### DAT structure

When compared to other members of the SLC6 gene family, mammalian DAT shows a high homology to various transporter structures like NET (~67%), SERT (~49%) and GABA (~45.5%) [6]. The mammalian DAT is a ~80 KDa glycoprotein. With its three dimensional crystallized structure still unknown, mammalian DAT is highly comparable to its prototype, the bacterial homologue, leucine transporter protein (LeuT) derived from *Aquifex aeolicus* which shares a 20% sequence identity to mammalian DAT. The three dimensional LeuT structure shows it to be a 12 transmembrane spanning domain (TMD) helical structure arranged in two pseudo-symmetrical inverted repeats: TMDs 1-5 and TMDs 6-10, with its N- and C-termini present within the cytosol. The amino acid sequence alignment between LeuT, DAT

and other Na<sup>+</sup>/Cl<sup>-</sup> dependent transporters revealed that various residues are conserved between these transporters (Fig. 4). TMDs 1, 3, 6 and 8 form the central substrate binding site with TMDs 1 and 6 being anti-parallel to each other having breaks in the helical structure about halfway across the membrane bilayer. Other TMDs surround the core site, providing support to this region. The LeuT structure shows the presence of two Na<sup>+</sup> ions near the leucine molecule at halfway across the bilayer (Fig. 5). These ions stabilize the LeuT core, TMDs 1 and 6 and the bound leucine molecule. Since leucine transport is not chloride dependent, the LeuT structure failed to show the presence of Cl<sup>-</sup> ion near the binding pocket, but instead had a Cl<sup>-</sup> ion bound near the surface of the protein. Many LeuT gating residues are found to be conserved in DAT and other Na<sup>+</sup>/Cl<sup>-</sup> dependent transporters, all of which play a role in substrate transport [27-33].

The recently crystallized eukaryotic DAT structure, *Drosophila melanogaster* DAT (dDAT) shares more than 50% sequence identity to mammalian DAT. The overall structure of dDAT is similar to LeuT except for the presence of a kink at the centre of TMD 12 as a result of P572, causing the second half of the TMD 12 to move away from the transporter. dDAT crystal structure predicted N-linked glycosylation sites and a disulphide bond in the extracellular loop 2 (EL2), critical for the trafficking of transporter to the plasma membrane. The binding pocket shows proximal binding of Na<sup>+</sup> and Cl<sup>-</sup> ions. Many important dDAT gating residues are found to be conserved in LeuT and human DAT (hDAT), playing a role in substrate recognition and transport. dDAT structure showed the presence of a cholesterol molecule anchored at the junction of TMD 5 and 7, which stabilizes DAT in an outward-open confirmation position (Fig. 6) [30, 34]. These transporters serve as a template in understanding the overall mammalian DAT structure. The mammalian DAT is also a 12 TMD structure

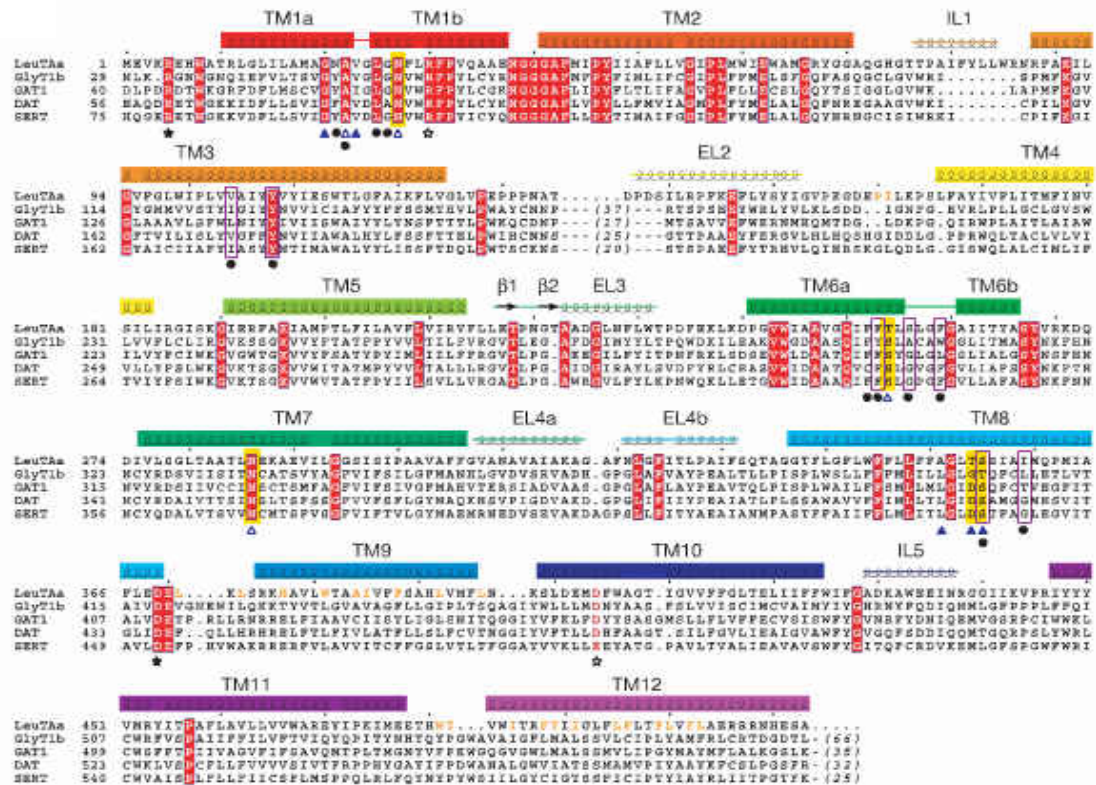


Image courtesy, Yamashita, A., et al., *Crystal structure of a bacterial homologue of Na<sup>+</sup>/Cl<sup>-</sup> dependent neurotransmitter transporters*. Nature, 2005. **437**(7056): p. 215-223, with permission [31].

Figure 4: Amino acid sequence alignment of *A. aeolicus* LeuT with hDAT homologues for glycine, GABA, DA and 5-HT using Psi-BLAST.

The conserved residues are highlighted in red while  $\alpha$ -helices and  $\beta$ -strands in LeuT are depicted in coils and arrows respectively. The open and filled triangles show residues involved in coordinating the Na<sup>+</sup> ions, Na1 and Na2 respectively while residues whose side-chains interact with Na<sup>+</sup> ions are further highlighted in yellow. The filled black circles indicate the residues involved in leucine binding and the residues whose side chains interact with the leucine are enclosed by purple boxes. The open and filled stars indicate the charged pairs at the extracellular and cytoplasmic entrances respectively. The residues in the LeuT dimer interface are shown in orange letters. For eukaryotic transporters, residues are truncated in the alignment and the numbers of the truncated residues are shown in parentheses.

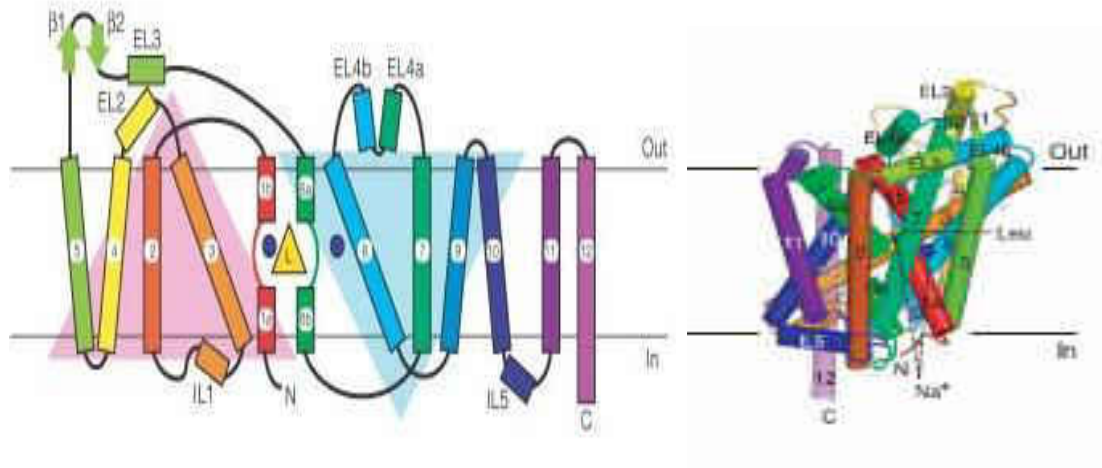


Image courtesy, Yamashita, A., et al., *Crystal structure of a bacterial homologue of Na<sup>+</sup>/Cl<sup>-</sup> dependent neurotransmitter transporters*. Nature, 2005. **437**(7056): p. 215-223, with permission [31].

Figure 5: LeuT structure.

LeuT is a 12 TMD spanning helical structure, with the first 10 TMD forming the central protein core. TMDs 1-10 are arranged in two pseudo-symmetrical inverted repeats in the membrane plane: TMDs 1-5 and TMDs 6-10. Leucine residue (yellow triangle) is seen here in the substrate binding site accompanied with two Na<sup>+</sup> ions (blue circles) bound in the sodium binding sites, halfway across the membrane bilayer in an occluded site lacking water.

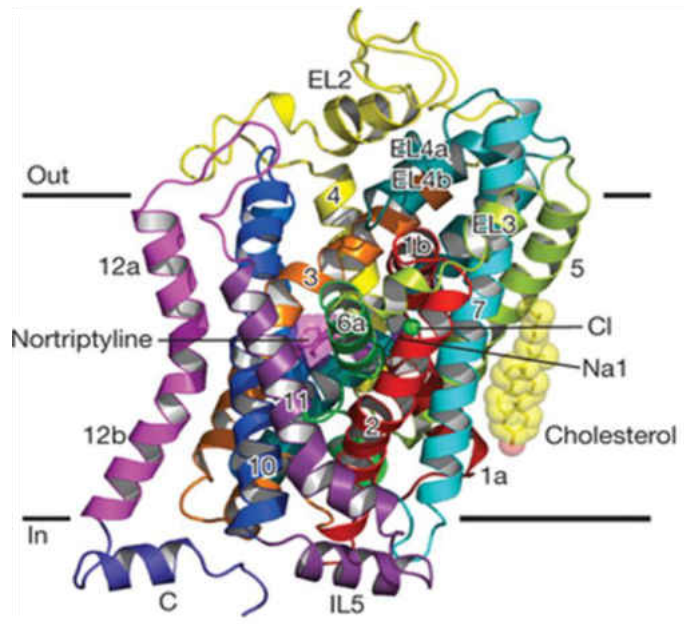


Image courtesy, Penmatsa, A., Wang, K.H. and Gouaux, E., *X-ray structure of dopamine transporter elucidates antidepressant mechanism*. Nature, 2013. **503**(7474): p. 85-90, with permission [30].

Figure 6: Drosophila DAT structure.

dDAT is shown in the presence of tricyclic antidepressant Nortriptyline,  $\text{Na}^+$  ions and  $\text{Cl}^-$  ions and a cholesterol molecule. It is a 12 TMD spanning helical structure similar to LeuT except for the presence of a kink at the centre of TMD 12 as a result of P572, causing the second half of the TMD 12 to move away from the transporter.

with its termini facing the cytosol and TMDs 1, 3, 6 and 8 forming the central substrate binding pocket [31, 35]. The hDAT is a 620 amino acid residue protein while the rat DAT (rDAT) is a 619 residue protein with hDAT having an extra G199. The rDAT differs from hDAT in 48 residues making its sequence 92% identical to hDAT. DAT undergoes at least four forms of post translational modifications: glycosylation, ubiquitination, phosphorylation and S-palmitoylation. These modifications facilitate the interaction between DAT and other proteins, altering DAT transport kinetics and/or change the distribution of DAT within the plasma membrane or between the cell surface and intercellular space [36-42]. Pharmacological manipulation of these post-translational modifications may lead to therapeutic routes to regulate DAT expression and function.

Glycosylation of mammalian DAT occurs on the Asn residues present on the EL2. While hDAT is glycosylated on N181, 188 and 205, rDAT is glycosylated on N181, 188, 196 and 204 (Fig. 7) [2, 35, 41, 43, 44]. Glycosylation helps stabilize DAT localization on the plasma membrane, maintain functional regulation, increase the DA  $V_{\max}$  and surface expression of DAT [42, 45]. It also plays an important role in susceptibility of DAT to the effect of drugs and disease. Ubiquitination of DAT occurs on the N-terminus determining if DAT internalization is temporary for it to be recycled back to the plasma membrane, or it is permanent leading to DAT degradation. Ubiquitinated DAT is sorted away from the constitutive recycling pathway and into a late endocytic pathway, resulting in lysosomal degradation [46, 47].

Phosphorylation has been widely studied on a cluster of Ser residues (2, 4, 7, 12, 13 and 21) on the N-terminus, out of which, S7 and S13 have been validated for



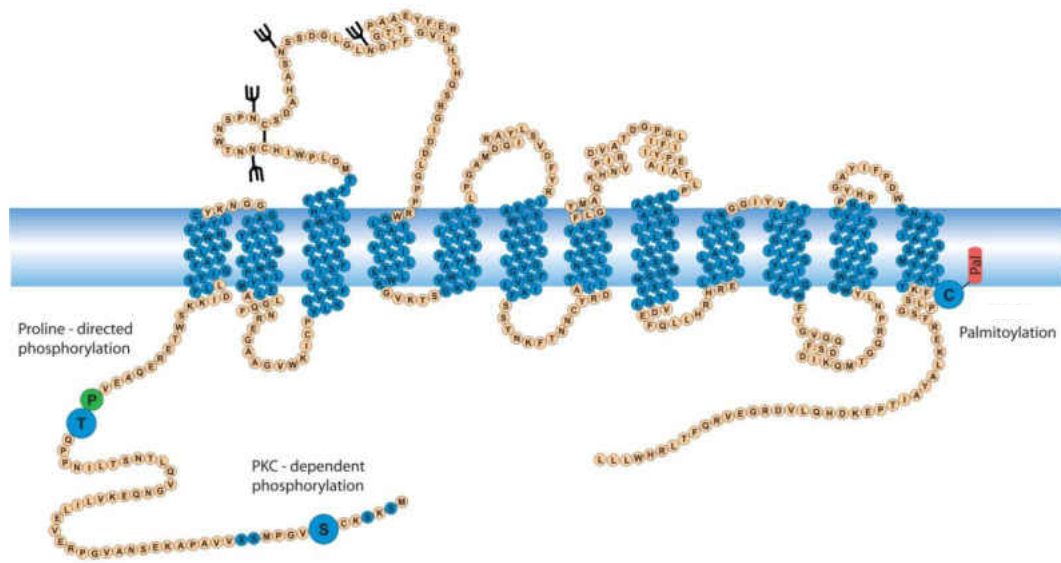


Image courtesy, Foster, J.D. and Vaughan, R.A., with permission.

Figure 7: Depiction of rDAT in its currently known phosphorylation and palmitoylation sites.

DAT is a 12 TMD helical structure with its N- and C-termini facing towards the cytosol. DAT is heavy glycosylated on its EL2. The rDAT structure depicts the known sites for phosphorylation (on the N-terminus) and palmitoylation (on the C-terminus).

phosphorylation by mass spectrometry and N-DAT in-vitro phosphorylation respectively. Phosphorylation on these residues is brought about by protein kinases such as protein kinase A (PKA), protein kinase C (PKC) and calcium/calmodulin-dependent protein kinase II (CaMKII), which play a role in mediating DA efflux [39-41, 48-50]. Apart from these Ser residues, the other site that has been validated by mass spectrometry to undergo phosphorylation on N-terminus is T53 (human equivalent being S53). This site is phosphorylated by extracellular signal regulated kinase (ERK), a proline directed kinase [38, 48, 51]. Not much is known about this site, but its proximity to TMD 1 and intracellular gate residue R60 suggests that phosphorylation at this site could play a role in regulating the binding and interaction of DAT with other associated proteins or Src homology 3 domain proteins thus affecting the opening and closing of intracellular gates and ion flow or efflux [48, 50, 52, 53].

A protein kinase C (PKC) activator, phorbol 12-myristate, 13-acetate (PMA) has been associated with down-regulation of DAT, reduction in the surface expression of DAT and its  $V_{max}$  [46, 54, 55]. While PKC- and CaMKII-mediated phosphorylation leads to down-regulation of DAT, clathrin and dynamin and/or lysosomal dependent endocytosis leading to dampening of DA uptake and AMPH-mediated DA efflux, ERK-mediated phosphorylation increases DA transport promoting DAT surface expression [46, 56-61].

The role of N-terminus in phosphorylation is confirmed by truncating the first 21 amino acid residues or deleting first 5 Ser residues on the N-terminus. This leads to reduction in PKC-mediated DAT phosphorylation, although it does not alter DAT localization, DA uptake or PKC-mediated internalization [40, 54, 56, 59, 62, 63].

DAT also undergoes S-palmitoylation, the reversible addition of a saturated fatty acid moiety (palmitate) via a thioester bond to C580 (human equivalent being C581) on the C-terminal rDAT, with additional sites still unidentified [36, 64]. Palmitoylation is known to control various functions of integral membrane proteins such as membrane binding, catalytic activity, trafficking, sub-cellular targeting, protein localization and turnover [47, 61, 65-72]. The main driving force in such a diverse role played by palmitoylation is the properties of the palmitate group, its hydrophobicity/membrane affinity and its preference for the cholesterol rich membrane rafts [71]. Loss or inhibition of palmitoylation strongly reduces transport  $V_{max}$ , opposes turnover, promotes transport capacity and PKC-stimulated down-regulation also affecting DAT degradation and lateral membrane mobility [36, 41, 56, 72-74].

Apart from the post-translational modifications that affect DAT function there also are many important amino acid residues that play a critical role in its function. Single nucleotide polymorphism (SNP) for these residues is seen to bring about DA efflux, affecting proper DAT function leading to various illnesses [8, 9, 41, 75-78].

The transport of DA across DAT occurs via the alternating access mechanism (Fig. 8) [3]. In this mechanism DAT undergoes a series of conformational changes from outward open to inward open so as to transport the substrate from the synapse, back into the pre-synaptic neuron. In this mechanism, there is the movement of two  $\text{Na}^+$  and one  $\text{Cl}^-$  ion along with DA from outside to inside of the neuron. DAT in a polarized state is in an outward open conformation, during which DA,  $\text{Na}^+$  and  $\text{Cl}^-$  ions move into the open conformation and take their places at the S1, Na1 and Cl binding sites respectively, with the bound ions having a major effect on substrate binding. Following the binding of DA at the binding pocket, DAT moves into an outward

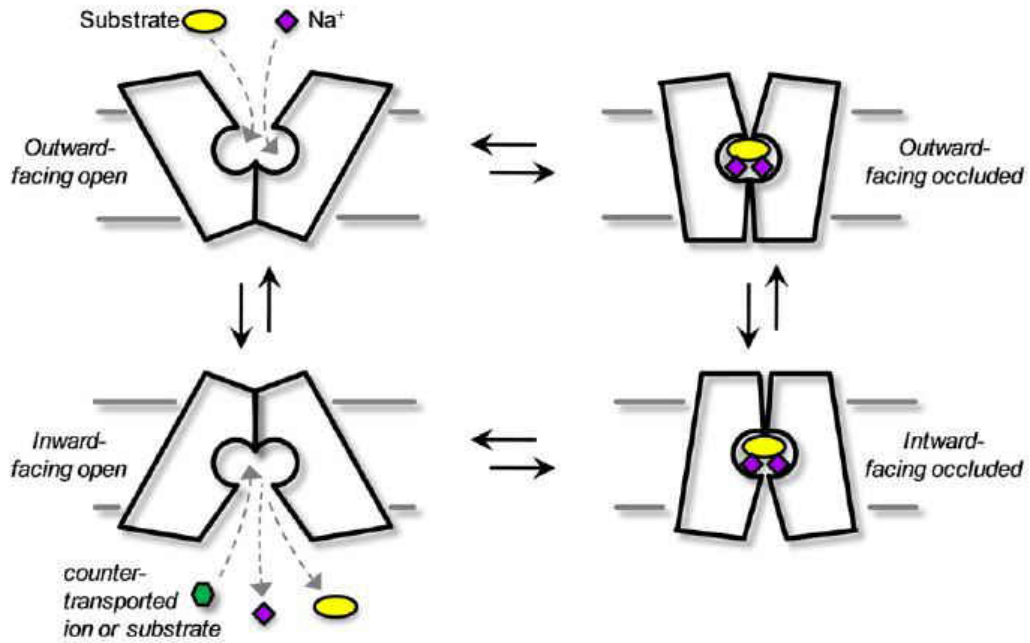


Image courtesy, Kristensen, A.S., et al., *SLC6 neurotransmitter transporters: structure, function, and regulation*. Pharmacological reviews, 2011. **63**(3): p. 585-640, with permission [3].

Figure 8: Alternating access mechanism for transportation of substrate.

A schematic representation of the conformational states in the alternating access mechanism for transporting substrate across SLC6 transporters. The outward facing conformation for the transporter allows the substrate and  $\text{Na}^+$  ions to bind at their respective binding sites. This binding triggers conformational changes within the transporter that makes it move into an outward facing occluded and then into an inward facing occluded conformation, where the extracellular and intracellular gates are closed. Ion interactions within the transporter leads to the opening of the intracellular gates and the transporter then shifts into the inward open conformation releasing the substrate and the ions into the cytosol.

facing occluded conformation, with  $\text{Cl}^-$  ions balancing the charge between the co-transported, DAT bound DA and  $\text{Na}^+$  ions. Since the presence of intracellular  $\text{Cl}^-$  ions positively regulates DAT turnover,  $\text{Cl}^-$  ions plays an important role in the conformational shift of DAT from outward occluded to inward occluded conformation. Once the S1, N1 and Cl sites are occupied, the second  $\text{Na}^+$  ion binds at the N2 binding site. This leads to the coupling between the  $\text{Cl}^-$  and  $\text{Na}^+$  ions, triggering DAT movement into an inward facing occluded conformation. This conformational change is brought about as a result of changes in the core substrate binding TMDs.

These conformational changes lead to the release of DA and  $\text{Na}^+$  ion from S1 and N1 binding sites respectively which leads to the weakening of the affinity of  $\text{Na}^+$  ion for the N2 binding site causing its release. The presence of this unbound  $\text{Na}^+$  ion causes DAT to move into the inward open conformation, causing the transport of DA along with the ions into the pre-synaptic neuron. Presence of physiologically high  $\text{Na}^+$  ion concentration on the extracellular side, forces DAT to move again into the outward open conformation [3, 79-85]. These conformational changes for DAT states are very well studied in LeuT and dDAT [30, 31, 86]. Studying homologue amino acid residues and computational modeling between these DAT structures and mammalian DAT provides a greater understanding of the functional importance of specific amino acid residues within the transporter. The alternating access mechanism for DA transport is assisted by the interaction between various different amino acid residues. The extracellular facing H193, D206, H375 and E396 residues helps in coordinating the  $\text{Zn}^{++}$  ion binding, which stabilizes DAT in the  $\text{Na}^+$  bound outward facing conformation. Along with these residues, D79 and Y335 play an important role in maintaining DA transport. Mutations at these residues affect DA binding at the S1 binding site, DA uptake capacity and conformational equilibrium of DAT [75, 76, 87].

Upon substrate binding, hDAT undergoes conformational changes, which leads to the formation of an extracellular gate. This gate is as a result of a salt bridge formed between R85 and D476 which are residues of TMD 1 and 8 respectively such that mutation at R85 causes complete loss of DAT function. The side chain of F320 also undergoes rotational isomerization so as to associate itself with Y156 forming an inner extracellular gate, a part of the occluded outward DAT structure. The closure of the extracellular gate is followed by the inward movement of TMD 1b and 6a segments. DAT undergoes further conformational changes making it move into an inward occluded structure, in which an intracellular gate is formed, as a result of a salt bridge between R60 and D436 which are residues located in the N-terminus close to cytoplasmic end of TMD 1 and at the cytoplasmic end of TMD 8 respectively. This salt bridge is stabilized by a cation- $\pi$  interaction between R60 and Y335 residues.

These gating residues are highly conserved in SLC6 neurotransmitter transporter and any mutation in these residues affects the conformational changes of the transporter [31, 34, 76, 88, 89]. Another important component that plays a pivoting role in maintaining DAT structure and function is the presence of cholesterol which helps in maintaining an outward facing conformation [30, 90].

#### DAT regulation and binding partners

DAT is regulated by post-translational modifications and its binding partners. DAT phosphorylation in-vitro is regulated by various different kinases such as PKA, PKC, CaMKII, ERK, mitogen-activated protein kinase (MAPK) and c-Jun N-terminal kinase (JNK) which influence sub-cellular localization and DAT transport [38, 48, 51, 91]. Phorbol ester-mediated PKC-stimulated DAT phosphorylation decreases DAT transport  $V_{max}$ , with long term PKC-stimulation driving DAT towards lysosomal

degradation reducing total DAT levels [46, 54, 56, 58, 61-63, 92]. PKC activated by PMA also increases DAT-mediated efflux, indicating either a direct role for DAT phosphorylation in efflux or attraction of interacting partners that facilitates efflux [93]. Truncation of N-terminal DAT leads to reduction in the PKC-stimulated phosphorylation without affecting DAT's ability to undergo internalization [59, 60]. Phosphorylation stabilizes the interaction of DAT and its binding partner  $\alpha$ -synuclein, which regulates DAT function and also causes DA efflux. While  $\alpha$ -synuclein interacts with DAT at its C-terminal residues 597-620, another binding partner, calcium/calmodulin-dependent protein kinase II alpha subunit (CaMKII $\alpha$ ) interacts at residues 598-620 regulating DAT function [41, 94]. In-vitro studies have shown CaMKII $\alpha$  regulating DAT phosphorylation at the N-terminus and also playing a role in amphetamine (AMPH)-mediated DA efflux. Inhibition of CaMKII $\alpha$  or mutation of the N-terminal phosphorylation residues attenuates AMPH-mediated DA efflux [95]. In contrast to the function of PKC, which causes reduction on DA uptake, ERK-activation leads to an increase in DA transport, indicating the bidirectional role of phosphorylation on DAT depending upon the kinases that acts on it and related signaling pathways [96-98]. Another important group of kinases are the MAPKs which are activated by both, PKC-dependent and independent mechanisms. D<sub>2</sub> DA receptor-stimulation leads to an increase in DA transport capacity and activation of the MAPK cascade by increasing intracellular Ca<sup>++</sup> ions and activating PKC. Inhibition of MAPK causes decrease in DA transport capacity and clathrin-dependent DAT redistribution from plasma membrane to cytosol [96, 99, 100].

An important 10 residue sequence on DAT C-terminus is the FREKLYAIA region which occupies residues 587-596. This sequence is highly conserved in other neurotransmitter transporters and is required for PKC regulated DAT internalization

and DAT trafficking. The neuronal GTPase Rin (Rit2) associates itself with FREKLYAIA and DAT/Rin interaction enhances the PKC-stimulated DAT endocytosis, with mutations in the amino acid residues 589 and 590 causing reduction in DAT endocytosis [56, 73, 74].

The DAT N-terminus also interacts with the soluble N-ethylmaleimide-sensitive factor attachment protein receptor (SNARE) protein, syntaxin 1A (syn 1A) and the receptor for activated C kinase (RACK1), both of which play a role in DAT trafficking regulated by PKC-activated phosphorylation. Syn 1A interacts with N-terminal residues 1-33 causing a reduction in DAT transport activity [41]. AMPH stimulates the interaction of DAT and syn 1A causing localization of syn 1A closer to DAT on the plasma membrane. This promotes DA efflux and localization of DAT into the membrane raft microdomains [101].

The membrane microdomain marker, Flotillin (flot1) is known to take part in clathrin-mediated PKC-stimulated DAT endocytosis and modulate the association of DAT with cholesterol rich membrane raft microdomains causing a decrease in membrane mobility. Disruption of flot1 causes alterations in DAT structure, function and impairment of PKC- and CaMKII-dependent DAT regulation. Flot1 also regulates AMPH-mediated DA efflux such that its absence reduces the effect of AMPH [92, 102-104].

DA D<sub>2</sub> receptors regulate DAT by direct interaction. This interaction is between residues 1-15 on the N-terminus of DAT and the intracellular loop 3 (IL3) of D<sub>2</sub> receptors. These interactions help recruit DAT to the plasma membrane and also increase DA uptake. The disruption of these interactions cause a decrease in DAT uptake capacity and locomotor activities (Fig. 9) [105].



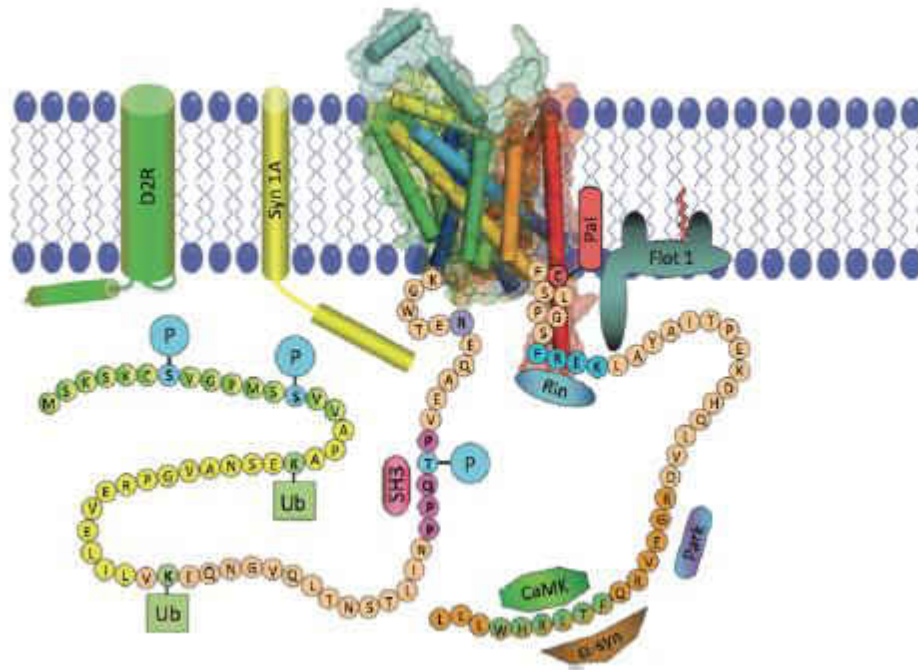


Image courtesy, Vaughan, R.A. and Foster, J.D., *Mechanisms of dopamine transporter regulation in normal and disease states*. Trends Pharmacol Sci, 2013. **34**(9): p. 489-96, with permission [41].

Figure 9: DAT and its binding partners.

DAT is a 12 TMD helical protein with its N- and C-termini facing towards the cytosol. These termini undergo post-translational modifications, such as phosphorylation and palmitoylation, and also interact with a large number of binding partners. These modifications and binding partners together play a regulatory role towards proper DAT function.

### Reciprocal roles of phosphorylation and palmitoylation

DAT has shown reciprocal roles for its post-translational modifications, phosphorylation and palmitoylation. Mutational and pharmacological studies demonstrate that these modifications are reciprocally regulated such that a pool of DAT upon being phosphorylated shows decrease palmitoylation levels and visa versa. While phosphorylation dictates DA transport capacity, DA efflux and DAT internalization, palmitoylation regulates DAT degradation and turnover. Although the actual mechanism for the reciprocal regulation of DAT in terms of phosphorylation and palmitoylation is not fully understood, it has been well studied in proteins such as  $\beta_2$ -adrenergic receptors and  $\alpha$ -amino-3-hydroxy-5-methyl-4-isoxazolepropionic acid (AMPA) receptors, where steric hindrance between these modifications oppose each other [106-110]. With the three dimensional structure for mammalian DAT not known, one of the explanations for this reciprocal phosphorylation and palmitoylation status in DAT could be their distinct occurrences on the membrane microdomain with phosphorylation causing increased DAT distribution in the membrane raft microdomain and palmitoylation driving the membrane raft partitioning in proteins [30, 56, 110, 111]. Also palmitoylation could affect the rest of the downstream C-terminus, which acts as a latch locking the transporter in the outward facing conformation, affecting the overall orientation of the active sites of DAT. Thus palmitoylation driven alteration could impact the interaction between the TMDs during DA transport, also affect DAT phosphorylation [10, 88, 110]. With phosphorylation and palmitoylation affecting various DAT properties such as membrane raft partitioning, lateral membrane mobility, surface expression and DA efflux, an impact on these modifications may cause dopaminergic imbalances that are associated with diseases such as ADHD, AD, PD, BPD and ASD [9, 110, 112-114].

## Psychostimulant drugs

DAT is a primary target of many psychostimulant drugs such as methamphetamine (METH), AMPH and cocaine (COC). These drugs target DAT interfering with its function and expression disrupting dopaminergic homeostasis.

COC is a NSS uptake blocker which competes with DA to bind at the substrate binding site. Once bound COC locks DAT in an outward facing conformation, restricting its ability to transport DA. This leads to accumulation of DA in the synapse causing euphoria, increased locomotion, hyperactivity, all caused as a result of activation of brain circuitry leading to stimulation of rewarding properties [115-119].

AMPH is a substrate that is involved in providing reward and reinforcing properties. At high concentrations, AMPH is a substrate competing with DA to be transported into the pre-synaptic neuron, where it is able to move into the synaptic vesicles via vesicular monoamine transporter (VMAT). Within the vesicles, AMPH acts as a weak base disrupting the proton gradient, needed for neurotransmitter packaging. This causes release of DA from the vesicles into the cytoplasm eventually to be effluxed, affecting transporter  $V_{max}$  and endocytosis. AMPH is also able to inhibit MAO or COMT which mediate DA oxidation and inactivation (Fig. 10) [3, 26, 40, 120-130]. Thus AMPH is able to disrupt DAT function and cause euphoria [129].

AMPH activates PKC, ERK and CaMKII-stimulated DAT phosphorylation, which regulates DAT-mediated DA efflux with inhibition of these kinases significantly reducing the DA efflux [40, 127, 131-135]. The role of phosphorylation in AMPH-mediated DA efflux is also evident by the fact that truncation of first 21 residues of the N-terminus or substituting the first 5 N-terminal Ser residues to Ala, leads to a

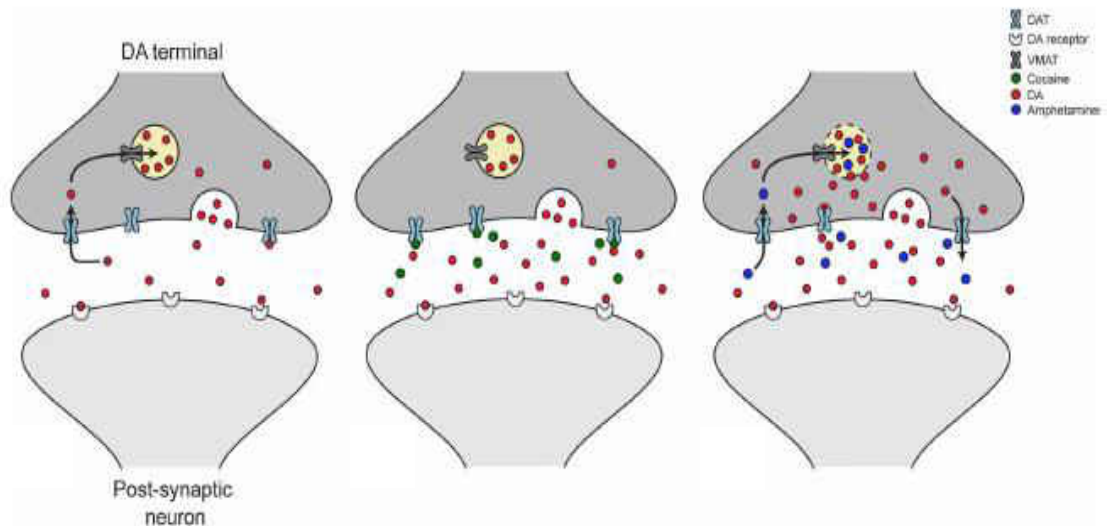


Image courtesy, Espana, R.A. and Jones, S.R., *Presynaptic dopamine modulation by stimulant self-administration*. Front Biosci (Schol Ed), 2013. **5**: p. 261-76, with permission [119].

Figure 10: Action of COC and AMPH on DAT.

After the transmission of neurological signal via the post-synaptic neurons, DA is taken-up by DAT into the pre-synaptic neurons to be repackaged into synaptic vesicles. COC competes with DA to bind at the substrate binding site of DAT. Once bound, COC locks DAT in an outward facing conformation, preventing the uptake of DA. This leads to an increase in the amounts of DA in the synapse, which binds to the DA receptors on the post-synaptic neurons, triggering excessive downstream signaling. AMPH also competes with DA to bind at the substrate binding site, and is able to be transported via DAT into the pre-synaptic neurons. Once in the pre-synaptic neuron, AMPH disrupts the vesicular packaging of DA, leading to an increase in cytosolic levels of DA. This DA is effluxed via DAT into the synapse increasing the synaptic levels of DA.

decrease in AMPH-stimulated DA efflux, without affecting DA uptake [136]. While PKC brings about phosphorylation by directly binding at the N-terminus, CaMKII binds at the C-terminus interacting with  $\alpha$ -synuclein presumably bringing about N-terminal phosphorylation. Upon phosphorylation, syn 1A interacts with N-terminal DAT stimulating AMPH-mediated DA efflux by shifting DAT towards a more efflux willing state (Fig. 11) [50, 137-140].

With the exact mechanism for AMPH-mediated DAT phosphorylation not fully clear, there could be many possibilities driving this phenomenon. AMPH could regulate the neuronal circuits or the neurotransmitter levels that are linked to signaling, causing a rise in phosphorylation. Also AMPH could affect the PKC sub-cellular localization, causing increase in phosphorylation within these regions. The uptake of AMPH into the pre-synaptic neuron causes an increase in the intracellular levels of  $\text{Ca}^{++}$ ,  $\text{H}^+$  or  $\text{Na}^+$  ions which affects kinases and phosphatases, causing a rise in phosphorylation. Evidence suggests that there exists a rapid DA efflux process that occurs non-traditionally, through a channel like mode of DAT. This mode is independent of the ion mediated DA efflux and is facilitated by  $\text{Zn}^{++}$  ions (Fig. 12) [140-142].

The inhibition of AKT upon the increase of AMPH-mediated CaMKII activity suggests the involvement of insulin signaling in DAT trafficking and DA homeostasis. This involvement is confirmed as the inhibition of insulin activated receptors cause a reduction in DA clearance due to the loss of DAT surface expression [140, 143, 144]. Also the inhibition of components of the insulin signaling pathway such as Akt and phosphatidylinositol 3-kinase (PI3K) cause a decrease in DA clearance and DAT surface expression with inhibition of PI3K causing reduction in AMPH-stimulated DA efflux [140, 145, 146].

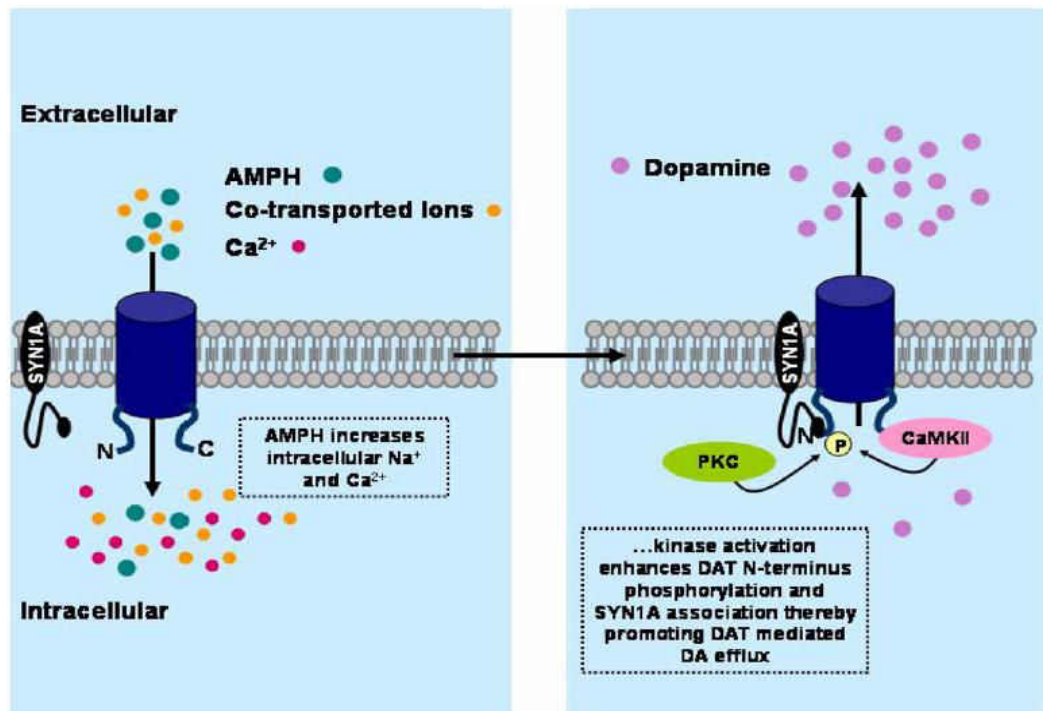


Image courtesy, Robertson, S.D., Matthies, H.J. and Galli, A., *A closer look at amphetamine-induced reverse transport and trafficking of the dopamine and norepinephrine transporters*. Mol Neurobiol, 2009. **39**(2): p. 73-80, with permission [140].

Figure 11: AMPH induced DAT efflux regulated by second messengers.

Transport of extracellular AMPH into the pre-synaptic neurons via DAT leads to increase in intracellular Ca<sup>++</sup> and Na<sup>+</sup> ions. This result in activation of kinases such as PKC and CAMKII that enhance DAT phosphorylation by interacting at the N- and C-termini of DAT respectively promoting DAT mediated DA efflux.

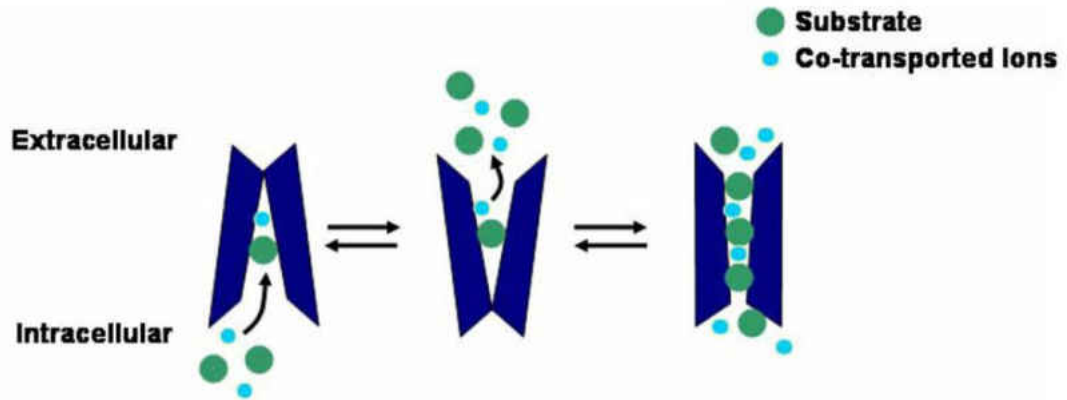


Image courtesy, Robertson, S.D., Matthies, H.J. and Galli, A., *A closer look at amphetamine-induced reverse transport and trafficking of the dopamine and norepinephrine transporters*. Mol Neurobiol, 2009. **39**(2): p. 73-80, with permission [140].

Figure 12: Schematic representation of transporter mediated monoamine efflux.

DAT present in the inward facing conformation is able to mediate efflux by binding to substrate and co-transporter ions. Presence of AMPH and intracellular  $\text{Na}^+$  ions causes DAT to acquire inward facing conformation where it binds to DA causing increase in efflux. This alternating access mechanism driven efflux is a slow exchange mechanism of efflux. AMPH is also able to induce a rapid efflux through a channel like mode of DAT which is facilitated by  $\text{Zn}^{++}$  ions upon AMPH-stimulation.

## DAT and diseases

Abnormalities or dysfunctions in DA homeostasis cause dopaminergic imbalances which are associated with neurological and neuropsychiatric diseases [147, 148]. Various DAT abnormalities occur as a result of nucleotide polymorphism seen in its coding and/or non-coding gene sequences [149].

### PD

PD is a progressive disorder characterized with loss of dopaminergic neurons in the SNc region of the brain leading to low levels of DA in the brain. There are two familial forms of PD, that are caused either by mutation or by over-expression of  $\alpha$ -synuclein and Parkin, both of which affect the regulatory aspect of DAT [41].  $\alpha$ -synuclein is a DAT interacting scaffolding protein whose actual role in PD is poorly understood. It interacts with C-terminal DAT regulating the recruitment of DAT on the plasma membrane [150, 151]. It also plays a role in SNc degradation causing DA-induced apoptosis [151]. Parkin, an E3 ubiquitin ligase, regulates ubiquitylation and degradation of DAT. Mutation in this protein leads to prevention of misfolded or unwanted DAT from being degraded. Thus the accumulation of the misfolded DAT leads to its oligomerization with properly folded DAT preventing it from travelling to the plasma membrane. This leads to decrease in DA uptake [41, 65, 152, 153].

### Angelman syndrome

Angelman syndrome is a neurological disorder which occurs as a result of a defective maternal inherited allele of the E3 ubiquitin ligase that leads to the reduction of CaMKII activity. This is brought about by increased inhibitory auto-phosphorylation [10, 41]. A mouse model for Angelman syndrome showed the accumulation of auto-



inhibited  $\alpha$ CamKII in the brain causing characteristics such as suppressed AMPH induced efflux. The mouse model also showed a decrease in synaptic DA levels, which was similar to PD like phenotype [154, 155].

## ADHD

ADHD is a neurological disorder having symptoms including hyperactivity, attention difficulty, impulsiveness and motor impairment [156]. ADHD affects 3-6% of children worldwide with symptoms continuing in adulthood in 5-6% of these cases, with a worldwide prevalence rate of ADHD being 5-7%. ADHD also has an estimated heritability rate of 0.7-0.9% with a large genetic variation among the individuals suffering from ADHD [157-160]. It has been hypothesized that ADHD characteristics arise as a result of impaired dopaminergic transmission and excess DA uptake [26, 130, 161]. Various SNPs in hDAT, V55A, R237E, I312F, V382A, R421N, A559V, E602G and R615C, have been identified in patients diagnosed with ADHD and/or bipolar disorder as well as few non diagnosed individuals [7, 18, 41, 114, 162-165]. These SNPs are located at different positions on DAT structure and play an important role in the proper expression and function of DAT.

V55A and V382A, located in the N-terminal and extracellular loop 4 (EL4) respectively, show a reduced DAT surface expression and a decreased DA transport capacity with V382A also destabilizing the extracellular gate [18, 166]. R421N has a compromised N2 binding site along with a large cation leak and DA efflux while I312F has a reduced DA transport capacity [114]. R615C, located at the  $\alpha$ CaMKII binding site on the C-terminus, shows increased phosphorylation and a greater DAT membrane raft microdomain localization. It also displays a constitutive level of DAT endocytosis and recycling, with a greater lateral mobility insensitive to AMPH. This

mutant is insensitivity to PKC-stimulated DAT trafficking and maintains AMPH-mediated DA efflux, with a decrease in DAT surface expression, DA transport  $V_{\max}$ . R615 is phosphorylated and forms a phosphorylation site motif with T613 [9, 41, 113, 167, 168]. Not much is known about R237E and E602G.

A559V is located on the extracellular end of TMD 12, and was first identified in two male siblings with ADHD. This mutant displays anomalous DA efflux (ADE) (reverse transport) with individuals showing signs of motor dysfunction. A559V displays reduction in ADE upon AMPH-stimulation with resistance to AMPH-mediated DAT cell surface distribution and normal levels of DA uptake. Recently, A559V was found in patients with autism spectrum disorder (ASD) and this mutant displayed impaired AMPH transport to the intracellular side of DAT and also failed to incur cell surface loss of DAT. In case of ASD patients, inhibition of PKC restored the AMPH-induced DAT trafficking and intracellular AMPH accumulation.

The diminished ability of A559V to transport AMPH via DAT into the pre-synaptic neuron could be as a result of the bulkier Val substitution. Also, since A559V has elevated D2 receptor signaling, application of D2 receptor blocker inhibits the ADE, thus indicating that increased signaling could play a role in the elevated PKC activity. Thus, N-terminal phosphorylation which promotes D2 receptor signaling through PKC could bring about DA dysfunction in ADHD and ASD individuals [7-9, 26, 30, 95, 114, 136, 164, 169-171].

Another DAT mutant associated with ASD is T356M. This mutant displays AMPH insensitive ADE, as seen in A559V hDAT, along with reduced DA uptake capacity despite having a normal surface expression [26, 77, 113].

### DAT association with lipid rafts and lateral membrane mobility

DAT is associated with cholesterol-rich membrane raft microdomains [56, 172, 173]. Membrane cholesterol is important for proper DAT function and it favors an outward facing conformation for DAT [90]. The depletion of cholesterol disrupts the membrane rafts microdomains which abolishes PKC-stimulated DAT down regulation, decreases DA transport activity and DAT surface expression [173]. Techniques like Fluorescence Recovery After Photobleaching (FRAP) and Fluorescence Correlation Spectroscopy (FCS) have shown that cholesterol affects lateral membrane mobility, such that disruption of cholesterol or cytoskeleton increases the mobility [172].

Membrane rafts are diverse, dynamic membrane microdomains that are rich in cholesterol and glycosphingolipids. Membrane rafts are associated with various cellular processes such as signal transduction, protein sorting and membrane trafficking. DAT is distributed between membrane raft and non-raft regions, with membrane rafts playing a role in compartmentalization of DAT affecting dopaminergic neuronal activity [41, 56, 174-176]. Evidence suggests DAT localized in membrane rafts microdomain have a lower DA binding potency and a reduced rate of DA clearance while DAT localized in membrane non-rafts microdomain have a greater DA binding potency and a greater DA clearance. Membrane rafts and non-rafts microdomains behave differently in their phosphorylation properties. PKC-mediated phosphorylated DAT is seen to be enriched in membrane rafts regions indicating that membrane rafts may serve as a platform for PKC-stimulated DA efflux. DAT internalization is seen to occur in membrane non-raft microdomain. Inappropriate localization of DAT within raft and non-raft microdomains adversely affects its

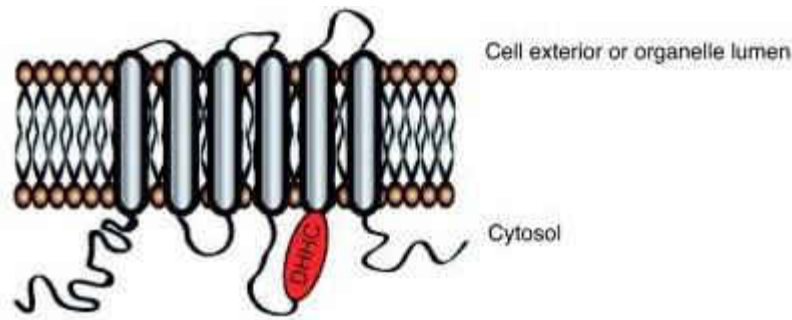
function [56, 136, 140].

The interaction of flot1 with DAT affects its lateral membrane mobility. Flot1 is important for proper membrane raft distribution and its presence reduces DAT lateral membrane mobility [92, 102]. Presence of flot1 causes retention of DAT on the cell surface mediating DA efflux [113, 177]. DAT is associated with cytoskeletal and lipid elements, which reduces its lateral membrane mobility. Disruption of these elements increase DAT mobility. This lateral membrane mobility is also affected by membrane raft microdomains, the disruption of which causes a decrease in DAT function,  $V_{\max}$  and  $K_m$  for DA [172].

#### DHHC palmitoyl transferases enzymes

S-palmitoylation is regulated by a large family of Asp-His-His-Cys (DHHC) enzymes which are palmitoyl acyltransferases (PAT). These enzymes palmitoylate large groups of proteins, among which DHHC2, 3, 7 and 15 are the most active. These DHHC enzymes are proteins with Cys rich domains (CRD) and a consensus signaling sequence of Asp-His-His-Cys residues, which are highly conserved from yeast to mammals (Fig.13) [178, 179]. Mammalian cells have a total of 23 DHHC enzymes, all of them containing 4-6 TMDs [179-182]. Most of these DHHC enzymes are associated with the golgi complex or endoplasmic reticulum (ER) but DHHC2 is localized within the dendritic vesicles of neurons and DHHC5, 20 and 21 are localized on the plasma membrane. DHHC2 is seen to cycle between the plasma membrane and endosomes with the C-terminus of DHHC2 playing a role in its membrane trafficking [72, 182-186]. Mutations in DHHC enzymes are associated with large number neurological disorders. Mutation of DHHC3 is associated with behavioral abnormalities. Microdeletions and SNPs within the DHHC8 gene is associated with

increased risk of schizophrenia. Mutations in DHHC15 and DHHC9 are associated with X-linked mental retardation [181, 187-190].



Consensus	1	10	20	30	40	50	51
	LKYCPXCQLIKPPRAHHCSSVCDRCVXXFDHHC	PWVNN	CVGER	NYRY	ELL	ELL	
DHHC1	DLHONLCDVDVSARSKHCSACNKCVCVGF	DHHC	KWLNN	CVGER	NYRL	ELL	FLHSV
DHHC2	IRYCDRCQLIKPDRCHHCSSVCDKCILKMD	DHHC	PWVNN	CVGFS	NYKF	ELL	ELL
DHHC3	VYKCPKCCSIKEDRAHHCSSVCKRCIRKMD	DHHC	PWVNN	CVGEN	NQKY	ELL	ELL
DHHC4	NSROPTCDLRKPARSKHCRLLCDRCVHRF	DHHC	VWVNN	CVGAW	NTRY	ELL	ELL
DHHC5	MKWCA TCRFYRPPRCSHCSVCDNCEVEF	DHHC	PWVNN	CVIGR	RRNYR	ELL	ELL
DHHC6	LQYCKVCCQAYKAPRSHHCRCNRCVMKMD	DHHC	PWINN	CVGHQ	NHAS	ELL	ELL
DHHC7	IYKCPKCCSIKEDRAHHCSSVCKRCIRKMD	DHHC	PWVNN	CVGEC	NQR	ELL	ELL
DHHC8	MKWCA TCHFYRPPRCSHCSVCDNCEVEF	DHHC	PWVNN	CVIGR	RRNYR	ELL	ELL
DHHC9	LKYCYTCKIFRPPRASHCSICDNCVERF	DHHC	PWVNN	CVGKR	NYR	ELL	ELL
DHHC11	NQYCHLCEVTASKKAKHCSACNKCVS	GF	DHHC	KWLNN	CVGRR	NYW	ELL
DHHC12	LRRGRHCLVLPRLRARHCRDCRRCVRRY	DHHC	PWMEN	CVGER	NHPL	ELL	ELL
DHHC13	RTFOTSCLIRKPLRSLHCHVCNSCVARF	DHHC	FDQHC	FWTGR	ICIGF	GNHH	YIF
DHHC14	LKYCF TCKIFRPPRASHCSICDNCVEQF	DHHC	PWVGN	CVGKR	NYR	ELL	ELL
DHHC15	VRFCDRCHLIKEDRCHHCSSVCAACV	LKMDHHC	PWVNN	CVIGF	SNYK	ELL	ELL
DHHC16	VSICKKCIYPKPARTHHCSSICNRCV	LKMDHHC	PWLNN	CVGHY	NHRY	ELL	ELL
DHHC17	SIFOSTCLIRKPVRSKHCGVGNRCIAK	F	DHHC	PWVGN	CVGAG	NHRY	ELL
DHHC18	LKYCF TCKMFRPPRTSHCSVCDNCEVEF	DHHC	PWVGN	CVGRR	NYR	ELL	ELL
DHHC19	LEWCPKCLFHRPPRTYHCPWCNICVED	F	DHHC	KWVNN	CVIGR	NFR	ELL
DHHC20	IRYCEK CQLIKEDRAHHCSSACDRCVL	KMDHHC	PWVNN	CVGFT	NYK	ELL	ELL
DHHC21	WELONKCNLMRPKRSHHCSSRCGHCV	RRMDHHC	PWINN	CVGED	NHWL	ELL	ELL
DHHC22	MSQRPPQCP PPS THFCRVCSRVTLR	H	DHHC	FFTGN	CVIGSR	NMR	ELL
DHHC23	EDWCAK CQLVREARAWHCRICGICV	RRMDHHC	PWINN	CVGES	NHQA	ELL	ELL
DHHC24	WAYCYOCCSQVPPRSGHCSACRVCIL	RRDHHC	RLLGC	CVGFH	NYR	ELL	ELL
DHHC25	VSICYTDCHSAIPRTACHCTVCCQR	IRKNDHHC	PWINN	CVIGED	NQKY	ELL	ELL

Image courtesy, Greaves, J. and Chamberlain, L.H., *DHHC palmitoyl transferases: substrate interactions and (patho)physiology*. Trends Biochem Sci, 2011. **36**(5): p. 245-53, with permission [190].

Figure 13: Membrane topology of DHHC proteins and its aligned sequences.

The DHHC proteins have 4-6 TMDs with its N- and C-termini facing toward the cytosol. The sequence alignment and consensus of 24 different mouse DHHC proteins, with amino acids residues 29-32 having a consensus sequence except for DHHC13 that has Gln at residue 30.

## CHAPTER II

### ADHD ASSOCIATED DOPAMINE TRANSPORTER MUTANT, A559V HAS ALTERED, RECIPROCAL PHOSPHORYLATION AND PALMITOYLATION STATUS

#### ABSTRACT

The dopaminergic system plays a role in controlling motor, cognitive and behavioral activities with the neurotransmitter dopamine (DA) modulating brain circuits involving mood, reward, sleep patterns and locomotion and the dopamine transporter (DAT; SLC6) maintaining DA homeostasis. DAT is a target for psychostimulant substrates such as amphetamine (AMPH) and psychostimulant uptake blockers such as cocaine (COC), both disrupting DAT function, impacting DA uptake with AMPH causing DA efflux. An attention-deficit hyperactivity disorder (ADHD) associated single nucleotide polymorphism (SNP) in human DAT (hDAT), A559V hDAT, displays anomalous DA efflux (ADE), with DA uptake, total and surface expression levels being similar to wildtype (WT). Here we investigate the phosphorylation and palmitoylation status for A559V and its rat homologue, A558V rat DAT (rDAT) using metabolic labeling and acyl-biotinyl exchange (ABE) respectively. We demonstrate that A559V and A558V display AMPH independent elevated phosphorylation, which in WT causes DA efflux and N-terminal phosphorylation, and decreased palmitoylation respectively. We also demonstrated that A558V rDAT displayed AMPH independent increased T53 phosphorylation. This increased phosphorylation may contribute to ADE seen for this polymorphism. We also showed C581 to be a palmitoylation site in hDAT and that the palmitoylation deficient C581A hDAT mutant displays enhanced basal and PMA stimulated phosphorylation consistent with reciprocal regulation of these modification as recently reported.

Palmitoylation studies on phosphorylation deficient mutants, T53A rDAT, S7A hDAT and S53A hDAT (human homologue for T53A rDAT) displayed increased palmitoylation, providing further evidence of the reciprocal nature of these post-translational modifications.

For A559V hDAT, we believe that the bulkier Val substitution in place of Ala at residue 559 may mechanistically hinder palmitoylation at C581, which could be the driving force for reciprocal N-terminal phosphorylation. This increased phosphorylation is associated with DA efflux as seen by AMPH-stimulation or by this polymorphism (A559V). T53A rDAT, S7A hDAT and S53A hDAT must be harboring similarly targeted phenomenon to bring about the reciprocal post-translational modifications.



## INTRODUCTION

The Dopamine transporter (DAT) is a 12 transmembrane spanning domain (TMD) helical structure belonging to the solute carrier 6 (SLC6) gene family which plays a critical role in maintaining and coordinating dopamine (DA) mediated signaling in the central nervous system (CNS) [2-6, 9, 11, 12, 14, 15].

Present on pre-synaptic neurons, DAT maintains the dynamics of DA neurotransmission by actively transporting extracellular DA from the synapses into the pre-synaptic neurons. This transport is highly regulated by many signaling pathways and post-translational modifications. DAT regulated DA homeostasis, prevents over stimulation of the post-synaptic receptors and also helps recycle DA for future neurotransmission [3, 110, 191]. Several neurological diseases such as schizophrenia, bipolar disorder (BPD), Parkinson's disease (PD), attention-deficit hyperactivity disorder (ADHD), autism spectrum disorder (ASD) and mood disorders such as depression, anxiety and obsessive compulsive disorder (OCD) are associated with abnormal DA homeostasis and/or polymorphisms in DAT, although the role of DAT dysfunction in these diseases is not clearly understood [6-10, 17-21, 26, 41, 112, 192].

DAT is a target for various addictive and therapeutic drugs that either act as uptake blockers, such as cocaine (COC), or act as substrates, such as amphetamine (AMPH), which stimulates DA efflux (reverse transport). In either of these cases there is an accumulation of DA in the synaptic space [191]. AMPH disrupts DAT function by affecting DA uptake, DAT surface expression and endocytosis. AMPH upon binding

at the substrate binding site is transported into the pre-synaptic neuron. Here it moves into the synaptic vesicles via vesicular monoamine transporter (VMAT). Being a weak base, accumulation of AMPH disrupts the proton gradient causing DA release from the synaptic vesicle which is then effluxed [3, 26, 40, 120-130]. This AMPH triggered DA efflux is driven by N-terminal DAT phosphorylation stimulated by protein kinases and proline directed kinases [57, 110].

DAT undergoes phosphorylation and palmitoylation, which play a regulatory role in DAT function. In-vitro studies have identified DAT to be phosphorylated on the N-terminus at residues S4, 7, 13 and T53 for rat DAT (rDAT) and S7, 13 for human DAT (hDAT) with phosphorylation causing DA efflux, down-regulation of DAT, reduction in DAT surface expression and  $V_{max}$  [9, 39-41, 48-54, 56, 62, 63, 91]. DAT is S-palmitoylated, a reversible addition of a saturated fatty acid moiety (palmitate) via a thioester bond, on its C-terminus at C580 in rDAT, with one or more palmitoylation sites currently unknown [36, 64]. Palmitoylation affects DAT transport kinetics, turnover, degradation and protein kinase-stimulated down regulation [36, 72]. DAT is reciprocally regulated for these two post-translational modifications [110].

A large number of DAT dysfunction occurs as a result of single nucleotide polymorphism (SNP), seen in its coding as well as non-coding gene sequences. Many of which are identified in patients diagnosed with neurological disorders. SNPs identified in hDAT are V55A, R237E, V382A, A559V, R615C, I312F and R421N [7, 18, 41, 114, 162-165]. The A559V hDAT mutant has been recently reported in several independent cases as well as individuals diagnosed with ADHD, ASD or BPD [9, 162, 164, 169]. Studies have shown that although A559V hDAT shows DA uptake, total and surface DAT expression similar to wildtype (WT), it displays anomalous DA

efflux (ADE). This mutant also showed resistance to AMPH-stimulated cell surface redistribution and a reduction in DA efflux [8, 9, 18, 193]. In patients suffering from ASD, A559V hDAT mutant displayed impaired AMPH transport via DAT. This mutant failed to incur cell surface loss of DAT and inhibition of PKC-mediated phosphorylation [169].

Since A559V hDAT displays ADE, a phenomenon associated with AMPH-mediated phosphorylation in WT, we investigated the phosphorylation status of this mutant along with its rat homologue, A558V rDAT, including T53, a proline directed phosphorylation site, specific for rDAT. With recent findings that DAT is reciprocally regulated for these post-translational modifications, we examine the palmitoylation status for A559V hDAT and A558V rDAT. We also investigate phosphorylation deficient mutants, T53A rDAT, S7A rDAT and S53A rDAT for palmitoylation levels in order to study their response to loss of specific phosphorylation sites. With C580 identified as a palmitoylation site in rDAT, we also investigate C581 (human equivalent being C580) for its palmitoylation status. Here we present insights on the increased phosphorylation status for A559V, which is associated with ADE, and its reciprocal nature in palmitoylation, along with site specific phosphorylation mutants in hDAT.

## EXPERIMENTAL METHODS

### Cell culture and site directed mutagenesis

Lewis lung carcinoma-porcine kidney (LLC-PK<sub>1</sub>) cells were transfected and selected to stably express WT DAT: hDAT and rDAT; mutant DAT: S7A hDAT, S53A hDAT, A559V hDAT, C581A hDAT, A558V rDAT and previously characterized T53A rDAT and C580A rDAT [36, 38, 49]. The codon substitutions were generated using the Stratagene QuikChange® Kit, with WT, hDAT or rDAT, pcDNA 3.0 plasmids as the template. Mutations were verified by sequencing (Eurofins MWG). LLC-PK<sub>1</sub> cells were grown in 12-well culture plates and were transfected with 1.4 µg plasmid/well and XtremeGene transfection reagent. Transformants were selected 24-48 hours later by adding 800 µg/mL geneticin (G418 sulfate) to the culture medium. Transfected LLC-PK<sub>1</sub> cells were maintained in  $\alpha$ -minimum essential medium (AMEM) supplemented with 2 mM L-glutamine, 5% fetal bovine serum (FBS), 200 µg/mL G418 sulfate and 1X penicillin/streptomycin. Cells were grown in an incubation chamber gassed with 5% CO<sub>2</sub> at 37°C. DAT expression level in transfected cells was verified by sodium dodecyl sulfate-polyacrylamide gel electrophoresis (SDS-PAGE) and immunoblotting of the cellular lysates against DAT specific antibodies.

### Acyl-biotinyl exchange (ABE)

Measurement of DAT palmitoylation was performed as described previously [36, 194]. Cell membranes [ $\sim$ 100 µg protein] pellet expressing WT or mutant DAT were solubilized in 200 µL lysis buffer (50 mM HEPES, pH 7.0, 2% SDS, 1 mM

ethylenediaminetetraacetic acid (EDTA)) containing protease inhibitors and 20 mM methyl methanethiosulfonate (MMTS) with end-over-end mixing for 1 hour at room temperature (RT). The excess MMTS was removed by 3 sequential 1 mL acetone precipitations followed by vortexing and centrifugation at 16,000 X g for 10 minutes at RT. Pelleted protein was solubilized in lysis buffer containing MMTS and protease inhibitor and incubated overnight at RT with end-over-end mixing.

The next day, following the removal of excess MMTS by 3 sequential acetone 1 mL precipitations, the precipitated protein pellet was re-suspended in 300  $\mu$ L 4SB buffer (4% SDS, 50 mM tris-HCl, 5 mM EDTA, pH 7.4). The solubilized pellet was divided into two equal portions and one was treated with 50 mM tris-HCl (pH 7.4) while the other was treated with 0.7 M hydroxylamine (NH<sub>2</sub>OH) (pH 7.4) with end-over-end mixing for 2 hours at RT. Excess hydroxylamine was removed by 3 sequential 1 mL acetone precipitations and the precipitated protein pellet was re-suspended in 240  $\mu$ L 4SB buffer and biotinylated by adding 900  $\mu$ L of 50 mM tris-HCl (pH 7.4) containing 0.4 mM sulfhydryl-reactive *N*-(6-(biotinamido)hexyl)-3'-(2'-pyridyldithio)-propionamide (HPDP-biotin) with end-over-end mixing for 1 hour at RT. Following the removal of the unreacted HPDP-biotin by 3 sequential acetone 1 mL precipitations, the final protein pellet was solubilized in 150  $\mu$ L lysis buffer. 10  $\mu$ L aliquots of ABE lysates were immunoblotted for DAT expression levels. ABE lysates were adjusted to contain equal amounts of total DAT protein and 0.1% SDS with lysis buffer and 50 mM tris-HCl (pH 7.4) respectively. Biotinylated proteins were extracted by incubating the ABE lysates with 25  $\mu$ L neutrAvidin resin with end-over-end mixing overnight at 4°C. The next day, the resin was washed thrice with 800  $\mu$ L RadioImmunoPrecipitation Assay (RIPA) buffer (1% triton X-100, 1% sodium deoxycholate, 1% SDS, 125 mM sodium phosphate, 150 mM sodium chloride, 2 mM

EDTA, 50 mM sodium fluoride) and palmitoylated proteins were eluted with 32  $\mu$ L 2X laemmli sample buffer containing 5% 2-mercaptoethanol. Following an incubation of elute for 20 minutes at RT, they were subjected to SDS-PAGE and immunoblotting for DAT using DAT specific antibody against C-terminus of hDAT or N-terminus of rDAT. In all experiments the level of signal intensity from Tris-HCl controls was less than 5% of  $\text{NH}_2\text{OH}$  treated samples. Experiments were independently performed three or more times and results are reported as mean  $\pm$  standard error. Statistical analyses were done by unpaired Student's t-test using graphpad prism software.

#### Cell membrane preparation

Cells expressing WT or mutant DAT were grown in 150 mm culture plates until ~80% confluent. After a quick wash with ice cold buffer B (0.25 M sucrose, 10 mM triethanolamine, 10 mM acetic acid, pH 7.8), cells were scraped using 1 mL buffer B containing protease inhibitors. The cells were collected and centrifuged at 3,000 X g for 5 minutes at 4°C followed by transfer of the pellet in 1 mL buffer C (0.25 M sucrose, 10 mM triethanolamine, 10 mM acetic acid, 1 mM EDTA, pH 7.8) containing protease inhibitor to a Dounce homogenizer. Cells were homogenized using 30 up and down strokes and cellular lysates were centrifuged at 800 X g for 10 minutes followed by centrifugation of the supernatant fraction again at 16,000 X g for 12 minutes. The resulting pellet containing the cell membranes was suspended in 1 mL SP buffer (0.32 M sucrose, 10 mM sodium phosphate, pH 7.4) containing protease inhibitor and assayed for protein content using BCA protein assay method.

#### DAT T53 phosphorylation assay

Cells expressing WT or mutant DAT were grown in 6-well culture plates until ~80%

confluent. After a quick wash with ice cold Kreb's-Ringer HEPES (KRH) buffer (25 mM HEPES, 125 mM sodium chloride, 1.3 mM calcium chloride, 4.8 mM potassium chloride, 1.2 mM potassium dihydrogen phosphate, 1.2 mM magnesium sulfate, 5.6 mM glucose, pH 7.4) cells were treated with vehicle or 10  $\mu$ M AMPH in KRH for 20 minutes at 37°C. Following washes with ice-cold KRH, the cells were solubilized with 200  $\mu$ L RIPA containing protease inhibitors with continuous rocking for 30 minutes. Cellular lysates were adjusted to contain equal amounts of total DAT protein using RIPA and pT53 DAT was immunoprecipitated using phospho-specific antibody against T53 DAT followed by SDS-PAGE and immunoblotting for DAT using DAT specific antibody against N-terminus of rDAT. Experiments were independently performed three or more times and results are reported as mean  $\pm$  standard error. Statistical analyses were done by unpaired Student's t-test using graphpad prism software.

#### Metabolic [ $^{32}$ ]PO $_4$ - labeling

Metabolic  $^{32}$ PO $_4$  labeling in cells expressing WT or mutant DAT was performed as previously described [40]. Cells were grown in 6-well culture plates until ~80% confluent after which they were incubated with phosphate free medium for 1 hour prior to labeling with the same medium containing 0.5 mCi/mL  $^{32}$ PO $_4$  for 2 hours at 37°C. Following metabolic labeling, cells were treated with vehicle or 10  $\mu$ M AMPH for 20 minutes at 37°C after which they were washed with ice-cold Buffer B before being scrapped in 500  $\mu$ L buffer B. The cellular lysates were centrifugated at 2,000 x g for 5 min at 4 °C, and the cell pellet was suspended in 700  $\mu$ L lysis buffer (10 mM triethanolamine/acetate buffer, pH 7.8, 2 mM EDTA, 150 mM sodium chloride, 15% sucrose, 0.1% triton X-100, 100 mM dithiothreitol (DTT)) containing protease

inhibitors followed by end-over-end mixing for 10 minutes at 4°C. The lysates were then centrifuged at 4,000 X g for 5 minutes at 4°C and the resulting supernatant was transferred, adjusted to contain 0.5% SDS and mixed. Following centrifugation at 20,000 X g for 30 minutes at 4°C, the final supernatant was collected for DAT immunoprecipitation. Cellular lysates were adjusted to contain equal amounts of total DAT protein using lysis buffer and <sup>32</sup>P-DAT was immunoprecipitated using DAT specific antibody against C-terminus of hDAT or N-terminus of rDAT followed by SDS-PAGE. Gels were vacuum dried for 2 hours at 72°C followed by exposure to X-Ray film to detect <sup>32</sup>P-DAT. The autoradiograms were developed and quantified using Quantity-1.0® analysis software. Experiments were independently performed three or more times and results are reported as mean ± standard error. Statistical analyses were done by unpaired Student's t-test using graphpad prism software.

#### Crosslinking immunoglobulin (IgG) to protein-A sepharose beads

Protein-A sepharose beads (0.4 gms) were hydrated with 0.2 M triethanolamine (pH 8.0) for 15 minutes with mixing every 5 minutes. The hydrated beads were washed thrice with 5 mL 0.2 M triethanolamine followed by a quick vortex and centrifugation at 1,000 X g for 2 minutes. After the third centrifugation the hydrated protein-A sepharose beads were incubated for 45 minutes at RT with primary antibody (Table 1) diluted in 10 mL of 0.2 M triethanolamine with end-over-end mixing. The incubated protein-A sepharose beads were washed twice with 5 mL 0.2 M triethanolamine and centrifuged at 1000 X g for 2 minutes. Following washes, the beads were incubated with dimethyl pimelimidate (DMP) mix (65 mg DMP/13 mL 0.2 M triethanolamine) for 45 minutes at RT with end-over-end mixing. The beads were then washed twice with 100 mM tris-HCl (pH 8.0) and finally with ImmunoPrecipitation (IPB) Buffer



Table 1. The volume of specific antibodies required for crosslinking with the protein-A beads based on the specificity of the antibodies.

<u>Primary Antibody</u>	<u>Volume (μL)</u>
DAT specific goat polyclonal antibody raised against amino acids 601 to 620 of the C-terminus of human DAT (Santa Cruz Biotechnology)	400 μL
DAT specific mouse monoclonal antibody raised against synthetic peptide 16 containing amino acids 42 to 59 of the N-terminus of rat DAT (Cell Essentials)	200 μL
DAT specific rabbit polyclonal antibody raised against phosphorylated T53 of the N-terminus of rat DAT (Arigobio)	120 μL

(50 mM tris-HCl, pH 8.0, 0.1% triton X-100) followed by being suspended and stored in 7-10 mL IPB containing 0.05% sodium azide at 4°C.

### Immunoprecipitation

Cellular lysates containing equal amounts of total DAT protein were incubated with 50 µL of a 50% slurry of protein sepharose-A beads cross-linked to the desired primary antibody and 450 µL IPB and incubated overnight with end-over-end mixing at 4°C. The next day, DAT bound, primary antibody cross-linked sepharose-A beads were washed thrice with 800 µL IPB containing 0.1% SDS followed by a quick vortex and centrifuged at 8,000 X g for 2 minutes. Immunoprecipitated proteins were eluted with 32 µL 2X laemmli sample buffer containing 5% 2-mercaptoethanol and subjected to SDS-PAGE and either immunoblotting for DAT or gels were dried for X-Ray film exposure.

### Immunoblotting

Lysates were mixed with concentrated laemmli sample buffer containing 5% 2-mercaptoethanol and subjected to SDS-PAGE using 4-20% tris/glycine-polyacrylamide gels. Proteins were resolved by electrophoresis (150 Volts for 1.45 hours) in 1X tris-glycine running buffer. The proteins were transferred to 0.2 µm polyvinylidene difluoride (PVDF) membranes (35 Volts for 1.45 hours) in 1X transfer buffer (25 mM tris, 192 mM glycine, 0.1% SDS, 20% methanol) at 4°C. Membranes were blocked overnight by incubation with 3% bovine serum albumin (BSA)/phosphate buffer saline (PBS; 1.37 M sodium chloride, 2.7 mM potassium chloride, 100 mM disodium phosphate, 18 mM potassium dihydrogen phosphate, pH 7.4) at 4°C. Blocked membranes were probed for 1 hour at RT with DAT specific goat

polyclonal antibody raised against amino acids 601 to 620 of the C-terminus of hDAT or DAT specific mouse monoclonal antibody raised against synthetic peptide 16 containing amino acids 42 to 59 of the N-terminus of rDAT (1:1000 dilution in 3% BSA/PBS). The bound antibodies were detected by incubating the PVDF membranes for 1 hour at RT with anti-goat or anti-mouse IgG 2° antibody linked to alkaline phosphatase (1:5000 dilution in 3% BSA/PBS), with 5 washes of 0.1% tween-20/PBS after each antibody treatment followed by incubation of the membranes with 3 ml alkaline phosphatase substrate for 5 minutes. The membranes were sandwiched between plastic film and imaged on a BioRad Image Doc System and quantified using Quantity-1.0® analysis software.

### Equipment

Transfected LLC-PK<sub>1</sub> cells were maintained in a Nuair 2700-30 water jacketed CO<sub>2</sub> incubator and handled in a Nuair class II type A/B3 class II biological safety cabinet laminar flow hood. Mutagenesis via PCR was performed using a thermocycler from Eppendorf.

The cellular lysates were centrifuged using a Beckman Coulter™ Microfuge® 16 or Microfuge® 22R microcentrifuge. The protein-A sepharose beads were centrifuged using Beckman Coulter™ J6-M1 swing bucket ultracentrifuge. Cellular pellets were solubilized using a Branson® water bath sonicator.

Cell membranes were assayed for protein content using Molecular Devices microplate reader.

SDS-PAGE and protein transfer to PVDF membranes was performed using an XCell SureLock™ electrophoresis apparatus and an XCell II™ Blot module electrophoresis

transfer cell respectively from Invitrogen. The power supply used to control both the electrophoresis apparatus and electrophoresis transfer cell was also from Invitrogen. Gels were dried using a Bio-Rad Hydro vacuum gel drier. Illuminescence from PVDF membranes and autoradiograms were imaged using a Bio-Rad gel documentation system and analyzed using Bio-Rad Quantity-1.0® software. All statistical analyses were done using graphpad prism software.

### Materials

AMEM, G418 sulfate, 1X Penicillin/Streptomycin, and L-Glutamine were from Corning Cellgro (Manassas, VA, USA); FBS was from Atlanta Biologicals (Atlanta, GA, USA); XtremeGene Transfection Reagent was from Roche (Indianapolis, IN, USA); Magnesium Sulfate, Glucose, AMPH, DMP, Sodium Azide, Colorburst Molecular Mass Standard Markers and anti-mouse IgG 2° antibody linked to alkaline phosphatase were from Sigma Aldrich (St. Louis, MO, USA); DAT specific goat polyclonal antibody raised against amino acids 601 to 620 of the C-terminus of hDAT and anti-goat IgG 2° antibody linked to alkaline phosphatase were from Santa Cruz Biotechnology (Dallas, TX, US); Triethanolamine and Hydroxylamine were from Acros Organics (New Jersey, USA); Dimethyl Sulfoxide (DMSO), Sucrose, HEPES, EDTA, Protease Inhibitor Tablets, Tween-20, Triton X-100, Acetic Acid, Sodium Deoxycholate, Sodium Chloride, Sodium Fluoride, BSA, Sodium Phosphate, Potassium Chloride, Disodium Phosphate, Calcium Chloride, Potassium Dihydrogen Phosphate, SDS, Methanol, Acetone, Glycine, 2-Mercaptoethanol, Tris-HCl, DTT, NeutrAvidin beads, MMTS and PVDF membranes were from Fisher Scientific (Waltham, MA, USA); 4-20% tris/glycine-polyacrylamide gels were from Lonza (Walkerville, MD, USA); Protein Sepharose-A beads was from GE Healthcare

Lifesciences (Piscataway, NJ, USA); HPDP-Biotin was from ProteoChem (Loves Park, IL, USA); DAT specific rabbit polyclonal antibody raised against phosphorylated T53 (pT53Ab) of the N-terminus of rat DAT was from PhosphoSolutions (Aurora, CO, USA); DAT specific mouse monoclonal antibody raised against synthetic peptide 16 containing amino acids 42 to 59 of the N-terminus of rDAT was from Cell Essentials (Boston, MA, USA);  $^{32}\text{PO}_4$  was from MP Biomedicals (Santa Ana, CA, USA) or Perkin Elmer (Waltham, MA, USA); Alkaline phosphatase substrate (ImmunStar) was from Bio-Rad (Hercules, CA, USA); X-Ray film was from GE Healthcare (Chicago, IL, USA).

## RESULTS

### ADHD associated SNP, A559V hDAT and its rat homologue, A558V rDAT, display increased phosphorylation

DAT phosphorylation is stimulated by protein kinases and proline directed kinases such as protein kinase C (PKC) and extracellular signal regulated pathway (ERK) respectively [40, 41, 49, 93, 95]. This phosphorylation is specific to the N-terminus such that truncation of the first 21 amino acid residues leads to significant reduction in phosphorylation levels. Drugs such as AMPH and PKC activators such as phorbol 12-myristate, 13-acetate (PMA) stimulate these kinases causing elevation of DAT phosphorylation which plays a role in DA efflux and DAT endocytosis [40, 49, 57, 129, 136, 140, 169, 195, 196].

First identified in two male siblings, ADHD associated SNP, A559V hDAT showed ~300% increase in basal ADE, independent of AMPH-mediated stimulation, and that AMPH stimulation blocked this efflux [8, 9, 169]. Since phosphorylation of DAT is critical for ADE, we examined the phosphorylation levels of A559V hDAT along with C581A hDAT, homologue for palmitoylation deficient mutant C580A rDAT which previously was shown to have increased phosphorylation levels [9, 36, 110]. LLC-PK<sub>1</sub> cells stably expressing WT, A559V hDAT or C581A hDAT were labeled with 0.5 mCi/mL <sup>32</sup>PO<sub>4</sub> and treated with vehicle or 10 μM AMPH. Equal amounts of DAT were immunoprecipitated for DAT and analyzed by SDS-PAGE/autoradiography (Fig. 14). WT DAT displayed typical level of phosphorylation with AMPH-mediated PKC-stimulation causing an increase in phosphorylation levels over basal (138 ± 8% of WT

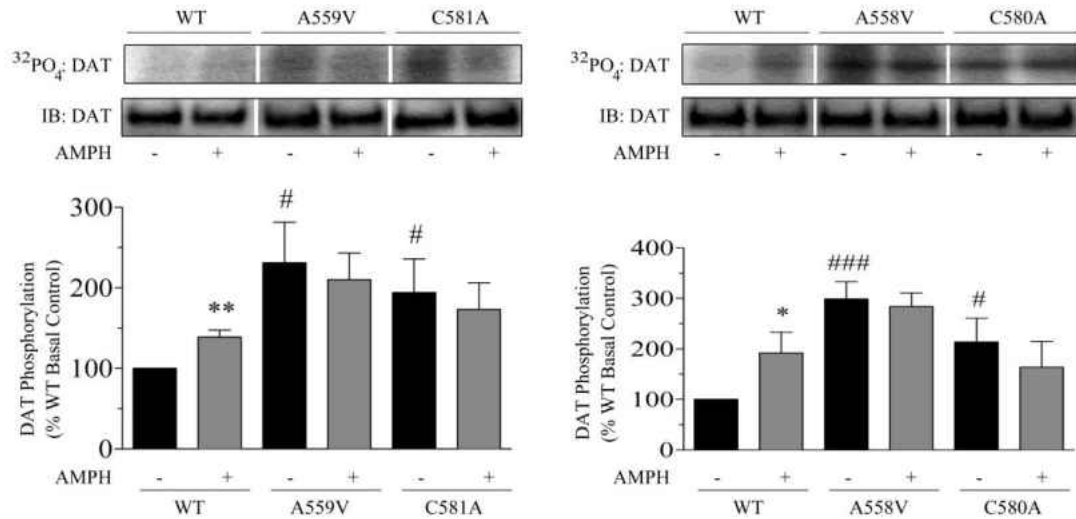


Figure 14: A559V hDAT, C581A hDAT and their rat homologues display increased basal phosphorylation levels.

LLC-PK<sub>1</sub> cells stably expressing the indicated hDAT or rDAT forms were labeled in parallel with 0.5 mCi/mL <sup>32</sup>PO<sub>4</sub> and treated with vehicle or 10 μM AMPH. Equal amounts of DAT determined by immunoblotting (IB) were immunoprecipitated for DAT specific antibody against C-terminus of hDAT or N-terminus of rDAT and subjected to SDS-PAGE/autoradiography.

Upper panels show representative autoradiograms and matching total DAT immunoblots. Vertical white dividing lines indicate the rearrangement of lanes from the same blot or autoradiogram. Histograms show the quantification of <sup>32</sup>PO<sub>4</sub> labeling (% WT basal control, mean ± S.E.; \*\* p ≤ 0.01, WT (hDAT) AMPH vs. WT basal; # p ≤ 0.05, indicated DAT forms basal vs. WT basal; \* p ≤ 0.05, WT (rDAT) AMPH vs. WT basal; ### p ≤ 0.001, A558V rDAT basal vs. WT basal; n=6 (rDAT WT, A558V rDAT and C580A rDAT), 5 (hDAT WT, A559V), 4 (C581A hDAT)). Statistical analyses were done by unpaired Student's t-test using graphpad prism software.

basal;  $p \leq 0.01$  vs. WT basal). In contrast to WT, A559V hDAT ( $231 \pm 50\%$  of WT basal;  $p \leq 0.05$  vs. WT basal) and C581A hDAT ( $194 \pm 41\%$  of WT basal;  $p \leq 0.05$  vs. WT basal) displayed elevated basal phosphorylation levels with AMPH-mediated PKC-stimulation having no effect on the already elevated phosphorylation levels. This increased basal phosphorylation level demonstrated by ADHD associated SNP, A559V, suggests that it may mechanistically be contributing to ADE seen in this polymorphism.

Identical experiments performed on A558V rDAT and C580A rDAT, rat homologues for A559V hDAT and C581A hDAT respectively displayed similar AMPH-stimulated increase in phosphorylation levels over basal for WT ( $192 \pm 41\%$  of WT basal;  $p \leq 0.05$  vs. WT basal). In contrast to WT, A558V rDAT ( $299 \pm 33\%$  of WT basal;  $p \leq 0.001$  vs. WT basal) and C580A rDAT ( $213 \pm 46\%$  of WT basal;  $p \leq 0.05$  vs. WT basal) displayed elevated basal phosphorylation level, which were insensitivity to AMPH-stimulation [9, 36, 110].

#### A558V rDAT displays increased phosphorylation at T53

Mass-spectrometry studies have identified T53 residue on the N-terminus to be a proline directed phosphorylation site driven by kinases such as mitogen-activated protein kinase (MAPK), c-Jun N-terminal kinase (JNK) and ERK [38, 48, 51, 197]. It is believed that the closeness of T53 to TMD 1 causes modifications at this site regulate the binding and interaction of DAT with other associated proteins affecting the opening and closing of intracellular gates and ion flow or efflux [48, 50, 52, 53]. We examined the phosphorylation status of T53 using a phospho-specific T53 antibody. LLC-PK<sub>1</sub> cells stably expressing WT, A558V rDAT or C580A rDAT, were treated with vehicle or 10  $\mu$ M AMPH and equal amounts of DAT were



immunoprecipitated for pT53 and analyzed by immunoblotting (Fig. 15) [9, 36, 38, 110]. WT DAT displayed typical levels of T53 phosphorylation with AMPH-mediated stimulation causing an increase in T53 phosphorylation levels over basal ( $154 \pm 17\%$  of WT basal;  $p \leq 0.01$  vs. WT basal). In contrast to WT, A558V rDAT ( $159 \pm 22\%$  of WT basal;  $p \leq 0.05$  vs. WT basal) and C580A rDAT ( $168 \pm 17\%$  of WT basal;  $p \leq 0.01$  vs. WT basal) displayed elevated T53 phosphorylation levels with AMPH-mediated stimulation having no effect on the already elevated T53 phosphorylation levels. This result demonstrated that AMPH mediates proline directed phosphorylation at T53 (human equivalent being S53) affecting DA functionality and could be a factor causing rapid up-regulation of DAT transport capacity, which is mediated kinases such as MAPK, JNK and ERK. Phosphorylation at this site could also contribute to ADE seen by this polymorphism.

#### Determining C581A hDAT to be palmitoylation deficient mutant

C580 is the only known palmitoylation site in rDAT such that Cys to Ala substitution causes a 60% reduction in palmitoylation levels and reciprocal increase in phosphorylation levels [36, 110]. With C581 being the human equivalent to C580, we hypothesized it to be a palmitoylation site. To determine if C581 is a palmitoylation site, we subjected LLC-PK<sub>1</sub> cells stably expressing WT or C581A hDAT to ABE (Fig. 16) [64, 194, 198]. In contrast to WT, C581A hDAT ( $49 \pm 8\%$  of WT;  $p \leq 0.01$  vs. WT) indeed displayed reduced palmitoylation levels indicating it is a palmitoylation site. This mutant also reciprocally demonstrated increased phosphorylation levels. The lack of complete loss of palmitoylation at C581A hDAT indicates the possibility of there being additional palmitoylation sites within hDAT.

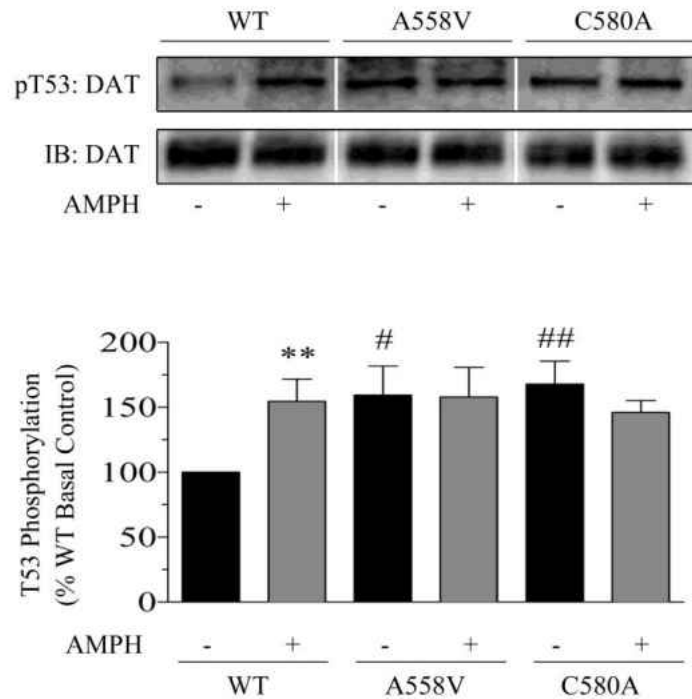


Figure 15: A558V rDAT shows increased basal T53 phosphorylation levels.

LLC-PK<sub>1</sub> cells stably expressing the indicated rDAT forms were treated with vehicle or 10  $\mu$ M AMPH. Equal amounts of DAT determined by immunoblotting (IB) were immunoprecipitated using T53 phospho-specific DAT antibody and subjected to immunoblotting.

Upper panel shows representative T53 phospho-specific DAT immunoblot and matching total DAT immunoblot. Vertical white dividing lines indicate the rearrangement of lanes from the same blot. Histogram shows the quantification of T53 phosphorylation (% WT basal control, mean  $\pm$  S.E.; \*\*  $p \leq 0.01$ , WT AMPH vs. WT basal; #  $p \leq 0.05$ , A558V rDAT basal vs. WT basal; ##  $p \leq 0.01$ , C580A rDAT basal vs. WT basal; n=7). Statistical analyses were done by unpaired Student's t-test using graphpad prism software.

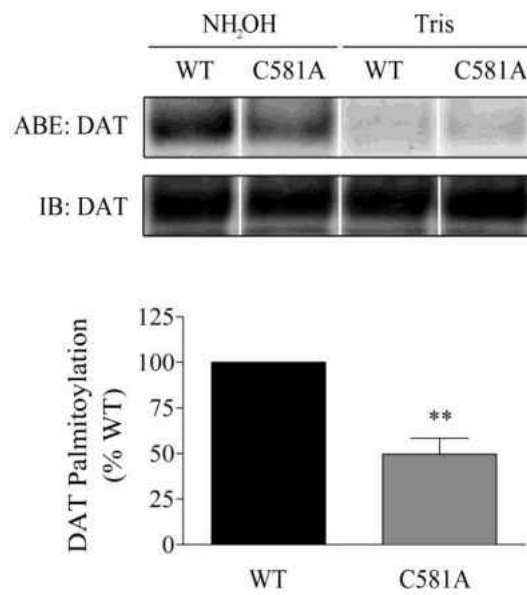


Figure 16: C581A hDAT is a palmitoylation deficient mutant.

LLC-PK<sub>1</sub> cells stably expressing WT or C581A hDAT were assessed for palmitoylation by ABE. Upon blocking the free Cys thiol residues with 20 mM MMTS, cell lysates were treated with 0.7 M NH<sub>2</sub>OH or 50 mM Tris-HCl (control) followed by reaction with 0.4 mM sulfhydryl-specific biotinylating reagent. Equal amounts of DAT determined by immunoblotting (IB) were subjected to neutrAvidin extraction followed by immunoblotting.

Upper panel shows representative ABE blot and matching total DAT immunoblot. Vertical white dividing lines indicate the rearrangement of lanes from the same blot. Histogram shows the quantification of DAT palmitoylation (% WT, mean  $\pm$  S.E.; \*\*  $p \leq 0.01$ , C581A vs. WT; n=4). Statistical analysis was done by unpaired Student's t-test using graphpad prism software.

ADHD associated SNP, A559V hDAT and its rat homologue, A558V rDAT, display decreased palmitoylation

We have shown that A559V hDAT and A558V rDAT have elevated basal phosphorylation levels consistent with ADE and that this increase in phosphorylation is insensitive to AMPH-stimulation. With DAT being reciprocally regulated by palmitoylation and phosphorylation, we next examined WT, A559V hDAT or A558V rDAT for their palmitoylation status by ABE (Fig. 17) [110]. In contrast to WT, A559V hDAT ( $69 \pm 5\%$  of WT;  $p \leq 0.01$  vs. WT) and A558V rDAT ( $61 \pm 4\%$  of WT;  $p \leq 0.01$  vs. WT) displayed decreased palmitoylation levels, demonstrating these DATs are palmitoylation deficient mutants. With the rationale for decreased palmitoylation not well understood, we believe that the Ala to Val substitution close to the palmitoylation site is a factor causing reduction in palmitoylation. The presence of bulkier Val may mechanistically be hindering palmitoylation at C581 [64, 194, 198].

Phosphorylation deficient hDAT and rDAT mutants show enhanced palmitoylation status

Among the many Ser/Thr residues on the DAT N-terminus, S7 and T53 residues on rDAT have been validated as phosphorylation sites (human equivalent being S7 and S53 respectively) [38, 49]. Activated by various kinases, N-terminal phosphorylation plays an important role in mediating DA efflux, regulating DAT binding to its partner proteins and down-regulation of DAT functional capacity [9, 39-41, 48, 49, 51, 91]. As DAT is reciprocally regulated [110], we examined T53A rDAT, S7A and S53A for their palmitoylation status (Fig. 18) [64, 194, 198].

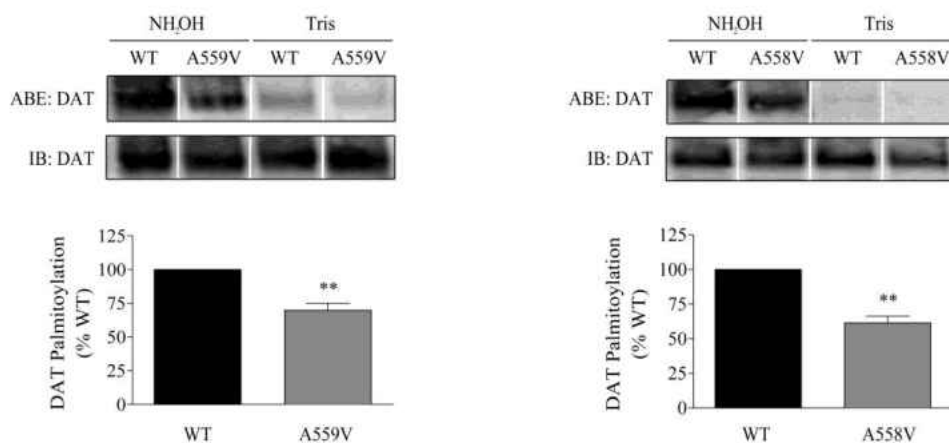


Figure 17: A559V hDAT and A558V rDAT display decreased palmitoylation levels. LLC-PK<sub>1</sub> cells stably expressing the indicated hDAT or rDAT forms were assessed for palmitoylation by ABE. Upon blocking the free Cys thiol residues with 20 mM MMTS, cell lysates were treated with 0.7 M NH<sub>2</sub>OH or 50 mM Tris-HCl (control) followed by reaction with 0.4 mM sulfhydryl-specific biotinylating reagent. Equal amounts of DAT determined by immunoblotting (IB) were subjected to neutrAvidin extraction followed by immunoblotting.

Upper panels show representative ABE blots and matching total DAT immunoblots. Vertical white dividing lines indicate the rearrangement of lanes from the same blot. Histograms show the quantification of DAT palmitoylation (% WT, mean  $\pm$  S.E.; \*\*  $p \leq 0.01$ , indicated DAT forms vs. WT; n=3). Statistical analyses were done by unpaired Student's t-test using graphpad prism software.

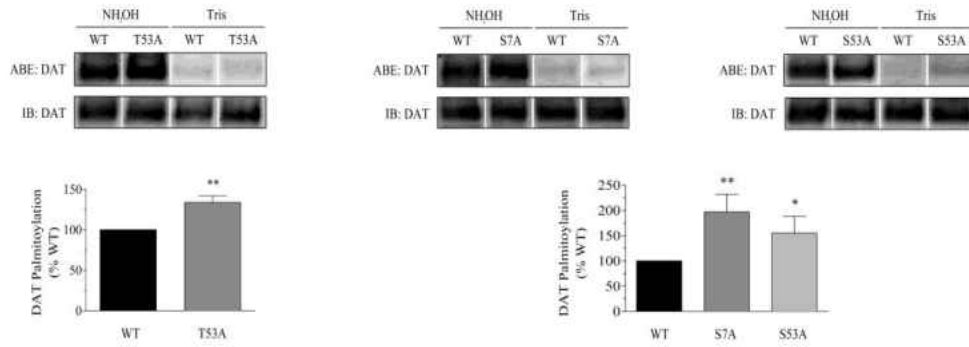


Figure 18: Phosphorylation deficient hDAT and rDAT mutants show enhanced palmitoylation levels.

LLC-PK<sub>1</sub> cells stably expressing the indicated hDAT or rDAT forms were assessed for palmitoylation by ABE. Upon blocking the free Cys thiol residues with 20 mM MMTS, cell lysates were treated with 0.7 M NH<sub>2</sub>OH or 50 mM Tris-HCl (control) followed by reaction with 0.4 mM sulfhydryl-specific biotinylating reagent. Equal amounts of DAT determined by immunoblotting (IB) were subjected to neutrAvidin extraction followed by immunoblotting.

Upper panels show representative ABE blots and matching total DAT immunoblots. Vertical white dividing lines indicate the rearrangement of lanes from the same blot. Histograms show the quantification of DAT palmitoylation (% WT, mean  $\pm$  S.E.; \*\*  $p \leq 0.01$ , indicated DAT forms vs. WT; \*  $p \leq 0.05$ , S53A hDAT vs. WT;  $n=8$  (hDAT WT), 4 (rDAT WT, T53A rDAT, S7A hDAT, S53A hDAT)). Statistical analyses were done by unpaired Student's t-test using graphpad prism software.

LLC-PK<sub>1</sub> cells stably expressing WT, T53A rDAT, S7A hDAT or S53A hDAT were subjected to ABE. In contrast to WT, T53A rDAT ( $133 \pm 8\%$  of WT;  $p \leq 0.01$  vs. WT), S7A hDAT ( $196 \pm 35\%$  of WT;  $p \leq 0.01$  vs. WT) and S53A hDAT ( $155 \pm 32\%$  of WT;  $p \leq 0.05$  vs. WT) displayed increased palmitoylation levels. These results strengthen the concept of reciprocal regulation of post-translational modifications, though the actual mechanism for such a reciprocal phenomenon in these mutants is still not well understood.

## DISCUSSION

DAT is an important neurotransmission regulator which controls the duration of DA neurotransmission by clearing the synapse of DA [3]. Abnormal levels of DA in the mesencephalon is associated with neurological disorders such as PD, AD, ADHD, ASD, BPD, drug abuse and addiction with some of these disorders also being associated with SNPs in DAT [6, 8-10, 16-21, 26, 41, 112, 199-201]. DAT undergoes various post-translational modifications, including phosphorylation and palmitoylation which plays a role in regulating DAT function affecting DAT down-regulation, membrane raft partitioning, membrane trafficking and mobility, DAT surface expression and  $V_{max}$  [8, 9, 26, 36, 48, 56, 62, 113, 114, 164, 169]. These post-translational modifications reciprocally regulate each other such that increased phosphorylation leads to decreased palmitoylation and visa versa [49, 56, 110, 111].

Drugs such as AMPH mediate PKC-stimulated increase in N-terminal DAT phosphorylation, a condition stimulating ADE [40, 136]. An ADHD associated rare hDAT SNP, A559V displays total and surface DAT levels and DA uptake levels similar to WT but shows DA efflux independent of AMPH stimulation suggesting that differences exist between WT and A559V hDAT towards their ability to interact with AMPH [9, 40, 162, 164, 169, 193, 202]. Studies with ASD showed A559V has a reduced ability to transport AMPH stating a conformational alteration might be hampering its dynamics to transport AMPH [169].

We here demonstrate A559V hDAT and its rat homologue, have elevated phosphorylation levels, including specific modification at T53, a proline directed



phosphorylation site specific for rDAT, supporting a role for phosphorylation at this site in DA efflux. In addition, elevated phosphorylation levels in this mutant were independent of AMPH-stimulation and AMPH failed to have an effect on the already elevated phosphorylation levels consistent with reduced ability of this mutant to transport AMPH. We also showed similar increased phosphorylation levels for C581A hDAT and C580A rDAT which are palmitoylation deficient mutants. Thus, we believe increased phosphorylation levels mechanistically contribute to ADE seen for this polymorphism. With T53 showing increased phosphorylation, we believe this proline directed phosphorylation site could be a factor causing a rapid increase in DAT transport capacity, which is mediated by MAPK, JNK and ERK. Similar phosphorylation occurring at S53 in hDAT could drive DA efflux.

With recent findings showing DAT is reciprocally regulated with regard to phosphorylation and palmitoylation, we analyzed the palmitoylation status for A559V hDAT and A558V rDAT to find that these mutants displayed decreased palmitoylation levels. We also demonstrate C581A hDAT, to be a palmitoylation deficient mutant, which showed reciprocal increased phosphorylation levels. With A559V hDAT and A558V rDAT displaying reciprocally regulated post-translational modifications, we believe that the close proximity of the mutated residue A559V to the known palmitoylation site, C581, could be the driving force.

A559 is located at the top extracellular side of TMD 12. It shares close proximity to C581, a palmitoylation site that is present on the intracellular side of TMD 12. The mutation of Ala to Val at 559 residue, makes this site bulkier that may cause structural change within TMD 12. This hindrance could make C581 move away from the DAT core region making it lose its flexibility. This could affect C581 from undergoing

palmitoylation and the C-terminus to cap the cytoplasmic gate. Thus this altered palmitoylation status of A559V hDAT and A558V rDAT could affect its phosphorylation status by an unknown mechanism which could stimulate ADE.

Another concept driving this reciprocal regulation of these post-translational modifications in A559V hDAT could be the N-terminal phosphorylation which is supported by PKC-stimulation. DAT is a 12 TMD helical structure with TMDs 1, 3, 6 and 8 forming the central core binding pocket with the substrate translocation occurring in DAT via an alternating access mechanism [3, 203]. With DAT phosphorylation and palmitoylation both occurring outside the core of the protein, we speculate that the amino acid residues involved in these post-translational modifications could be interacting with binding partners, gating residues in a process of impacting the overall functioning, structure and orientation, duration of transport cycle of DAT which in turn affect other post-translational modifications [10, 36, 41, 53, 88, 110, 204].

We also demonstrated increased palmitoylation status for phosphorylation deficient mutants including T53A rDAT, S7A hDAT and S53A hDAT. Although the actual mechanism for this phenomenon is not known we believe these mutants would be harboring similarly targeted phenomenon to bring about this reciprocal post-translational modifications. Together these results strongly support reciprocal regulation for phosphorylation and palmitoylation in DAT.

## CHAPTER III

### ALTERED MEMBRANE LOCALIZATION AND MOBILITY IN ADHD ASSOCIATED DOPAMINE TRANSPORTER MUTANT A559V LINKED TO ALTERED PHOSPHORYLATION/PALMITOYLATION STATUS

#### ABSTRACT

In the central nervous system, the presynaptic dopamine transporter (DAT, SLC6A3) regulates synaptic dopamine (DA) signaling by clearing the DA from the synapse into the presynaptic neuron. Dysregulated DA clearance and/or DAT associated polymorphisms have been linked to several neurological diseases including bipolar disorder (BPD), Parkinson's disease (PD), attention-deficit hyperactivity disorder (ADHD) and autism although the role of DAT dysfunction in these diseases is not clearly understood. ADHD associated human DAT (hDAT) single nucleotide polymorphism (SNP) A559V hDAT displays ADE and elevated N-terminal phosphorylation independent of amphetamine (AMPH) stimulation. With membrane rafts being the preferred site for localization of phosphorylated DAT, we here demonstrate increased DAT localization in membrane raft microdomains over non-raft microdomains for A559V hDAT and its rat homologue, A558V rat DAT (rDAT) and mutants having elevated phosphorylation levels. This enrichment of phosphorylated DAT in membrane raft microdomain is driven by AMPH-stimulation in the wildtype (WT).

With palmitoylation known to influence membrane trafficking and mobility, we confirm palmitoylation to be a factor regulating lateral membrane mobility, such that stimulation of phosphorylation drives an increase in lateral membrane mobility via a

reciprocal decrease in palmitoylation. We also demonstrate A559V hDAT, A558V and other palmitoylation deficient mutants have increased lateral membrane mobility with reciprocal results for phosphorylation deficient mutants T53A rDAT, S7A hDAT, S53A hDAT (human homologue for T53A rDAT).

With enhanced localization of phosphorylated DAT in membrane raft microdomain, we believe membrane rafts serve as a platform for ADE displayed by A559V hDAT. For ADHD associated A559V, we believe that its closeness to the palmitoylation site, C581, is a factor causing its decrease in palmitoylation status, which in-turn drives the increase in lateral membrane mobility. This decrease in palmitoylation is also the driving force for increased phosphorylation levels and localization of DAT in membrane raft region.

Although we lack a complete understanding of how palmitoylation affects lateral membrane mobility and membrane microdomain distribution, together, our data provides valuable information regarding palmitoylation being a factor contributing towards regulating DAT localization in membrane raft and its lateral membrane mobility for ADHD associated A559V and other phosphorylation and palmitoylation deficient DAT mutants.

## INTRODUCTION

The neurotransmitter dopamine (DA) plays a critical role in controlling motor activities, reward, pleasure and locomotive abilities [6, 9, 14]. The rapid synaptic clearance of DA is controlled by the dopamine transporter (DAT), a 12 transmembrane spanning domain (TMD) plasma membrane protein belonging to the solute carrier 6 (SLC6) gene family of  $\text{Na}^+/\text{Cl}^-$  coupled transporters [2-4, 6, 9, 31, 35, 205, 206]. Functionally, this clearance of DA via DAT controls the intensity and duration of the dopaminergic signaling maintaining DA homeostasis.

DAT is the primary target for abused psychoactive drugs such as amphetamine (AMPH) and cocaine (COC), which act as substrate and uptake blocker respectively [2, 3, 205, 206]. While DAT bound COC prevents the binding and movement of DA into the pre-synaptic neuron, affecting DAT regulatory properties, AMPH is transported via DAT into the pre-synaptic neuron, where it disrupts the potential gradient of the synaptic vesicles eventually causing DA efflux (reverse transport) without affecting DA transport capacity, DA uptake and the surface expression of DAT [3, 40, 48, 115-117, 119, 196]. DAT is associated with many neurological and psychological diseases, in which DAT either has dysfunction and/or polymorphism. Such disorders are schizophrenia, bipolar disorder (BPD), Parkinson's disease (PD), autism spectrum disorder (ASD), obsessive compulsive disorder (OCD), attention-deficit hyperactivity disorder (ADHD) and addiction although the actual role of DAT dysfunctions and/or polymorphisms in these disorders is not well understood [6, 9, 17, 18, 20, 191, 207].

DAT undergoes tightly regulated post-translational modifications. The two modifications that are of our interest are phosphorylation and palmitoylation. These modifications are reciprocally regulated and between them modulate functions such as protein-protein interaction, membrane trafficking, DAT signaling and lateral membrane mobility [9, 36, 56, 60, 95, 102, 127, 137, 208, 209]. DAT is phosphorylated by kinases such as protein kinase C (PKC) or calcium/calmodulin-dependent protein kinase II (CaMKII) which cause DAT interaction with binding partners, anomalous DA efflux (ADE), DAT down-regulation, endocytosis and reduction in DA transport capacity [46, 57, 58, 210, 211]. AMPH is able to trigger PKC-stimulated N-terminal DAT phosphorylation and trigger DA efflux [40, 57, 202, 212].

DAT undergoes S-palmitoylation, the reversible addition of a saturated fatty acid moiety (palmitate) via a thioester bond to Cys. Palmitoylation is brought about by specific enzymes called palmitoyl acyltransferases (PATs) while removal of the palmitate group is catalyzed by palmitoyl-protein thioesterases (PPTs) [69]. Palmitoylation affects DAT transport kinetics, degradation and protein kinase stimulated down regulation [36, 72]. The driving force behind palmitoylation is thought to be the properties of the palmitate group, its hydrophobicity/membrane affinity and its preference for the cholesterol rich membrane rafts [71].

DAT present on the plasma membrane is distributed between cholesterol-rich membrane raft microdomains and cholesterol poor membrane non-raft microdomain with membrane rafts playing a role in compartmentalization of cellular processes associated with DAT internalization, lateral membrane mobility and endocytotic cargo delivery regulating DAT function [56, 90, 137, 172, 175, 213, 214]. PKC-stimulated

phosphorylated DAT is localized in membrane raft microdomains over non-raft microdomains suggesting that membrane rafts are preferred sites for DAT phosphorylation localization [56, 136, 140]. With AMPH-mediated PKC-stimulation causing DA efflux, membrane rafts may serve as a platform for this efflux.

A recently discovered ADHD, BPD and ASD associated single nucleotide polymorphism (SNP) in human DAT (hDAT) is A559V [9, 162, 164, 169]. This SNP displayed ADE independent of AMPH-stimulation and altered DAT transport function [9, 18, 193]. Findings have shown that A559V hDAT has increased basal phosphorylation, a condition promoting ADE [8, 9, 169] [Chapter II].

With membrane rafts being the preferred site for phosphorylated DAT localization, we studied the membrane microdomain distribution for ADHD associated SNP, A559V hDAT and its rat homologue, A558V rat DAT (rDAT) along with palmitoylation deficient mutants (C581A hDAT and C580A rDAT) which showed reciprocal elevated phosphorylation. We also studied the effect of AMPH on the membrane raft and non-raft microdomain localization for these mutants.

Being a plasma membrane protein, membrane trafficking of DAT is an important component of its regulatory function, with dysregulation of membrane trafficking known to be a risk determinant for many disorders [167, 172]. With previous studies having shown A559V hDAT and A558V rDAT to be palmitoylation deficient mutants, we studied the lateral membrane mobility for A559V hDAT, A558V rDAT and other palmitoylation and phosphorylation deficient mutants. We also studied the effect of AMPH and phorbol 12-myristate, 13-acetate (PMA) on mobility, further analyzing if palmitoylation is a factor driving lateral membrane mobility.

## EXPERIMENTAL METHODS

### Cell culture and site directed mutagenesis

Plasmids containing the coding sequence for mutant DATs were generated by codon substitution in a pcDNA 3.0 vector containing WT hDAT or rDAT using the Stratagene QuikChange® Kit and were verified by sequencing (Eurofins MWG). Lewis lung carcinoma-porcine kidney (LLC-PK<sub>1</sub>) cells were transfected with individual plasmids and selected for stable DAT expression with 800 µg/ml geneticin (G418 sulfate). Plasmids containing coding sequence for EYFP-tagged WT DATs were generated by insertion of the WT hDAT or rDAT coding sequence between the Kpn I and ECoR I endonuclease cleavage sites in an EYFP-C1 (Clontech) vector. Plasmids containing the coding sequence for EYFP-tagged DAT mutants were generated by codon substitution in the EYFP-C1 vector containing WT hDAT or rDAT sequence using the Stratagene QuikChange® Kit and were verified by sequencing (Eurofins MWG). Neuronal (N<sub>2</sub>A) cells were transiently transfected with the EYFP-DAT vectors to express yellow fluorescent protein (YFP)-tagged DATs.

LLC-PK<sub>1</sub>/N<sub>2</sub>A cells were grown in 12-well culture plates and were transfected with 1.4 µg plasmid/well and XtremeGene transfection reagent (Roche). Stable transformants were selected 24-48 hours post transfection while transient transformants were used for experiments 24-48 hours post transfection. For stable transfections, the cells were maintained under selection by adding 800 µg/mL G418 sulfate to the culture medium. Transfected LLC-PK<sub>1</sub> cells were maintained in  $\alpha$ -



minimum essential medium (MEM) supplemented with 2 mM L-glutamine, 5% fetal bovine serum (FBS), 200 µg/mL G418 sulfate and 1X penicillin/streptomycin while transfected N<sub>2</sub>A cells were maintained in dulbecco's modified eagle's medium (DMEM) supplemented with 10% FBS and 1X penicillin/streptomycin. Cells were incubated in an incubation chamber gassed with 5% CO<sub>2</sub> at 37°C. DAT expression levels in transfected cells was verified by sodium dodecyl sulfate-polyacrylamide gel electrophoresis (SDS-PAGE) and immunoblotting of the cellular lysates against DAT specific antibodies. The YFP-DAT expressing cells were additionally checked for the fluorescence levels by confocal microscopy.

#### Confocal microscopy and fluorescence recovery after photobleaching (FRAP)

N<sub>2</sub>A cells transiently expressing YFP-tagged WT or mutant DAT were plated on 1 mm glass coverslips and allowed to grow to ~50% confluence before confocal imaging and FRAP analysis was performed using a Zeiss 510 META laser scanning confocal microscope.

For palmitoylation inhibition studies, cells were treated with vehicle or 15 µM 2-bromopalmitate (2BP) for 3 hours at 37°C prior to confocal imaging and FRAP analysis. For phosphorylation stimulation studies, cells were treated with vehicle or 10 µM AMPH or 1 µM PMA for 20 minutes or 30 minutes respectively at 37°C prior to confocal imaging and FRAP analysis.

During each FRAP run, cells were excited at 488/514 nm with an argon laser (2% power) through a 100X oil immersion objective followed by separation of the excited wavelength from the emitted wavelength using a 530 nm long pass filter. Following the excitation, a series of images were captured at ~4 seconds intervals to establish a

fluorescence intensity baseline for a 30  $\mu\text{m}$  diameter circular region of interest (ROI) on the cellular plasma membrane. The ROIs were then photobleached at 514 nm with an argon laser (100% power), keeping the pinhole fully open to ensure complete bleaching through the ROI. Following photobleaching, a total of 100 images were captured for analysis of the time taken for fluorescence recovery ( $T_{1/2}$ ) after photobleaching. This analysis was done using ImageJ software and the exponential recovery function ( $F(x) = F_{\infty} + A(\exp(-x\tau))$ ). Experiments were independently performed three or more times with three or more independent cells being examined in each experiment. Results are reported as mean  $\pm$  standard error. Statistical analyses were done by unpaired Student's t-test using graphpad prism software.

#### Sucrose density gradient centrifugation

Membrane raft fractions were isolated by a modified discontinuous sucrose density gradient centrifugation technique [90]. LLC-PK<sub>1</sub> cells stably expressing WT or mutant DATs were grown in 150 mm culture plates until ~80% confluent. After a quick wash with ice-cold Krebs's-Ringer HEPES (KRH) buffer (25 mM HEPES, 125 mM sodium chloride, 1.3 mM calcium chloride, 4.8 mM potassium chloride, 1.2 mM potassium dihydrogen phosphate, 1.2 mM magnesium sulfate, 5.6 mM glucose, pH 7.4) cells were treated with vehicle or 10  $\mu\text{M}$  AMPH for 20 minutes at 37°C. Following washes the cells were solubilized with 750  $\mu\text{L}$  1% BRIJ-58 in TNEB (10 mM tris-HCl, 150 mM sodium chloride, 1 mM EDTA, pH 7.5) for 1 hour at 4°C with end-over-end mixing. After centrifugation of the lysate at 1,000 X g for 10 minutes at room temperature, 750  $\mu\text{L}$  of the supernatant fraction was brought to 40% sucrose concentration by adding equal volume of 80% sucrose in TNEB. This 40% sucrose-supernatant mix was underlayered into the bottom of an SW41 centrifuge tube

containing a discontinuous sucrose gradient composed of 5.5 mL of 30% sucrose under 5 mL of 5% sucrose in TNEB. The tubes were centrifuged at 36,000 rpm for 18 hours at 4°C followed by collection of 500 µL fractions from each tube, starting from the top of the tube. 25 µL of each fraction was mixed with 7 µL 5X laemmli sample buffer and subjected to SDS-PAGE and immunoblotting for DAT. The polyvinylidene difluoride (PVDF) membranes were stripped of antibodies and reprobed for transferrin receptor and flotillin-1. Fractions were also assayed for total protein and cholesterol using BCA protein assay and a cholesterol E assay kit (Wako) respectively. The total protein and cholesterol levels were quantified using a molecular devices microplate reader at the appropriate wavelength. Fractions 1-8 did not contain detectable levels of DAT or other protein markers (data not shown). Experiments were independently performed three or more times. Results are reported as mean ± standard error. Statistical analyses were done by One-Way ANOVA with Tukey's post-hoc test using graphpad prism software.

### Immunoblotting

SDS-PAGE was performed using 4-20% tris/glycine-polyacrylamide gels. Proteins were resolved by electrophoresis (150 Volts for 1.45 hours) in 1X tris-glycine running buffer. The proteins were transferred to 0.2 µm PVDF membranes (35 Volts for 1.45 hours) in 1X transfer buffer (25 mM tris, 192 mM glycine, 0.1% SDS, 20% methanol) at 4°C. Membranes were blocked overnight by incubation with 3% bovine serum albumin (BSA)/phosphate buffer saline (PBS; 1.37 M sodium chloride, 2.7 mM potassium chloride, 100 mM disodium phosphate, 18 mM potassium dihydrogen phosphate, pH 7.4) at 4°C. Blocked membranes were probed for 1 hour at RT with DAT specific goat polyclonal antibody raised against amino acids 601 to 620 of the C-

terminus of hDAT or DAT specific mouse monoclonal antibody raised against synthetic peptide 16 containing amino acids 42 to 59 of the N-terminus of rDAT (1:1000 dilution in 3% BSA/PBS). The bound antibodies were detected by incubating the PVDF membranes for 1 hour at RT with anti-goat or anti-mouse immunoglobulin (IgG) 2° antibody linked to alkaline phosphatase (1:5000 dilution in 3% BSA/PBS), with 5 washes of 0.1% tween-20/PBS after each antibody treatment followed by incubation of the membranes with 3 ml alkaline phosphatase substrate for 5 minutes. The membranes were sandwiched between plastic film and imaged on a BioRad Image Doc System and quantified using Quantity-1.0® analysis software.

### Equipment

Transfected LLC-PK<sub>1</sub> and N<sub>2</sub>A cells were maintained in a Nuair 2700-30 water jacketed CO<sub>2</sub> incubator and handled in a Nuair class II type A/B3 biological safety cabinet laminar flow hood. Mutagenesis via PCR was performed using a thermocycler from Eppendorf.

Cellular lysates were centrifuged using a Beckman Coulter™ Microfuge® 16 or Microfuge® 22R microcentrifuge. Sucrose density gradients were centrifuged using an SW41 swing bucket rotor in a Beckman Coulter™ LE-80 ultracentrifuge.

Total protein and cholesterol levels were assayed using Molecular Devices microplate reader.

Confocal imaging and FRAP studies for YFP-tagged DATs was perform using a Zeiss (Germany) 510 META laser scanning confocal microscope and the image analysis was done using Image J software (NIH).

SDS-PAGE and protein transfer to PVDF membranes was performed using an XCell SureLock™ electrophoresis apparatus and an XCell II™ Blot module electrophoresis transfer cell respectively from Invitrogen. The power supply used to control both the electrophoresis apparatus and electrophoresis transfer cell was also from Invitrogen. Illuminescence from PVDF membranes were imaged using a Bio-Rad gel documentation system and analyzed using Bio-Rad Quantity-1.0® software. All statistical analyses were done using graphpad prism software.

### Materials

DMEM, AMEM, G418 sulfate, 1X Penicillin/Streptomycin, and L-Glutamine were from Corning Cellgro (Manassas, VA, USA); FBS was from Atlanta Biologicals (Atlanta, GA, USA); XtremeGene Transfection Reagent was from Roche (Indianapolis, IN, USA); Magnesium Sulfate, Glucose, AMPH, 2-BP, Colorburst Molecular Mass Standard Markers, Brij-58 and anti-mouse IgG 2° antibody linked to alkaline phosphatase were from Sigma Aldrich (St. Louis, MO, USA); Dimethyl Sulfoxide (DMSO), Sucrose, HEPES, EDTA, Protease Inhibitor Tablets, Tween-20, Triton X-100, Sodium Chloride, BSA, Sodium Phosphate, Potassium Chloride, Disodium Phosphate, Calcium Chloride, Potassium Dihydrogen Phosphate, SDS, Methanol, Tris-HCl, Glycine and PVDF membranes were from Fisher Scientific (Waltham, MA, USA); 4-20% tris/glycine-polyacrylamide gels were from Lonza (Walkerville, MD, USA); DAT specific mouse monoclonal antibody raised against synthetic peptide 16 containing amino acids 42 to 59 of the N-terminus of rDAT was from Cell Essentials (Boston, MA, USA); Alkaline phosphatase substrate (ImmunStar) was from Bio-Rad (Hercules, CA, USA); DAT specific goat polyclonal antibody raised against amino acids 601 to 620 of the C-terminus of hDAT and anti-goat IgG 2°

antibody linked to alkaline phosphatase were from Santa Cruz Biotechnology (Dallas, TX, US); PMA was from Calbiochem (San Diego, CA, USA); transferrin receptor and flotillin-1 were from BD Sciences (San Jose, CA, USA); cholesterol E assay kit was from Wako Diagnostics (Richmond, VA, USA).

## RESULTS

### ADHD associated SNP, A559V hDAT and its rat homologue, A558V rDAT, display increased membrane raft microdomain association

DAT undergoes N-terminal phosphorylation which is stimulated by protein kinases and proline directed kinases such as PKC and extracellular signal regulated pathway (ERK) respectively [40, 41, 49, 93, 95]. This phosphorylation is elevated upon treatment of PKC activators such as PMA and/or psychostimulant drugs such as AMPH such that this elevated phosphorylation mediates DA efflux and is accompanied by DAT endocytosis [40, 49, 129, 136, 140, 195, 196].

DAT is partitioned between membrane raft and non-raft microdomains that appear to affect multiple biochemical and regulatory properties of DAT. The membrane microdomain distribution of DAT suggests membrane rafts to be sites of relative lower constitutive phosphorylation and/or higher dephosphorylation which could be related to compartmentalization [56]. Previous studies have shown PMA-stimulation to cause an increase in localization of phosphorylated DAT in membrane raft microdomains suggesting it to be the preferred site for localization of phosphorylated DAT [40, 56].

An ADHD associated SNP, A559V hDAT, shows ADE which was supported by elevated levels of basal phosphorylation [8, 9, 136]. With phosphorylated DAT localized in membrane raft microdomains, we examined the membrane microdomain distribution for A559V, and its rat homologue, A558V rDAT along with other palmitoylation deficient mutants, C581A hDAT and C580A rDAT, which showed

elevated phosphorylation levels [36, 56, 110] [Chapter II]. LLC-PK<sub>1</sub> cells stably expressing WT, A559V hDAT, C581A hDAT or their respective rat homologues were subjected to 1% Brij-58 lysis followed by sucrose density gradient centrifugation and immunoblotting (Fig. 19). In contrast to WT which showed typical levels of membrane raft and non-raft distribution, A559V hDAT, A558V rDAT and mutants with elevated phosphorylation levels displayed increased membrane raft microdomain localization over non-raft microdomain distribution (Raft: hDAT WT,  $51 \pm 1$ ; A559V hDAT,  $62 \pm 2$ ; C581A hDAT,  $69 \pm 1$ ; rDAT WT,  $41 \pm 3$ ; A558V rDAT,  $55 \pm 2$ ; C580A rDAT,  $57 \pm 1$ ). With AMPH mediating PKC-stimulated phosphorylation that is associated with ADE, we examined the effect of AMPH on WT, A559V hDAT, C581A hDAT and their respective rat homologues. LLC-PK<sub>1</sub> cells stably expressing WT, A559V hDAT, C581A hDAT or their respective rDAT homologues were treated with vehicle or 10  $\mu$ M AMPH, followed by 1% Brij-58 lysis, sucrose density gradient centrifugation and immunoblotting (Fig. 20). In contrast to WT which showed typical levels of membrane raft and non-raft distribution, AMPH-stimulation resulted in increased DAT membrane raft microdomain localization over non-raft microdomain distribution (Raft: hDAT WT (basal),  $47 \pm 2$ ; hDAT WT (AMPH),  $64 \pm 1$ ; rDAT WT (basal),  $33 \pm 3$ ; rDAT WT (AMPH),  $59 \pm 3$ ). A559V hDAT, A558V rDAT and mutants with elevated phosphorylation levels failed to show any additional shift in membrane raft microdomain distribution from its earlier elevated DAT membrane raft localization.

These results indicate that mutants displaying ADE and/or elevated phosphorylation, show increased membrane raft localization, suggesting membrane raft microdomains serve as platforms for ADE.



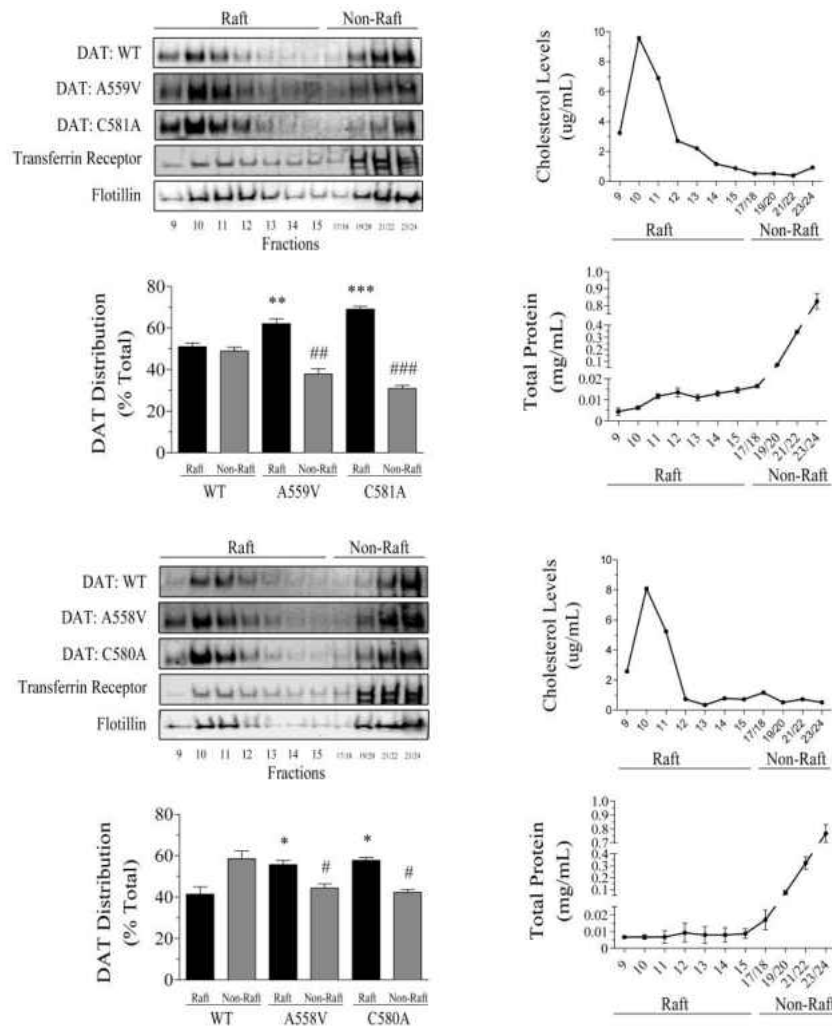


Figure 19: A559V hDAT and A558V rDAT display increased membrane raft microdomain localization.

LLC-PK<sub>1</sub> cells stably expressing the indicated hDAT or rDAT forms were subjected to 1% Brij-58 lysis followed by sucrose density gradient centrifugation. Aliquots of gradient fractions 9-24 were immunoblotted using the indicated antibodies. Representative blots for DAT, transferrin receptor and flotillin distribution between membrane raft and non-raft populations are shown. Designation of raft - non-raft are indicated above the blots. The gradient fractions were also analyzed for total protein and cholesterol contents with mean  $\pm$  S.E. for each fraction shown in the scatterplots on the right.

Fig 19: continued.

Histograms show the quantification of DAT in raft (black bar) and non-raft (gray bars) fractions (% Total, mean  $\pm$  S.E.; \*\*  $p \leq 0.01$ , A559V hDAT (raft) vs. WT (raft); \*\*\*  $p \leq 0.01$ , C581A hDAT (raft) vs. WT (raft); \*  $p \leq 0.05$ , indicated DAT forms (raft) vs. WT (raft); ##  $p \leq 0.01$ , A559V hDAT (non-raft) vs. WT (non-raft); ###  $p \leq 0.01$ , C581A hDAT (non-raft) vs. WT (non-raft); #  $p \leq 0.05$ , indicated DAT forms (non-raft) vs. WT (non-raft); n=8 (hDAT WT), 6 (rDAT WT, A559V hDAT, A558V rDAT), 3 (C581A hDAT, C580A rDAT)). Statistical analyses were done by One-Way ANOVA with Tukey's post-hoc test using graphpad prism software.

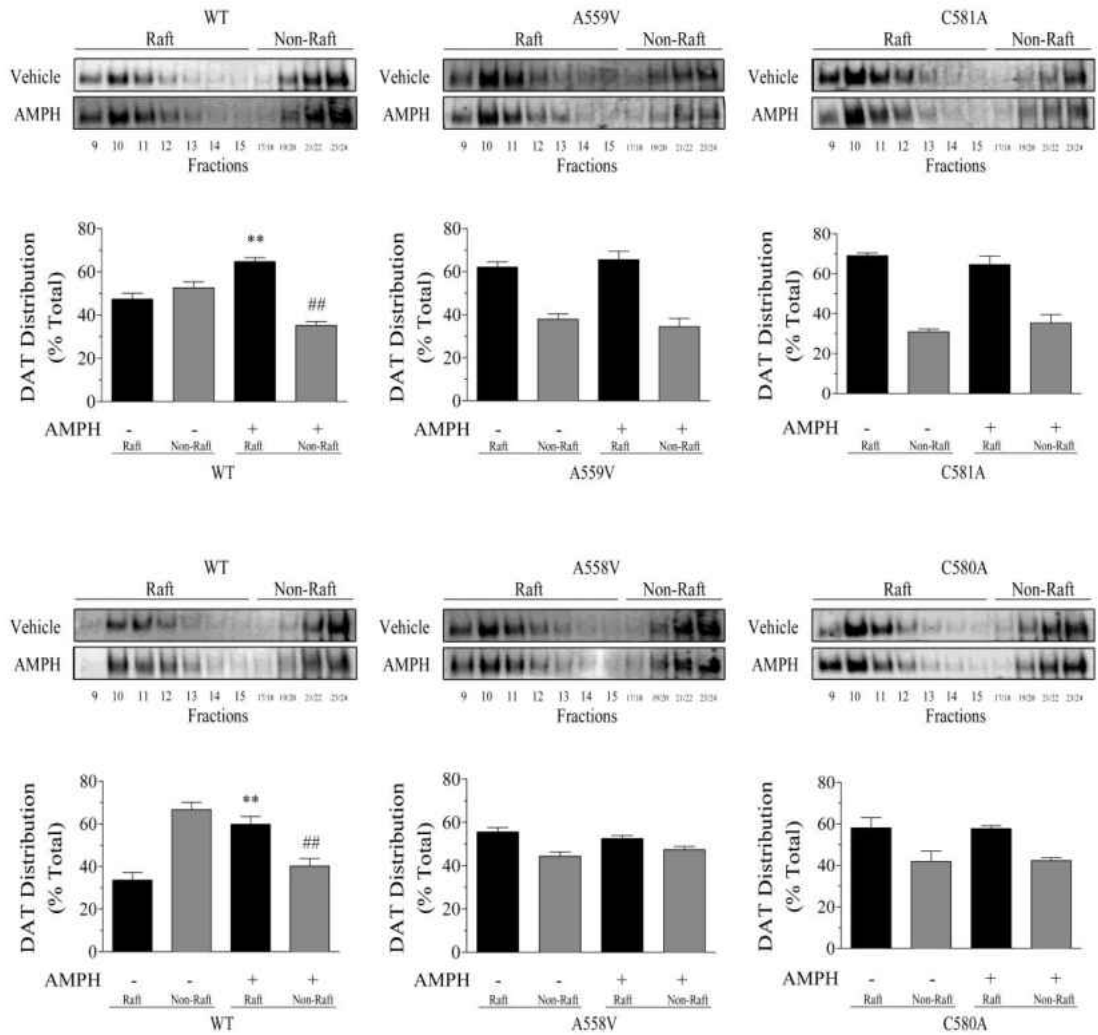


Figure 20: AMPH induces an increase in WT DAT membrane raft microdomain localization.

LLC-PK<sub>1</sub> cells stably expressing the indicated hDAT or rDAT forms were treated with vehicle or 10  $\mu$ M AMPH followed by 1% Brij-58 lysis. The lysates were subjected to sucrose density gradient centrifugation and aliquots of gradient fractions 9-24 were immunoblotted for DAT. Representative blots for DAT distribution between membrane raft and non-raft populations are shown. Designation of raft - non-raft are indicated above the blots.

Fig 20: continued.

Histograms show the quantification of DAT in raft [black bar] and non-raft [gray bars] fractions (% Total, mean  $\pm$  S.E.; \*\*  $p \leq 0.01$ , hDAT WT, rDAT WT (raft) (AMPH) vs. WT hDAT WT, rDAT WT (raft) (basal); ##  $p \leq 0.01$ , hDAT WT, rDAT WT (non-raft) (AMPH) vs. WT hDAT WT, rDAT WT (non-raft) (basal); n=3). Statistical analyses were done by One-Way ANOVA with Tukey's post-hoc test using graphpad prism software.

ADHD associated SNP, A559V hDAT and its rDAT homologue, A558V rDAT,  
display increased lateral membrane mobility

Membrane trafficking is an important DAT regulatory factor and it plays a role in maintaining DAT functional homeostasis. Previous studies have shown A559V hDAT and A558V rDAT to be palmitoylation deficient mutants [Chapter II]. Since palmitoylation influences membrane trafficking, mobility and microdomain distribution, we examined the lateral membrane mobility for A559V hDAT, A558V rDAT and other palmitoylation deficient mutants.

N<sub>2</sub>A cells transiently expressing YFP-tagged WT, A559V hDAT, C581A hDAT or their rat homologues were subjected to FRAP analysis (Fig. 21). In contrast to WT, A559V hDAT, C581A hDAT and their rat homologues displayed increased lateral membrane mobility (lower T<sub>1/2</sub> values) (T<sub>1/2</sub>: hDAT WT, 45 ± 4; A559V hDAT, 24 ± 2; C581A hDAT, 20 ± 41; rDAT WT, 40 ± 4; A558V rDAT, 21 ± 2; C580A rDAT, 20 ± 2). Our experiments [Chapter II] as well as previous studies [8, 9, 169] have shown that A559V hDAT displays elevated levels of phosphorylation which is associated with phosphorylation stimulated ADE. With AMPH stimulating PKC-mediated phosphorylation, we also examined the effect of AMPH on the lateral membrane mobility of WT, A559V hDAT and their rat homologues. The lateral membrane mobility was also studied in presence of PMA, a positive control for phosphorylation stimulation.

N<sub>2</sub>A cells transiently expressing YFP-tagged WT, A559V hDAT or their rat homologues were treated with vehicle or 10 μM AMPH or 1 μM PMA, followed by FRAP analysis (Fig. 22). AMPH and PMA treatments resulted in an increase in lateral membrane mobility (lower T<sub>1/2</sub> values) for WT, A559V hDAT and A558V rDAT

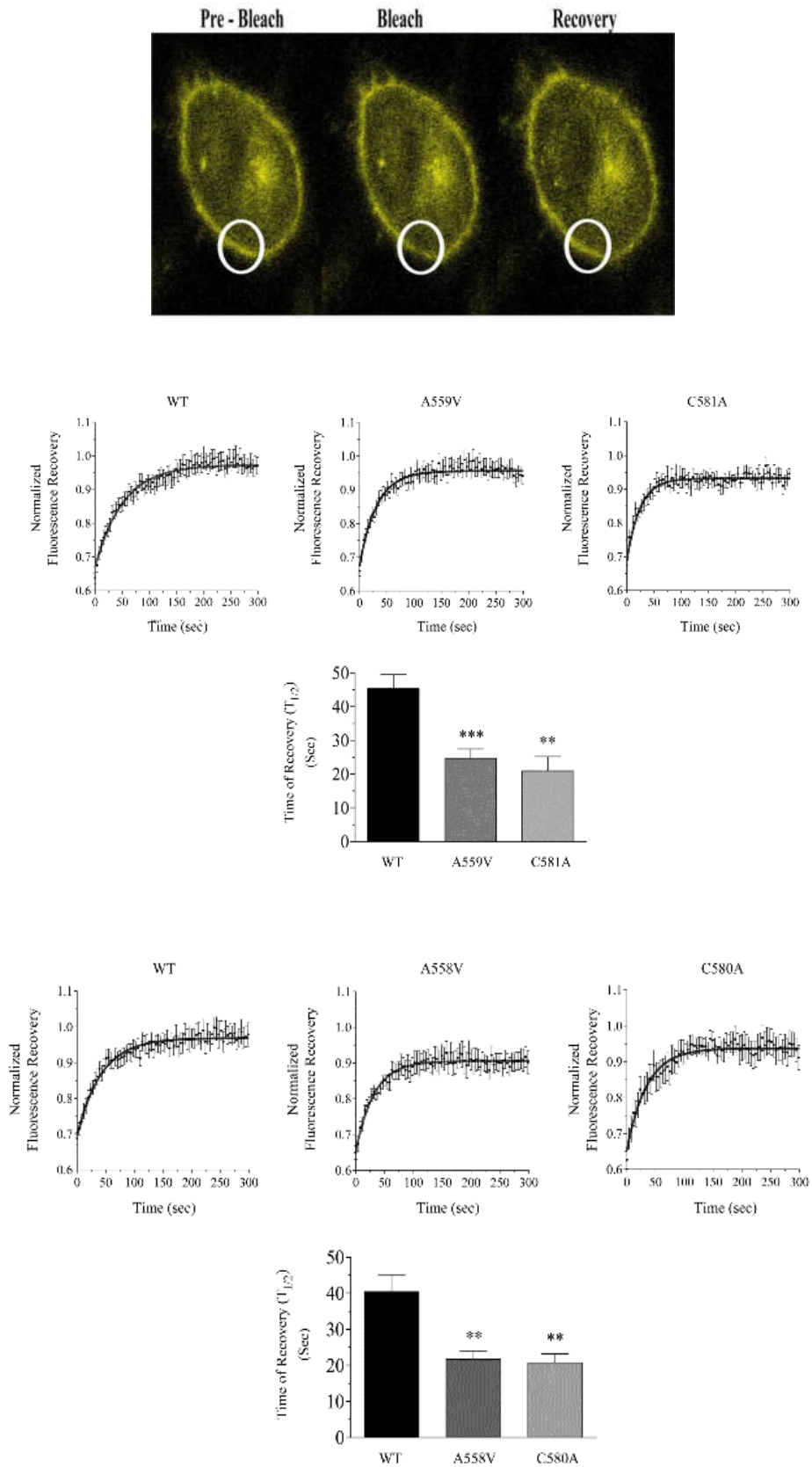


Figure 21: A559V hDAT and C581A and their rDAT homologues display increased lateral membrane mobility.

Fig 21: continued.

N<sub>2</sub>A cells transiently expressing the indicated YFP-tagged hDAT or rDAT forms were subjected to FRAP analysis. The confocal images depict representative YFP-tagged DAT cell fluorescence at pre-bleach, bleached and after recovery time points during FRAP analysis with the circle showing the ROI used for photobleaching. The recovery curves display the fluorescence recovery for each DAT line after photobleaching. The histograms show the quantification of the time taken (sec) by each DAT to recover post photobleaching (Time of Recovery (sec), mean  $\pm$  S.E.; \*\*\*  $p \leq 0.001$ , A559V hDAT vs. WT; \*\*  $p \leq 0.01$ , indicated DAT forms vs. WT; n=30 (hDAT WT), 36 (rDAT WT), 23 (A559V hDAT), 22 (A558V rDAT), 12 (C581A hDAT), 22 (C580A rDAT); n=number of cells analyzed). Statistical analyses were done by unpaired Student's t-test using graphpad prism.

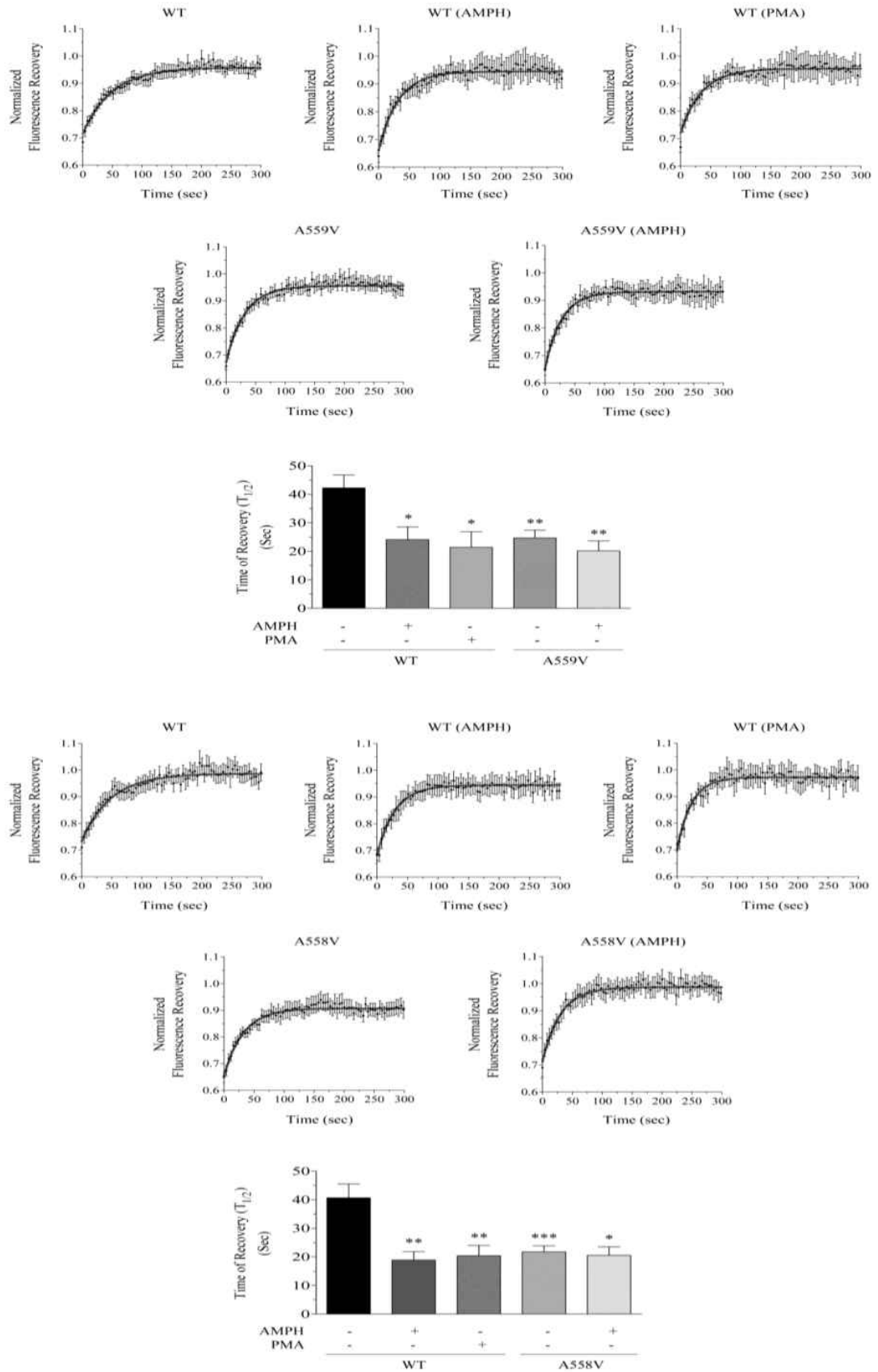


Figure 22: A559V hDAT and A558V rDAT display increased lateral membrane mobility equivalent to that induced by AMPH treatment.



Fig 22: continued.

N<sub>2</sub>A cells transiently expressing the indicated YFP-tagged hDAT or rDAT forms were treated with vehicle or 10  $\mu$ M AMPH or 1  $\mu$ M PMA followed by FRAP analysis. The recovery curves display the fluorescence recovery for each DAT line after photobleaching. The histograms show the quantification of the time taken [sec] by each DAT to recover post photobleaching (Time of Recovery (sec), mean  $\pm$  S.E.; \*  $p \leq 0.05$ , indicated DAT forms (AMPH), (PMA) vs. WT (basal); \*\*  $p \leq 0.01$ , indicated DAT forms (basal), (AMPH), (PMA) vs. WT (basal); \*\*\*  $p \leq 0.001$ , A558V rDAT (basal) vs. WT (basal); n=21 (hDAT WT basal, rDAT WT basal), 10 (hDAT WT AMPH, rDAT WT AMPH, A558V rDAT AMPH), 9 (hDAT WT PMA, A559V hDAT PMA), 22 (A558V rDAT basal), 13 (rDAT WT PMA), 23 (A559V hDAT basal); n=number of cells analyzed). Statistical analyses were done by unpaired Student's t-test using graphpad prism.

failed to show a significant AMPH-induced shift in its lateral mobility, from its already increased level of lateral membrane mobility (lower  $T_{1/2}$  values) which is similar to the mobility for WT upon AMPH treatment ( $T_{1/2}$ : hDAT WT (basal),  $42 \pm 4$ ; hDAT (AMPH),  $24 \pm 4$ ; hDAT (PMA),  $21 \pm 5$ ; A559V hDAT (basal),  $24 \pm 2$ ; A559V hDAT (AMPH),  $20 \pm 3$ ; rDAT WT (basal),  $40 \pm 4$ ; rDAT (AMPH),  $18 \pm 2$ ; rDAT (PMA),  $20 \pm 3$ ; A558V rDAT (basal),  $21 \pm 2$ ; A558V rDAT (AMPH),  $20 \pm 3$ ). Here we see an increase in lateral membrane mobility for palmitoylation deficient mutants. With AMPH or PMA-stimulation indirectly reducing palmitoylation, we believe palmitoylation is the driving force for lateral membrane mobility. For A559V hDAT, the Ala to Val substitution at 559 position could be the driving force for alter palmitoylation, which could lead to increased lateral membrane mobility further driving phosphorylation and membrane raft distribution, affecting DAT's trafficking ability from the plasma membrane into the cytosol and altering lateral mobility within the plasma membrane [71, 215, 216].

#### Palmitoylation is a factor affecting lateral membrane mobility

S-Palmitoylation is known to affect various cellular factors and DAT transport regulation [36]. Thus we also anticipated lateral membrane mobility to be one of the factors that is affected by palmitoylation as it is a lipid modification and its presence could lead to restricted lateral mobility. In order to understand if palmitoylation plays a role in lateral membrane mobility, we examined lateral membrane mobility upon 2BP treatment, an irreversible PAT inhibitor, which prevents palmitoylation.

N<sub>2</sub>A cells transiently expressing YFP-tagged WT hDAT were treated with vehicle or 15  $\mu$ M 2BP for 3 hours, followed by FRAP analysis (Fig. 23). 2BP treatment resulted in an increase in lateral membrane mobility (lower  $T_{1/2}$  values) for WT ( $T_{1/2}$ : hDAT

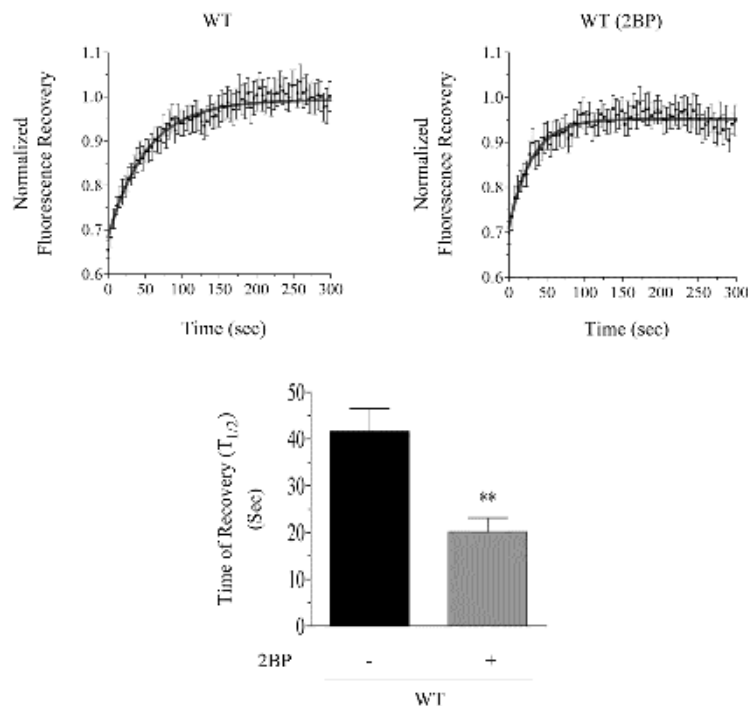


Figure 23: Inhibition of DAT palmitoylation results in increased lateral membrane mobility.

N<sub>2</sub>A cells transiently expressing YFP-tagged WT hDAT was treated with vehicle or 15  $\mu$ M 2BP for 3 hours followed by FRAP analysis. The recovery curves display the fluorescence recovery for DAT after photobleaching in the absence or presence of 2BP treatment. The histogram shows the quantification of the time taken (sec) by each DAT to recover post photobleaching (Time of Recovery (sec), mean  $\pm$  S.E.; \*  $p \leq 0.01$ , WT (2BP) vs. WT (basal); n=20 (hDAT WT basal), 13 (hDAT WT 2BP); n=number of cells analyzed). Statistical analyses were done by unpaired Student's t-test using graphpad prism.

WT (basal),  $41 \pm 4$ ; hDAT (2BP),  $20 \pm 3$ ). With 2BP having no known ability to activate PKC or other kinases [217], we were able to show that palmitoylation is a factor regulating lateral membrane mobility. However, this decreased palmitoylation also leads to increased phosphorylation in a reciprocal manner making it difficult to determine which is a major driving factor.

#### Phosphorylation deficient mutants display decreased lateral membrane mobility

Previous studies have shown that DAT undergoes reciprocal regulation of phosphorylation and palmitoylation [110]. With palmitoylation being a factor driving lateral membrane mobility, we examined the lateral membrane mobility for phosphorylation deficient mutants display increased palmitoylation levels [110] [Chapter II]. N<sub>2</sub>A cells transiently expressing YFP-tagged WT, T53A rDAT, S7A hDAT or S53A hDAT (human homologue for T53A rDAT) were subjected to FRAP analysis (Fig. 24). In contrast to WT, T53A rDAT, S7A hDAT and S53A hDAT showed a decrease in lateral membrane mobility (higher T  $\frac{1}{2}$  values) (T  $\frac{1}{2}$ : hDAT WT,  $38 \pm 4$ ; rDAT WT,  $38 \pm 5$ ; S53A hDAT,  $53 \pm 51$ ; S7A hDAT,  $66 \pm 11$ ; T53A rDAT,  $61 \pm 10$ ). Thus phosphorylation deficient mutants displayed decreased lateral membrane mobility. We believe a reciprocal increase in palmitoylation in these mutants leads to this decrease in lateral membrane mobility.

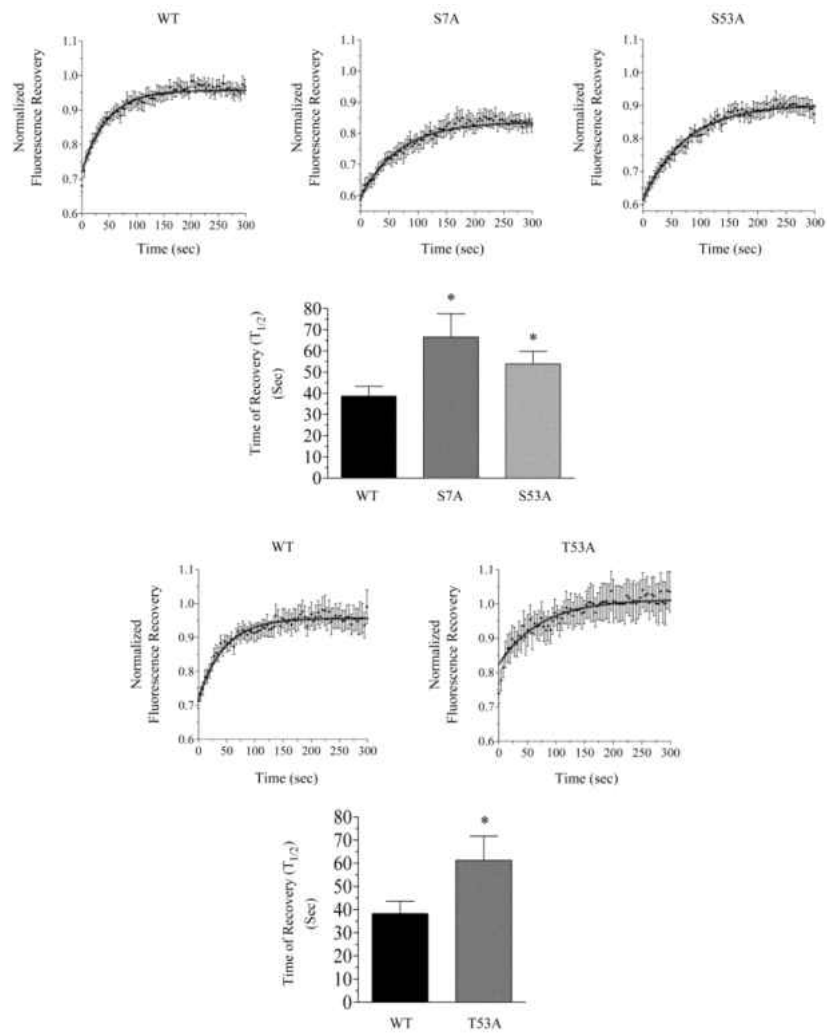


Figure 24: Phosphorylation deficient mutants display decreased lateral membrane mobility.

$N_2A$  cells transiently expressing the indicated YFP-tagged hDAT or rDAT forms were subjected to FRAP analysis. The recovery curves display the fluorescence recovery for each DAT line after photobleaching. The histograms show the quantification of the time taken (sec) by each DAT to recover post photobleaching (Time of Recovery (Sec), mean  $\pm$  S.E.; \*  $p \leq 0.005$ , indicated DAT forms vs. WT;  $n=25$  (hDAT WT), 19 (rDAT WT, S7A hDAT), 22 (S53A hDAT), 12 (T53A rDAT);  $n$ =number of cells analyzed). Statistical analyses were done by unpaired Student's t-test using graphpad prism.

## DISCUSSION

DAT plays an important role in maintaining DA homeostasis thus controlling the clearance of DA from the synapse. Dopaminergic signaling modulates brain activities such as pleasure, motor and cognitive behavior, attention and sleep patterns [2, 3]. DAT, like other transporters is targeted by drugs such as AMPH and COC which affects the overall function of DAT resulting in an increase in synaptic levels of DA [2, 3, 205, 206]. AMPH is known to mediate PKC-stimulated DAT phosphorylation which is associated with DA efflux. A SNP in hDAT associated with ADHD, A559V hDAT displays anomalous DA efflux (ADE) and increased phosphorylation independent of AMPH stimulation [8, 9, 40, 57, 202, 212] [Chapter II]. With PKC-stimulated phosphorylated DAT enriched in membrane raft regions our study showed A559V hDAT, and its rat homologue, A558V rDAT have increased membrane raft microdomain localization. This increased localization was independent of AMPH stimulation, which in WT induced a shift towards membrane raft localization. With rafts being the primary site for DAT phosphorylation and/or phosphorylated DAT localization, we believe membrane rafts serve as a platform for ADE, possibly by increased interaction with raft localized binding partners such as Syntaxin 1A (Syn 1A). Thus membrane rafts could play a role in compartmentalization affecting overall DAT function and could be associated with various neurological disorders [56, 90, 137, 172, 175, 213, 214]. With studies showing DAT undergoing reciprocal regulation for phosphorylation and palmitoylation, A559V hDAT, reciprocally showed lower levels of palmitoylation [Chapter II]. This shows that these post-translational

modifications together play a role in affecting the membrane raft distribution, with phosphorylated DAT aggregating in the membrane raft regions, possibly due to increased interaction with binding partners and palmitoylation helping in membrane raft partitioning by having stable membrane anchoring and integral membrane protein interaction [30, 56, 110, 111, 218].

An important factor in proper DAT function is the membrane trafficking of DAT on the plasma membrane and towards internalization which is affected by these post-translational modifications. Dysregulation of membrane trafficking is associated with many neurological disorders [167, 172]. With palmitoylation affecting membrane mobility and membrane trafficking, our study showed increased lateral membrane mobility for A559V hDAT and other palmitoylation deficient mutants with opposite results for phosphorylation deficient mutants.

With AMPH and PMA-mediated increases in DAT phosphorylation and 2BP-mediated decreases in DAT palmitoylation increasing lateral membrane mobility in WT DAT, we believe palmitoylation to be the driving force for this change in membrane mobility. We believe, for A559V hDAT, the substitution of Val for Ala in close proximity to the palmitoylation site may be the reason for the decrease in palmitoylation. A559 is located at the top extracellular side of TMD 12 and C581 is located at the bottom intracellular side of TMD 12 and the bulkier Val substitution may cause structural changes within TMD 12. This change could make C581 move away from the DAT core region making it lose its flexibility also affecting C581's ability to cap at the cytoplasmic gate. Thus this altered palmitoylation status of A559V hDAT and A558V rDAT which could affect its phosphorylation status by an unknown mechanism which stimulates ADE.

This decreased presence of saturated fatty acid moiety (palmitate) could affect DAT's interaction with binding partners and cholesterol leading to altering its membrane distribution and function, causing an increase in lateral membrane mobility. This in turn could be the driving force for an increase in phosphorylation leading to localization of phosphorylated DAT in membrane raft microdomains, potentially serving as a platform for ADE. We believe other phosphorylation or palmitoylation deficient mutants might show similar unknown mechanisms, so as to show reciprocal regulation of these post-translational modifications.

Currently our knowledge is limited on understanding how these modifications affect lateral membrane mobility and microdomain localization, but our study provides valuable insights.



## REFERENCES

1. Sudhof, T.C., *The synaptic vesicle cycle*. Annual review of neuroscience, 2004. **27**: p. 509-547.
2. Chen, N.H., M.E. Reith, and M.W. Quick, *Synaptic uptake and beyond: the sodium- and chloride-dependent neurotransmitter transporter family SLC6*. Pflugers Arch, 2004. **447**(5): p. 519-31.
3. Kristensen, A.S., et al., *SLC6 neurotransmitter transporters: structure, function, and regulation*. Pharmacological reviews, 2011. **63**(3): p. 585-640.
4. Blakely, R.D. and A.L. Bauman, *Biogenic amine transporters: regulation in flux*. Current opinion in neurobiology, 2000. **10**(3): p. 328-336.
5. Beckman, M.L. and M.W. Quick, *Neurotransmitter transporters: regulators of function and functional regulation*. The Journal of membrane biology, 1998. **164**(1): p. 1-10.
6. Giros, B. and M.G. Caron, *Molecular characterization of the dopamine transporter*. Trends in pharmacological sciences, 1993. **14**(2): p. 43-49.
7. Hahn, M.K. and R.D. Blakely, *The functional impact of SLC6 transporter genetic variation*. Annual review of pharmacology and toxicology, 2007. **47**: p. 401-441.
8. Mazei-Robison, M.S., et al., *Anomalous dopamine release associated with a human dopamine transporter coding variant*. The Journal of neuroscience : the official journal of the Society for Neuroscience, 2008. **28**(28): p. 7040-7046.
9. Bowton, E., et al., *Dysregulation of dopamine transporters via dopamine D2 autoreceptors triggers anomalous dopamine efflux associated with attention-deficit hyperactivity disorder*. The Journal of neuroscience : the official journal of the Society for Neuroscience, 2010. **30**(17): p. 6048-6057.
10. Pramod, A.B., et al., *SLC6 transporters: structure, function, regulation, disease association and therapeutics*. Molecular aspects of medicine, 2013. **34**(2-3): p. 197-219.
11. Alcaro, A., R. Huber, and J. Panksepp, *Behavioral functions of the mesolimbic dopaminergic system: an affective neuroethological perspective*. Brain research reviews, 2007. **56**(2): p. 283-321.
12. Le Moal, M. and H. Simon, *Mesocorticolimbic dopaminergic network: functional and regulatory roles*. Physiological reviews, 1991. **71**(1): p. 155-234.
13. Koob, G.F. and F.E. Bloom, *Cellular and molecular mechanisms of drug dependence*. Science (New York, N.Y.), 1988. **242**(4879): p. 715-723.
14. Palmiter, R.D., *Dopamine signaling in the dorsal striatum is essential for motivated behaviors: lessons from dopamine-deficient mice*. Annals of the New York Academy of Sciences, 2008. **1129**: p. 35-46.
15. Bannon, M.J., *The dopamine transporter: role in neurotoxicity and human disease*. Toxicology and applied pharmacology, 2005. **204**(3): p. 355-360.
16. Kopin, I.J., *The pharmacology of Parkinson's disease therapy: an update*. Annual review of pharmacology and toxicology, 1993. **33**: p. 467-495.

17. Hayden, E.P. and J.I. Nurnberger, *Molecular genetics of bipolar disorder*. Genes, brain, and behavior, 2006. **5**(1): p. 85-95.
18. Mazei-Robison, M.S. and R.D. Blakely, *Expression studies of naturally occurring human dopamine transporter variants identifies a novel state of transporter inactivation associated with Val382Ala*. Neuropharmacology, 2005. **49**(6): p. 737-749.
19. Kalivas, P.W. and N.D. Volkow, *The neural basis of addiction: a pathology of motivation and choice*. The American journal of psychiatry, 2005. **162**(8): p. 1403-1413.
20. Faraone, S.V. and J. Biederman, *Neurobiology of attention-deficit hyperactivity disorder*. Biological psychiatry, 1998. **44**(10): p. 951-958.
21. Temlett, J.A., *Parkinson's disease: biology and aetiology*. Current opinion in neurology, 1996. **9**(4): p. 303-307.
22. Di Chiara, G., et al., *Functions of dopamine in the extrapyramidal and limbic systems. Clues for the mechanism of drug actions*. Arzneimittel-Forschung, 1992. **42**(2A): p. 231-237.
23. Willner P., S.-K.J., *The mesolimbic dopamine system: from motivation to action*. 1992: John Wiley and Sons. 387-400.
24. Chinta, S.J. and J.K. Andersen, *Dopaminergic neurons*. The international journal of biochemistry & cell biology, 2005. **37**(5): p. 942-946.
25. White, F.J., *Synaptic regulation of mesocorticolimbic dopamine neurons*. Annu Rev Neurosci, 1996. **19**: p. 405-36.
26. Gowrishankar, R., M.K. Hahn, and R.D. Blakely, *Good riddance to dopamine: roles for the dopamine transporter in synaptic function and dopamine-associated brain disorders*. Neurochem Int, 2014. **73**: p. 42-8.
27. Patel, A., G. Uhl, and M.J. Kuhar, *Species differences in dopamine transporters: postmortem changes and glycosylation differences*. Journal of neurochemistry, 1993. **61**(2): p. 496-500.
28. Patel, A.P., et al., *Developmentally regulated glycosylation of dopamine transporter*. Brain research. Developmental brain research, 1994. **83**(1): p. 53-58.
29. Zhou, Z., et al., *LeuT-desipramine structure reveals how antidepressants block neurotransmitter reuptake*. Science (New York, N.Y.), 2007. **317**(5843): p. 1390-1393.
30. Penmatsa, A., K.H. Wang, and E. Gouaux, *X-ray structure of dopamine transporter elucidates antidepressant mechanism*. Nature, 2013. **503**(7474): p. 85-90.
31. Yamashita, A., et al., *Crystal structure of a bacterial homologue of Na<sup>+</sup>/Cl<sup>-</sup>-dependent neurotransmitter transporters*. Nature, 2005. **437**(7056): p. 215-223.
32. Forrest, L.R., *Structural biology. (Pseudo-)symmetrical transport*. Science, 2013. **339**(6118): p. 399-401.
33. Manepalli, S., et al., *Monoamine transporter structure, function, dynamics, and drug discovery: a computational perspective*. AAPS J, 2012. **14**(4): p. 820-31.
34. Cheng, M.H., et al., *Insights into the Modulation of Dopamine Transporter Function by Amphetamine, Orphenadrine, and Cocaine Binding*. Frontiers in neurology, 2015. **6**: p. 134.
35. Giros, B., et al., *Cloning, pharmacological characterization, and chromosome assignment of the human dopamine transporter*. Molecular pharmacology, 1992. **42**(3): p. 383-390.

36. Foster, J.D. and R.A. Vaughan, *Palmitoylation controls dopamine transporter kinetics, degradation, and protein kinase C-dependent regulation*. The Journal of biological chemistry, 2011. **286**(7): p. 5175-5186.
37. Nagahara, N., et al., *Protein cysteine modifications: (1) medical chemistry for proteomics*. Current medicinal chemistry, 2009. **16**(33): p. 4419-4444.
38. Foster, J.D., et al., *Dopamine transporter phosphorylation site threonine 53 regulates substrate reuptake and amphetamine-stimulated efflux*. The Journal of biological chemistry, 2012. **287**(35): p. 29702-29712.
39. Foster, J.D., B. Pananusorn, and R.A. Vaughan, *Dopamine transporters are phosphorylated on N-terminal serines in rat striatum*. The Journal of biological chemistry, 2002. **277**(28): p. 25178-25186.
40. Cervinski, M.A., J.D. Foster, and R.A. Vaughan, *Psychoactive substrates stimulate dopamine transporter phosphorylation and down-regulation by cocaine-sensitive and protein kinase C-dependent mechanisms*. The Journal of biological chemistry, 2005. **280**(49): p. 40442-40449.
41. Vaughan, R.A. and J.D. Foster, *Mechanisms of dopamine transporter regulation in normal and disease states*. Trends Pharmacol Sci, 2013. **34**(9): p. 489-96.
42. German, C.L., et al., *Regulation of the Dopamine and Vesicular Monoamine Transporters: Pharmacological Targets and Implications for Disease*. Pharmacol Rev, 2015. **67**(4): p. 1005-24.
43. Eshleman, A.J., et al., *Drug interactions with the dopamine transporter in cryopreserved human caudate*. The Journal of pharmacology and experimental therapeutics, 2001. **296**(2): p. 442-449.
44. Ribeiro, P. and N. Patocka, *Neurotransmitter transporters in schistosomes: structure, function and prospects for drug discovery*. Parasitol Int, 2013. **62**(6): p. 629-38.
45. Li, L.-B.B., et al., *The role of N-glycosylation in function and surface trafficking of the human dopamine transporter*. The Journal of biological chemistry, 2004. **279**(20): p. 21012-21020.
46. Daniels, G.M. and S.G. Amara, *Regulated trafficking of the human dopamine transporter. Clathrin-mediated internalization and lysosomal degradation in response to phorbol esters*. The Journal of biological chemistry, 1999. **274**(50): p. 35794-35801.
47. Miranda, M., et al., *Three ubiquitin conjugation sites in the amino terminus of the dopamine transporter mediate protein kinase C-dependent endocytosis of the transporter*. Mol Biol Cell, 2007. **18**(1): p. 313-23.
48. Gorentla, B.K., et al., *Proline-directed phosphorylation of the dopamine transporter N-terminal domain*. Biochemistry, 2009. **48**(5): p. 1067-1076.
49. Moritz, A.E., et al., *Phosphorylation of dopamine transporter serine 7 modulates cocaine analog binding*. The Journal of biological chemistry, 2013. **288**(1): p. 20-32.
50. Carvelli, L., R.D. Blakely, and L.J. DeFelice, *Dopamine transporter/syntaxin 1A interactions regulate transporter channel activity and dopaminergic synaptic transmission*. Proceedings of the National Academy of Sciences of the United States of America, 2008. **105**(37): p. 14192-14197.
51. Ramamoorthy, S., T.S. Shippenberg, and L.D. Jayanthi, *Regulation of monoamine transporters: Role of transporter phosphorylation*. Pharmacol Ther, 2011. **129**(2): p. 220-38.

52. Sparks, A.B., et al., *Distinct ligand preferences of Src homology 3 domains from Src, Yes, Abl, Cortactin, p53bp2, PLCgamma, Crk, and Grb2*. Proceedings of the National Academy of Sciences of the United States of America, 1996. **93**(4): p. 1540-1544.
53. Beuming, T., et al., *The binding sites for cocaine and dopamine in the dopamine transporter overlap*. Nature neuroscience, 2008. **11**(7): p. 780-789.
54. Huff, R.A., et al., *Phorbol esters increase dopamine transporter phosphorylation and decrease transport Vmax*. Journal of neurochemistry, 1997. **68**(1): p. 225-232.
55. Xiong, J., et al., *Fenpropathrin, a Widely Used Pesticide, Causes Dopaminergic Degeneration*. Mol Neurobiol, 2015.
56. Foster, J.D., et al., *Phorbol ester induced trafficking-independent regulation and enhanced phosphorylation of the dopamine transporter associated with membrane rafts and cholesterol*. Journal of neurochemistry, 2008. **105**(5): p. 1683-1699.
57. Melikian, H.E. and K.M. Buckley, *Membrane trafficking regulates the activity of the human dopamine transporter*. The Journal of neuroscience : the official journal of the Society for Neuroscience, 1999. **19**(18): p. 7699-7710.
58. Loder, M.K. and H.E. Melikian, *The dopamine transporter constitutively internalizes and recycles in a protein kinase C-regulated manner in stably transfected PC12 cell lines*. The Journal of biological chemistry, 2003. **278**(24): p. 22168-22174.
59. Granas, C., et al., *N-terminal truncation of the dopamine transporter abolishes phorbol ester- and substance P receptor-stimulated phosphorylation without impairing transporter internalization*. The Journal of biological chemistry, 2003. **278**(7): p. 4990-5000.
60. Vaughan, R.A., *Phosphorylation and regulation of psychostimulant-sensitive neurotransmitter transporters*. The Journal of pharmacology and experimental therapeutics, 2004. **310**(1): p. 1-7.
61. Hong, W.C. and S.G. Amara, *Differential targeting of the dopamine transporter to recycling or degradative pathways during amphetamine- or PKC-regulated endocytosis in dopamine neurons*. FASEB journal : official publication of the Federation of American Societies for Experimental Biology, 2013. **27**(8): p. 2995-3007.
62. Zhang, L., L.L. Coffey, and M.E. Reith, *Regulation of the functional activity of the human dopamine transporter by protein kinase C*. Biochemical pharmacology, 1997. **53**(5): p. 677-688.
63. Kitayama, S., T. Dohi, and G.R. Uhl, *Phorbol esters alter functions of the expressed dopamine transporter*. European journal of pharmacology, 1994. **268**(2): p. 115-119.
64. Kang, R., et al., *Neural palmitoyl-proteomics reveals dynamic synaptic palmitoylation*. Nature, 2008. **456**(7224): p. 904-9.
65. Jiang, H., Q. Jiang, and J. Feng, *Parkin increases dopamine uptake by enhancing the cell surface expression of dopamine transporter*. The Journal of biological chemistry, 2004. **279**(52): p. 54380-54386.
66. Greaves, J., et al., *The fat controller: roles of palmitoylation in intracellular protein trafficking and targeting to membrane microdomains (Review)*. Molecular membrane biology, 2009. **26**(1): p. 67-79.
67. Greaves, J. and L.H. Chamberlain, *Palmitoylation-dependent protein sorting*. The Journal of cell biology, 2007. **176**(3): p. 249-254.

68. Linder, M.E. and R.J. Deschenes, *Palmitoylation: policing protein stability and traffic*. Nature reviews. Molecular cell biology, 2007. **8**(1): p. 74-84.
69. Resh, M.D., *Palmitoylation of ligands, receptors, and intracellular signaling molecules*. Science's STKE : signal transduction knowledge environment, 2006. **2006**(359).
70. Munday, A.D. and J.A.A. López, *Posttranslational protein palmitoylation: promoting platelet purpose*. Arteriosclerosis, thrombosis, and vascular biology, 2007. **27**(7): p. 1496-1499.
71. Salaun, C., J. Greaves, and L.H. Chamberlain, *The intracellular dynamic of protein palmitoylation*. The Journal of cell biology, 2010. **191**(7): p. 1229-1238.
72. Greaves, J., J.A. Carmichael, and L.H. Chamberlain, *The palmitoyl transferase DHHC2 targets a dynamic membrane cycling pathway: regulation by a C-terminal domain*. Mol Biol Cell, 2011. **22**(11): p. 1887-95.
73. Navaroli, D.M., et al., *The plasma membrane-associated GTPase Rin interacts with the dopamine transporter and is required for protein kinase C-regulated dopamine transporter trafficking*. The Journal of neuroscience : the official journal of the Society for Neuroscience, 2011. **31**(39): p. 13758-13770.
74. Holton, K.L., M.K. Loder, and H.E. Melikian, *Nonclassical, distinct endocytic signals dictate constitutive and PKC-regulated neurotransmitter transporter internalization*. Nature neuroscience, 2005. **8**(7): p. 881-888.
75. Kitayama, S., et al., *Dopamine transporter site-directed mutations differentially alter substrate transport and cocaine binding*. Proceedings of the National Academy of Sciences of the United States of America, 1992. **89**(16): p. 7782-7785.
76. Loland, C.J., et al., *Generation of an activating Zn(2+) switch in the dopamine transporter: mutation of an intracellular tyrosine constitutively alters the conformational equilibrium of the transport cycle*. Proc Natl Acad Sci U S A, 2002. **99**(3): p. 1683-8.
77. Hamilton, P.J., et al., *De novo mutation in the dopamine transporter gene associates dopamine dysfunction with autism spectrum disorder*. Mol Psychiatry, 2013. **18**(12): p. 1315-23.
78. Fraser, R., et al., *An N-terminal threonine mutation produces an efflux-favorable, sodium-primed conformation of the human dopamine transporter*. Mol Pharmacol, 2014. **86**(1): p. 76-85.
79. Chen, N. and M.E. Reith, *Interaction between dopamine and its transporter: role of intracellular sodium ions and membrane potential*. J Neurochem, 2004. **89**(3): p. 750-65.
80. Borre, L., et al., *The second sodium site in the dopamine transporter controls cation permeation and is regulated by chloride*. J Biol Chem, 2014. **289**(37): p. 25764-73.
81. Zomot, E., et al., *Mechanism of chloride interaction with neurotransmitter:sodium symporters*. Nature, 2007. **449**(7163): p. 726-30.
82. Erreger, K., et al., *Currents in response to rapid concentration jumps of amphetamine uncover novel aspects of human dopamine transporter function*. J Neurosci, 2008. **28**(4): p. 976-89.
83. Zhao, C. and S.Y. Noskov, *The role of local hydration and hydrogen-bonding dynamics in ion and solute release from ion-coupled secondary transporters*. Biochemistry, 2011. **50**(11): p. 1848-56.

84. Shi, L., et al., *The mechanism of a neurotransmitter:sodium symporter--inward release of Na<sup>+</sup> and substrate is triggered by substrate in a second binding site.* Mol Cell, 2008. **30**(6): p. 667-77.
85. Norgaard-Nielsen, K. and U. Gether, *Zn<sup>2+</sup> modulation of neurotransmitter transporters.* Handb Exp Pharmacol, 2006(175): p. 1-22.
86. Singh, S.K., et al., *A competitive inhibitor traps LeuT in an open-to-out conformation.* Science, 2008. **322**(5908): p. 1655-61.
87. Norregaard, L., et al., *Delineation of an endogenous zinc-binding site in the human dopamine transporter.* EMBO J, 1998. **17**(15): p. 4266-73.
88. Kniazeff, J., et al., *An intracellular interaction network regulates conformational transitions in the dopamine transporter.* J Biol Chem, 2008. **283**(25): p. 17691-701.
89. Pedersen, A.V., T.F. Andreassen, and C.J. Loland, *A conserved salt bridge between transmembrane segments 1 and 10 constitutes an extracellular gate in the dopamine transporter.* The Journal of biological chemistry, 2014. **289**(50): p. 35003-35014.
90. Hong, W.C. and S.G. Amara, *Membrane cholesterol modulates the outward facing conformation of the dopamine transporter and alters cocaine binding.* J Biol Chem, 2010. **285**(42): p. 32616-26.
91. Gnegy, M.E., *The effect of phosphorylation on amphetamine-mediated outward transport.* European journal of pharmacology, 2003. **479**(1-3): p. 83-91.
92. Sorkina, T., J. Caltagarone, and A. Sorkin, *Flotillins regulate membrane mobility of the dopamine transporter but are not required for its protein kinase C dependent endocytosis.* Traffic, 2013. **14**(6): p. 709-24.
93. Johnson, L.A., et al., *Regulation of amphetamine-stimulated dopamine efflux by protein kinase C beta.* J Biol Chem, 2005. **280**(12): p. 10914-9.
94. Butler, B., et al., *Dopamine Transporter Activity Is Modulated by alpha-synuclein.* J Biol Chem, 2015.
95. Fog, J.U., et al., *Calmodulin kinase II interacts with the dopamine transporter C terminus to regulate amphetamine-induced reverse transport.* Neuron, 2006. **51**(4): p. 417-29.
96. Moron, J.A., et al., *Mitogen-activated protein kinase regulates dopamine transporter surface expression and dopamine transport capacity.* J Neurosci, 2003. **23**(24): p. 8480-8.
97. Chefer, V.I., et al., *Kappa-opioid receptor activation prevents alterations in mesocortical dopamine neurotransmission that occur during abstinence from cocaine.* Neuroscience, 2000. **101**(3): p. 619-27.
98. Zapata, A., et al., *Regulation of dopamine transporter function and cell surface expression by D3 dopamine receptors.* J Biol Chem, 2007. **282**(49): p. 35842-54.
99. Mayfield, R.D. and N.R. Zahniser, *Dopamine D2 receptor regulation of the dopamine transporter expressed in Xenopus laevis oocytes is voltage-independent.* Molecular pharmacology, 2001. **59**(1): p. 113-121.
100. Yan, Z., et al., *D(2) dopamine receptors induce mitogen-activated protein kinase and cAMP response element-binding protein phosphorylation in neurons.* Proceedings of the National Academy of Sciences of the United States of America, 1999. **96**(20): p. 11607-11612.

101. Lee, K.H., et al., *Syntaxin 1A and receptor for activated C kinase interact with the N-terminal region of human dopamine transporter*. *Neurochem Res*, 2004. **29**(7): p. 1405-9.
102. Cremona, M.L., et al., *Flotillin-1 is essential for PKC-triggered endocytosis and membrane microdomain localization of DAT*. *Nat Neurosci*, 2011. **14**(4): p. 469-77.
103. Pizzo, A.B., et al., *The membrane raft protein Flotillin-1 is essential in dopamine neurons for amphetamine-induced behavior in Drosophila*. *Mol Psychiatry*, 2013. **18**(7): p. 824-33.
104. Pizzo, A.B., et al., *Amphetamine-induced behavior requires CaMKII-dependent dopamine transporter phosphorylation*. *Mol Psychiatry*, 2014. **19**(3): p. 279-81.
105. Lee, F.J., et al., *Dopamine transporter cell surface localization facilitated by a direct interaction with the dopamine D2 receptor*. *EMBO J*, 2007. **26**(8): p. 2127-36.
106. Lin, D.T., et al., *Regulation of AMPA receptor extrasynaptic insertion by 4.1N, phosphorylation and palmitoylation*. *Nat Neurosci*, 2009. **12**(7): p. 879-87.
107. Moffett, S., et al., *Palmitoylated cysteine 341 modulates phosphorylation of the beta2-adrenergic receptor by the cAMP-dependent protein kinase*. *J Biol Chem*, 1996. **271**(35): p. 21490-7.
108. Moffett, S., et al., *Altered phosphorylation and desensitization patterns of a human beta 2-adrenergic receptor lacking the palmitoylated Cys341*. *EMBO J*, 1993. **12**(1): p. 349-56.
109. Salaun, C., J. Greaves, and L.H. Chamberlain, *The intracellular dynamic of protein palmitoylation*. *J Cell Biol*, 2010. **191**(7): p. 1229-38.
110. Moritz, A.E., et al., *Reciprocal Phosphorylation and Palmitoylation Control Dopamine Transporter Kinetics*. *J Biol Chem*, 2015.
111. Blaskovic, S., M. Blanc, and F.G. van der Goot, *What does S-palmitoylation do to membrane proteins?* *FEBS J*, 2013. **280**(12): p. 2766-74.
112. Blakely, R.D., A. Ortega, and M.B. Robinson, *The brain in flux: genetic, physiologic, and therapeutic perspectives on transporters in the CNS*. *Neurochem Int*, 2014. **73**: p. 1-3.
113. Sakrikar, D., et al., *Attention deficit/hyperactivity disorder-derived coding variation in the dopamine transporter disrupts microdomain targeting and trafficking regulation*. *J Neurosci*, 2012. **32**(16): p. 5385-97.
114. Hansen, F.H., et al., *Missense dopamine transporter mutations associate with adult parkinsonism and ADHD*. *J Clin Invest*, 2014. **124**(7): p. 3107-20.
115. Wise, R.A. and M.A. Bozarth, *Brain mechanisms of drug reward and euphoria*. *Psychiatr Med*, 1985. **3**(4): p. 445-60.
116. Kuhar, M.J., M.C. Ritz, and J.W. Boja, *The dopamine hypothesis of the reinforcing properties of cocaine*. *Trends Neurosci*, 1991. **14**(7): p. 299-302.
117. Koob, G.F. and E.J. Nestler, *The neurobiology of drug addiction*. *The Journal of neuropsychiatry and clinical neurosciences*, 1997. **9**(3): p. 482-497.
118. Jones, S.R., et al., *Dopamine neuronal transport kinetics and effects of amphetamine*. *Journal of neurochemistry*, 1999. **73**(6): p. 2406-2414.
119. Espana, R.A. and S.R. Jones, *Presynaptic dopamine modulation by stimulant self-administration*. *Front Biosci (Schol Ed)*, 2013. **5**: p. 261-76.
120. Uhl, G.R. and P.S. Johnson, *Neurotransmitter transporters: three important gene families for neuronal function*. *J Exp Biol*, 1994. **196**: p. 229-36.

121. Heikkila, R.E., et al., *Amphetamine: evaluation of d- and l-isomers as releasing agents and uptake inhibitors for 3H-dopamine and 3H-norepinephrine in slices of rat neostriatum and cerebral cortex*. J Pharmacol Exp Ther, 1975. **194**(1): p. 47-56.
122. Sulzer, D. and S. Rayport, *Amphetamine and other psychostimulants reduce pH gradients in midbrain dopaminergic neurons and chromaffin granules: a mechanism of action*. Neuron, 1990. **5**(6): p. 797-808.
123. Sulzer, D., et al., *Weak base model of amphetamine action*. Ann N Y Acad Sci, 1992. **654**: p. 525-8.
124. Ramsson, E.S., et al., *High doses of amphetamine augment, rather than disrupt, exocytotic dopamine release in the dorsal and ventral striatum of the anesthetized rat*. J Neurochem, 2011. **119**(6): p. 1162-72.
125. Ramsson, E.S., et al., *Amphetamine augments action potential-dependent dopaminergic signaling in the striatum in vivo*. J Neurochem, 2011. **117**(6): p. 937-48.
126. Richards, T.L. and N.R. Zahniser, *Rapid substrate-induced down-regulation in function and surface localization of dopamine transporters: rat dorsal striatum versus nucleus accumbens*. J Neurochem, 2009. **108**(6): p. 1575-84.
127. Saunders, C., et al., *Amphetamine-induced loss of human dopamine transporter activity: an internalization-dependent and cocaine-sensitive mechanism*. Proc Natl Acad Sci U S A, 2000. **97**(12): p. 6850-5.
128. German, C.L., G.R. Hanson, and A.E. Fleckenstein, *Amphetamine and methamphetamine reduce striatal dopamine transporter function without concurrent dopamine transporter relocalization*. J Neurochem, 2012. **123**(2): p. 288-97.
129. Sulzer, D., et al., *Mechanisms of neurotransmitter release by amphetamines: a review*. Prog Neurobiol, 2005. **75**(6): p. 406-33.
130. Daberkow, D.P., et al., *Amphetamine paradoxically augments exocytotic dopamine release and phasic dopamine signals*. J Neurosci, 2013. **33**(2): p. 452-63.
131. Baucum, A.J., 2nd, et al., *Methamphetamine increases dopamine transporter higher molecular weight complex formation via a dopamine- and hyperthermia-associated mechanism*. J Neurosci, 2004. **24**(13): p. 3436-43.
132. Chi, L. and M.E. Reith, *Substrate-induced trafficking of the dopamine transporter in heterologously expressing cells and in rat striatal synaptosomal preparations*. J Pharmacol Exp Ther, 2003. **307**(2): p. 729-36.
133. Kahlig, K.M., J.A. Javitch, and A. Galli, *Amphetamine regulation of dopamine transport. Combined measurements of transporter currents and transporter imaging support the endocytosis of an active carrier*. J Biol Chem, 2004. **279**(10): p. 8966-75.
134. Sorkina, T., et al., *Oligomerization of dopamine transporters visualized in living cells by fluorescence resonance energy transfer microscopy*. J Biol Chem, 2003. **278**(30): p. 28274-83.
135. Kahlig, K.M., et al., *Regulation of dopamine transporter trafficking by intracellular amphetamine*. Mol Pharmacol, 2006. **70**(2): p. 542-8.
136. Khoshbouei, H., et al., *N-terminal phosphorylation of the dopamine transporter is required for amphetamine-induced efflux*. PLoS Biol, 2004. **2**(3): p. E78.



137. Binda, F., et al., *Syntaxin 1A interaction with the dopamine transporter promotes amphetamine-induced dopamine efflux*. Mol Pharmacol, 2008. **74**(4): p. 1101-8.
138. Dipace, C., et al., *Amphetamine induces a calcium/calmodulin-dependent protein kinase II-dependent reduction in norepinephrine transporter surface expression linked to changes in syntaxin 1A/transporter complexes*. Mol Pharmacol, 2007. **71**(1): p. 230-9.
139. Sung, U., et al., *A regulated interaction of syntaxin 1A with the antidepressant-sensitive norepinephrine transporter establishes catecholamine clearance capacity*. J Neurosci, 2003. **23**(5): p. 1697-709.
140. Robertson, S.D., H.J. Matthies, and A. Galli, *A closer look at amphetamine-induced reverse transport and trafficking of the dopamine and norepinephrine transporters*. Mol Neurobiol, 2009. **39**(2): p. 73-80.
141. Kahlig, K.M., et al., *Amphetamine induces dopamine efflux through a dopamine transporter channel*. Proc Natl Acad Sci U S A, 2005. **102**(9): p. 3495-500.
142. Scholze, P., et al., *The role of zinc ions in reverse transport mediated by monoamine transporters*. J Biol Chem, 2002. **277**(24): p. 21505-13.
143. Wei, Y., et al., *Dopamine transporter activity mediates amphetamine-induced inhibition of Akt through a Ca<sup>2+</sup>/calmodulin-dependent kinase II-dependent mechanism*. Mol Pharmacol, 2007. **71**(3): p. 835-42.
144. Doolen, S. and N.R. Zahniser, *Protein tyrosine kinase inhibitors alter human dopamine transporter activity in Xenopus oocytes*. J Pharmacol Exp Ther, 2001. **296**(3): p. 931-8.
145. Carvelli, L., et al., *PI 3-kinase regulation of dopamine uptake*. J Neurochem, 2002. **81**(4): p. 859-69.
146. Garcia, B.G., et al., *Akt is essential for insulin modulation of amphetamine-induced human dopamine transporter cell-surface redistribution*. Mol Pharmacol, 2005. **68**(1): p. 102-9.
147. Miller, G.W., et al., *Dopamine transporters and neuronal injury*. Trends Pharmacol Sci, 1999. **20**(10): p. 424-9.
148. McHugh, P.C. and D.A. Buckley, *The structure and function of the dopamine transporter and its role in CNS diseases*. Vitam Horm, 2015. **98**: p. 339-69.
149. Haddley, K., et al., *Molecular genetics of monoamine transporters: relevance to brain disorders*. Neurochem Res, 2008. **33**(4): p. 652-67.
150. Swant, J., et al., *alpha-Synuclein stimulates a dopamine transporter-dependent chloride current and modulates the activity of the transporter*. J Biol Chem, 2011. **286**(51): p. 43933-43.
151. Lee, F.J., et al., *Direct binding and functional coupling of alpha-synuclein to the dopamine transporters accelerate dopamine-induced apoptosis*. FASEB J, 2001. **15**(6): p. 916-26.
152. Moszczynska, A., et al., *Parkin disrupts the alpha-synuclein/dopamine transporter interaction: consequences toward dopamine-induced toxicity*. J Mol Neurosci, 2007. **32**(3): p. 217-27.
153. Kitada, T., et al., *Mutations in the parkin gene cause autosomal recessive juvenile parkinsonism*. Nature, 1998. **392**(6676): p. 605-8.
154. Steinkellner, T., et al., *Ca(2+)/calmodulin-dependent protein kinase IIalpha (alphaCaMKII) controls the activity of the dopamine transporter: implications for Angelman syndrome*. J Biol Chem, 2012. **287**(35): p. 29627-35.

155. Weeber, E.J., et al., *Derangements of hippocampal calcium/calmodulin-dependent protein kinase II in a mouse model for Angelman mental retardation syndrome*. J Neurosci, 2003. **23**(7): p. 2634-44.
156. Childress, A.C. and S.A. Berry, *Pharmacotherapy of attention-deficit hyperactivity disorder in adolescents*. Drugs, 2012. **72**(3): p. 309-25.
157. Polanczyk, G., et al., *The worldwide prevalence of ADHD: a systematic review and meta-regression analysis*. Am J Psychiatry, 2007. **164**(6): p. 942-8.
158. Willcutt, E.G., et al., *Validity of DSM-IV attention deficit/hyperactivity disorder symptom dimensions and subtypes*. J Abnorm Psychol, 2012. **121**(4): p. 991-1010.
159. Levy, F., et al., *Attention-deficit hyperactivity disorder: a category or a continuum? Genetic analysis of a large-scale twin study*. J Am Acad Child Adolesc Psychiatry, 1997. **36**(6): p. 737-44.
160. Stevenson, J., *Evidence for a genetic etiology in hyperactivity in children*. Behav Genet, 1992. **22**(3): p. 337-44.
161. Levy, F., *The dopamine theory of attention deficit hyperactivity disorder (ADHD)*. Aust N Z J Psychiatry, 1991. **25**(2): p. 277-83.
162. Grunhage, F., et al., *Systematic screening for DNA sequence variation in the coding region of the human dopamine transporter gene (DAT1)*. Mol Psychiatry, 2000. **5**(3): p. 275-82.
163. Cargill, M., et al., *Characterization of single-nucleotide polymorphisms in coding regions of human genes*. Nat Genet, 1999. **22**(3): p. 231-8.
164. Mazei-Robison, M.S., et al., *Sequence variation in the human dopamine transporter gene in children with attention deficit hyperactivity disorder*. Neuropharmacology, 2005. **49**(6): p. 724-36.
165. Ueno, S., et al., *Identification of a novel polymorphism of the human dopamine transporter (DAT1) gene and the significant association with alcoholism*. Mol Psychiatry, 1999. **4**(6): p. 552-7.
166. Lin, Z. and G.R. Uhl, *Human dopamine transporter gene variation: effects of protein coding variants V55A and V382A on expression and uptake activities*. Pharmacogenomics J, 2003. **3**(3): p. 159-68.
167. Kovtun, O., et al., *Single-quantum-dot tracking reveals altered membrane dynamics of an attention-deficit/hyperactivity-disorder-derived dopamine transporter coding variant*. ACS Chem Neurosci, 2015. **6**(4): p. 526-34.
168. Amanchy, R., et al., *A curated compendium of phosphorylation motifs*. Nat Biotechnol, 2007. **25**(3): p. 285-6.
169. Bowton, E., et al., *SLC6A3 coding variant Ala559Val found in two autism probands alters dopamine transporter function and trafficking*. Transl Psychiatry, 2014. **4**: p. e464.
170. Hoogman, M., et al., *The dopamine transporter haplotype and reward-related striatal responses in adult ADHD*. Eur Neuropsychopharmacol, 2013. **23**(6): p. 469-78.
171. Mergy, M.A., et al., *The rare DAT coding variant Val559 perturbs DA neuron function, changes behavior, and alters in vivo responses to psychostimulants*. Proc Natl Acad Sci U S A, 2014. **111**(44): p. E4779-88.
172. Adkins, E.M., et al., *Membrane mobility and microdomain association of the dopamine transporter studied with fluorescence correlation spectroscopy and fluorescence recovery after photobleaching*. Biochemistry, 2007. **46**(37): p. 10484-97.

173. Jones, K.T., J. Zhen, and M.E. Reith, *Importance of cholesterol in dopamine transporter function*. J Neurochem, 2012. **123**(5): p. 700-15.
174. Brown, D.A. and E. London, *Structure and function of sphingolipid- and cholesterol-rich membrane rafts*. J Biol Chem, 2000. **275**(23): p. 17221-4.
175. Pike, L.J., *Rafts defined: a report on the Keystone Symposium on Lipid Rafts and Cell Function*. J Lipid Res, 2006. **47**(7): p. 1597-8.
176. Pike, L.J., *Growth factor receptors, lipid rafts and caveolae: an evolving story*. Biochim Biophys Acta, 2005. **1746**(3): p. 260-73.
177. Boudanova, E., et al., *Dopamine transporter endocytic determinants: carboxy terminal residues critical for basal and PKC-stimulated internalization*. Mol Cell Neurosci, 2008. **39**(2): p. 211-7.
178. Keller, C.A., et al., *The gamma2 subunit of GABA(A) receptors is a substrate for palmitoylation by GODZ*. J Neurosci, 2004. **24**(26): p. 5881-91.
179. Sharma, C., X.H. Yang, and M.E. Hemler, *DHHC2 affects palmitoylation, stability, and functions of tetraspanins CD9 and CD151*. Mol Biol Cell, 2008. **19**(8): p. 3415-25.
180. Lemonidis, K., et al., *The Golgi S-acylation machinery comprises zDHHC enzymes with major differences in substrate affinity and S-acylation activity*. Mol Biol Cell, 2014. **25**(24): p. 3870-83.
181. Fukata, Y. and M. Fukata, *Protein palmitoylation in neuronal development and synaptic plasticity*. Nat Rev Neurosci, 2010. **11**(3): p. 161-75.
182. Tsutsumi, R., Y. Fukata, and M. Fukata, *Discovery of protein-palmitoylating enzymes*. Pflugers Arch, 2008. **456**(6): p. 1199-206.
183. Bijlmakers, M.J. and M. Marsh, *The on-off story of protein palmitoylation*. Trends Cell Biol, 2003. **13**(1): p. 32-42.
184. Rocks, O., et al., *The palmitoylation machinery is a spatially organizing system for peripheral membrane proteins*. Cell, 2010. **141**(3): p. 458-71.
185. Ohno, Y., et al., *Intracellular localization and tissue-specific distribution of human and yeast DHHC cysteine-rich domain-containing proteins*. Biochim Biophys Acta, 2006. **1761**(4): p. 474-83.
186. Noritake, J., et al., *Mobile DHHC palmitoylating enzyme mediates activity-sensitive synaptic targeting of PSD-95*. J Cell Biol, 2009. **186**(1): p. 147-60.
187. Huang, K., et al., *Neuronal palmitoyl acyl transferases exhibit distinct substrate specificity*. FASEB J, 2009. **23**(8): p. 2605-15.
188. Mansouri, M.R., et al., *Loss of ZDHHC15 expression in a woman with a balanced translocation t(X;15)(q13.3;cen) and severe mental retardation*. Eur J Hum Genet, 2005. **13**(8): p. 970-7.
189. Raymond, F.L., et al., *Mutations in ZDHHC9, which encodes a palmitoyltransferase of NRAS and HRAS, cause X-linked mental retardation associated with a Marfanoid habitus*. Am J Hum Genet, 2007. **80**(5): p. 982-7.
190. Greaves, J. and L.H. Chamberlain, *DHHC palmitoyl transferases: substrate interactions and (patho)physiology*. Trends Biochem Sci, 2011. **36**(5): p. 245-53.
191. Giros, B., et al., *Hyperlocomotion and indifference to cocaine and amphetamine in mice lacking the dopamine transporter*. Nature, 1996. **379**(6566): p. 606-12.
192. Schmitt, K.C. and M.E. Reith, *Regulation of the dopamine transporter: aspects relevant to psychostimulant drugs of abuse*. Ann N Y Acad Sci, 2010. **1187**: p. 316-40.

193. Dreher, J.C., et al., *Variation in dopamine genes influences responsivity of the human reward system*. Proc Natl Acad Sci U S A, 2009. **106**(2): p. 617-22.
194. Wan, J., et al., *Palmitoylated proteins: purification and identification*. Nat Protoc, 2007. **2**(7): p. 1573-84.
195. Khoshbouei, H., et al., *Amphetamine-induced dopamine efflux. A voltage-sensitive and intracellular Na<sup>+</sup>-dependent mechanism*. J Biol Chem, 2003. **278**(14): p. 12070-7.
196. Amara, S.G. and J.L. Arriza, *Neurotransmitter transporters: three distinct gene families*. Curr Opin Neurobiol, 1993. **3**(3): p. 337-44.
197. Lu, K.P., Y.C. Liou, and X.Z. Zhou, *Pinning down proline-directed phosphorylation signaling*. Trends Cell Biol, 2002. **12**(4): p. 164-72.
198. Drisdell, R.C., et al., *Assays of protein palmitoylation*. Methods, 2006. **40**(2): p. 127-34.
199. Seeman, P. and H.B. Niznik, *Dopamine receptors and transporters in Parkinson's disease and schizophrenia*. FASEB J, 1990. **4**(10): p. 2737-44.
200. Wise, R.A., *Drug-activation of brain reward pathways*. Drug Alcohol Depend, 1998. **51**(1-2): p. 13-22.
201. Volkow, N.D., et al., *Depressed dopamine activity in caudate and preliminary evidence of limbic involvement in adults with attention-deficit/hyperactivity disorder*. Arch Gen Psychiatry, 2007. **64**(8): p. 932-40.
202. Gorentla, B.K. and R.A. Vaughan, *Differential effects of dopamine and psychoactive drugs on dopamine transporter phosphorylation and regulation*. Neuropharmacology, 2005. **49**(6): p. 759-68.
203. Forrest, L.R., et al., *Mechanism for alternating access in neurotransmitter transporters*. Proc Natl Acad Sci U S A, 2008. **105**(30): p. 10338-43.
204. Krishnamurthy, H. and E. Gouaux, *X-ray structures of LeuT in substrate-free outward-open and apo inward-open states*. Nature, 2012. **481**(7382): p. 469-74.
205. Torres, G.E., R.R. Gainetdinov, and M.G. Caron, *Plasma membrane monoamine transporters: structure, regulation and function*. Nat Rev Neurosci, 2003. **4**(1): p. 13-25.
206. Gether, U., et al., *Neurotransmitter transporters: molecular function of important drug targets*. Trends Pharmacol Sci, 2006. **27**(7): p. 375-83.
207. Kurian, M.A., et al., *Homozygous loss-of-function mutations in the gene encoding the dopamine transporter are associated with infantile parkinsonism-dystonia*. J Clin Invest, 2009. **119**(6): p. 1595-603.
208. Zahniser, N.R. and S. Doolen, *Chronic and acute regulation of Na<sup>+</sup>/Cl<sup>-</sup>-dependent neurotransmitter transporters: drugs, substrates, presynaptic receptors, and signaling systems*. Pharmacol Ther, 2001. **92**(1): p. 21-55.
209. Torres, G.E., et al., *Oligomerization and trafficking of the human dopamine transporter. Mutational analysis identifies critical domains important for the functional expression of the transporter*. J Biol Chem, 2003. **278**(4): p. 2731-9.
210. Melikian, H.E., *Neurotransmitter transporter trafficking: endocytosis, recycling, and regulation*. Pharmacology & therapeutics, 2004. **104**(1): p. 17-27.
211. Zahniser, N.R. and A. Sorkin, *Rapid regulation of the dopamine transporter: role in stimulant addiction?* Neuropharmacology, 2004. **47 Suppl 1**: p. 80-91.
212. Chen, N., et al., *Inhibition by arachidonic acid and other fatty acids of dopamine uptake at the human dopamine transporter*. Eur J Pharmacol, 2003. **478**(2-3): p. 89-95.

213. Simons, K. and D. Toomre, *Lipid rafts and signal transduction*. Nat Rev Mol Cell Biol, 2000. **1**(1): p. 31-9.
214. Bjerggaard, C., et al., *Surface targeting of the dopamine transporter involves discrete epitopes in the distal C terminus but does not require canonical PDZ domain interactions*. J Neurosci, 2004. **24**(31): p. 7024-36.
215. Aicart-Ramos, C., R.A. Valero, and I. Rodriguez-Crespo, *Protein palmitoylation and subcellular trafficking*. Biochim Biophys Acta, 2011. **1808**(12): p. 2981-94.
216. Charych, E.I., et al., *Interplay of palmitoylation and phosphorylation in the trafficking and localization of phosphodiesterase 10A: implications for the treatment of schizophrenia*. J Neurosci, 2010. **30**(27): p. 9027-37.
217. Davda, D., et al., *Profiling targets of the irreversible palmitoylation inhibitor 2-bromopalmitate*. ACS Chem Biol, 2013. **8**(9): p. 1912-7.
218. Levental, I., et al., *Palmitoylation regulates raft affinity for the majority of integral raft proteins*. Proc Natl Acad Sci U S A, 2010. **107**(51): p. 22050-4.